AD-A088 893 ARMY ENGINEER WATERWAYS EXPERIMENT STATION VICKSBURG--ETC F/G 8 3
EROSION CONTROL OF SCOUR DURING CONSTRUCTION; REPORT 2. LITERAT-- TC(U)
AUG 80 L Z HALES
UNCLASSIFIED WES/TR/HL-80-3-2 NL

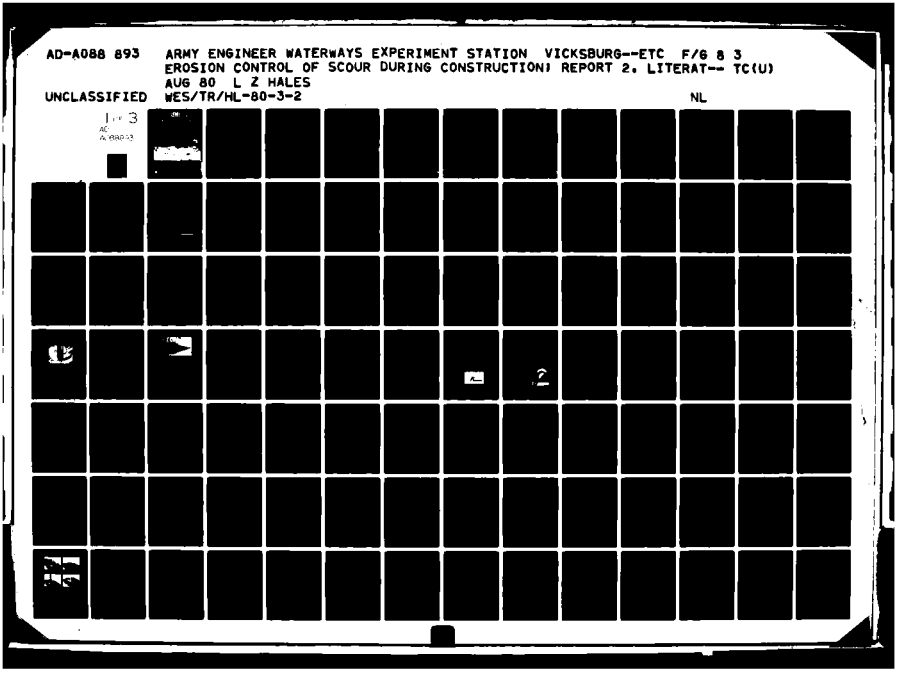

LEVEL II

12

TECHNICAL REPORT HL-80-3

EROSION CONTROL OF SCOUR DURING CONSTRUCTION

Report 2

LITERATURE SURVEY OF THEORETICAL, EXPERIMENTAL, AND PROTOTYPE INVESTIGATIONS

by

Lyndell Z. Hales

Hydraulics Laboratory
U. S. Army Engineer Waterways Experiment Station
P. O. Box 631, Vicksburg, Miss. 39180

August 1980

Report 2 of a Series

Prepared for Office, Chief of Engineers, U. S. Army
Washington, D. C. 20314

Destroy this report when no longer needed. Do not return it to the originator.

The findings in this report are not to be construed as an official Department of the Army position unless so designated by other authorized documents.

The contents of this report are not to be used for advertising, publication, or promotional purposes. Citation of trade names does not constitute an official endorsement or approval of the use of such commercial products.

(14) WES/TR/HL-80-3-2 (9) Technical rpt. 1 Oct 77-31 Oct 79

Unclassified
SECURITY CLASSIFICATION OF THIS PAGE (When Data Entered)

REPORT DOCUMENTATION PAGE

READ INSTRUCTIONS BEFORE COMPLETING FORM

1. REPORT NUMBER: Technical Report HL-80-3
2. GOVT ACCESSION NO.: AD-A088893
3. RECIPIENT'S CATALOG NUMBER:
4. TITLE (and Subtitle): (6) EROSION CONTROL OF SCOUR DURING CONSTRUCTION; Report 2, LITERATURE SURVEY OF THEORETICAL, EXPERIMENTAL, AND PROTOTYPE INVESTIGATIONS
5. TYPE OF REPORT & PERIOD COVERED: Report 2 of a series
6. PERFORMING ORG. REPORT NUMBER:
7. AUTHOR(s): (10) Lyndell Z. Hales
8. CONTRACT OR GRANT NUMBER(s):
9. PERFORMING ORGANIZATION NAME AND ADDRESS: U. S. Army Engineer Waterways Experiment Station, Hydraulics Laboratory, P. O. Box 631, Vicksburg, Miss. 39180
10. PROGRAM ELEMENT, PROJECT, TASK AREA & WORK UNIT NUMBERS: (12) 207
11. CONTROLLING OFFICE NAME AND ADDRESS: Office, Chief of Engineers, U. S. Army, Washington, D. C. 20314
12. REPORT DATE: (11) Aug 1980
13. NUMBER OF PAGES: 202
14. MONITORING AGENCY NAME & ADDRESS (if different from Controlling Office):
15. SECURITY CLASS. (of this report): Unclassified
15a. DECLASSIFICATION/DOWNGRADING SCHEDULE:
16. DISTRIBUTION STATEMENT (of this Report): Approved for public release; distribution unlimited.
17. DISTRIBUTION STATEMENT (of the abstract entered in Block 20, if different from Report):
18. SUPPLEMENTARY NOTES:
19. KEY WORDS (Continue on reverse side if necessary and identify by block number):
Construction practices
Erosion control
Prototypes
Scour
20. ABSTRACT (Continue on reverse side if necessary and identify by block number):

Waves breaking on structures in the coastal zone cause bottom material to be tossed into suspension and carried from the region by longshore or other currents. The scour holes that develop may require substantial amounts of material for rehabilitation and may even endanger the functional integrity of the structure. A substantial amount of work has been performed to investigate and understand local scour of noncohesive material in unidirectional flow,

(Continued)

DD FORM 1 JAN 73 1473 EDITION OF 1 NOV 65 IS OBSOLETE

Unclassified
SECURITY CLASSIFICATION OF THIS PAGE (When Data Entered)

411209

20. ABSTRACT (Continued).

Relatively little effort has been spent on the study of the problem of local scour around structures under wave action. Less work has been performed on the problem of scour under the dual processes of wave motion and unidirectional flow.

Many of the theoretical investigations regarding scour and erosion under wave-induced effects have been founded on earlier work regarding scour and sediment transport mechanics developed from river aspects. These unidirectional theories have been modified to account for the increased shear stress and pressure variations induced by the oscillatory wave field. This report is a survey of the existing literature that has been directed toward understanding the sediment transport by wave and current actions, and the scouring and erosion problems that result around major structures as a result of these phenomena. The primary forcing function is the incoming surface gravity wave train in most cases, and refraction causes concentrations of wave energy that increase scouring potential. The bottom hydrography is altered, and this is reflected in changes to the refraction patterns of the wave system. Theoretical and numerical work to couple wave characteristics, refraction, diffraction, and sediment transport mechanics to deduce resulting bottom configurations is truly in its infancy. However, the basic theoretical groundwork has been laid on which more sophisticated and analytically sound developments can be built to provide reliable engineering computations of scour near coastal structures.

PREFACE

The study reported herein was authorized as a part of the Civil Works Research and Development Program by the Office, Chief of Engineers (OCE). This particular work unit, Erosion Control of Scour During Construction, is part of the Improvement of Operations and Maintenance Techniques (IOMT) Program. Mr. Milt Millard and Mr. William Godwin were the OCE Technical Monitors of the IOMT program during preparation and publication of this report.

This study was conducted during the period 1 October 1977 through 31 October 1979 by personnel of the Hydraulics Laboratory of the U. S. Army Engineer Waterways Experiment Station (WES) under the general supervision of Messrs. H. B. Simmons, Chief of the Hydraulics Laboratory; F. A. Herrmann, Jr., Assistant Chief of the Hydraulics Laboratory; R. A. Sager, Chief of the Estuaries Division and IOMT Program Coordinator; Dr. R. W. Whalin, Chief of the Wave Dynamics Division; Mr. D. D. Davidson, Chief of the Wave Research Branch; and Dr. J. R. Houston, Research Engineer and Principal Investigator for the Erosion Control of Scour During Construction work unit. Dr. L. Z. Hales, Research Hydraulic Engineer, performed the study described herein and prepared this report.

Commanders and Directors of WES during the conduct of the investigation and the preparation and publication of this report were COL John L. Cannon, CE, and COL Nelson P. Conover, CE. Technical Director was Mr. F. R. Brown.

CONTENTS

CONVERSION FACTORS, U. S. CUSTOMARY TO METRIC (SI) UNITS OF MEASUREMENT

U. S. customary units of measurement used in this report can be converted to metric (SI) units as follows:

Multiply	By	To Obtain
cubic yards	0.7645549	cubic metres
feet	0.3048	metres
feet per second	0.3048	metres per second
inches	25.4	millimetres
knots (international)	0.5144444	metres per second
miles (U. S. statute)	1.609344	kilometres
mils	0.0254	millimetres
pounds (mass)	0.4535924	kilograms
square yards	0.8361274	square metres
squares	9.290304	square metres
tons (2000 lb, mass)	907.1847	kilograms
yards	0.9144	metres

EROSION CONTROL OF SCOUR DURING CONSTRUCTION

LITERATURE SURVEY OF THEORETICAL, EXPERIMENTAL, AND PROTOTYPE INVESTIGATIONS

PART I: INTRODUCTION

1. It is frequently necessary to construct engineering works of improvement in the surf and nearshore zone to protect harbor entrances, recreational beaches, and navigation channels. These structures are usually built from quarried rock and/or precast concrete and are usually placed in position by crane operating from the structure itself or on a barge. When these structures are erected in the coastal zone they may alter currents which normally occur at the location due to the bathymetry and wave climate peculiar to the location. Waves breaking on the new structure will cause bottom material to be tossed into suspension and transported out of the region by longshore or other currents. This removal of material is often not compensated by an influx of additional material; and the result is a scour hole, or erosion, which develops along the toe of the structure.

2. Substantial research work has been done with regard to the understanding of local scour of noncohesive material in steady, unidirectional flow. Very little effort has been spent on the study of local scour under wave action, probably because of the unsteady nature of the flow field. Even less work has been performed on the problem of scour under the dual processes of wave motion and unidirectional flow.

3. In the nearshore zone, both unidirectional and oscillatory flows may influence scour near structures. The orbital motions of individual water particles associated with waves in deep water are nearly circular. In intermediate water depths the orbits are elliptical, degenerating at the bottom to a straight-line to-and-fro motion with periods equal to the surface wave. Although tidal currents are periodic, their periodicity is so large that they may be considered to be unidirectional relative to the much shorter period gravity-wave-induced

current fluctuations. Longshore wave-induced currents also may be considered to be unidirectional.

4. Studies of sediment transport and scour become very complex when the combined effects of gravity waves and steady unidirectional currents are considered (Komar 1976). The transport results from wave action placing the sediment in motion but producing little or no net transport; however, the unidirectional currents provide the major net transport mechanism for both water and sediment. The unidirectional currents could conceivably be weak in magnitude and still account for a large transport since the sediment is already in motion as a result of wave action.

5. This report is a survey of the present state of knowledge of local scour and erosion of noncohesive sediments in the presence of both oscillatory flow caused by gravity waves and unidirectional currents such as tidal currents or longshore wave-induced currents. Much work has been founded on the sedimentation aspects of scour and erosion of river systems; hence, initial attention will be devoted to these considerations which form the basis for later theoretical and experimental investigations into the wave-induced sediment processes.

PART II: STEADY UNIDIRECTIONAL FLOW

6. When a liquid begins to flow over a bed of loose and cohesionless particles, hydrodynamic forces begin to be exerted upon the particles; and as the flow intensity increases, there is an increase in the magnitude of the hydrodynamic forces on the particles. A condition is eventually reached where the bed particles are unable to resist the forces, and movement is initiated. Owing to the stochastic nature of the problem, all particles on the bed surface do not begin to move at once. This implicitly brings out the fact that the flow has changed from laminar to turbulent, and the impact of the liquid on the particles tends to dislodge some elements with the combined drag and uplift forces contributing to their transport.

Laminar Versus Turbulent Flow Aspects

7. The drag forces exerted by a liquid on its boundary are an inherent property of the liquid, determined in slow motion by the dynamic viscosity of the liquid. At higher rates of flow, there is added transfer of momentum normal to the boundary that is greater than molecular transfer, the flow changes to turbulent, and the added momentum transfer is incorporated into an eddy viscosity that is much greater than the dynamic viscosity. Most flows that occur in practical applications are turbulent, where this term denotes motion in which irregular fluctuations are superposed on the main flow. These fluctuations are so complex that they are not readily amenable to mathematical treatment; however, their effects are as if the viscosity of the liquid were increased by factors of hundreds or even thousands (Schlichting 1968). Time-averages of the turbulent motion must be considered in an analysis because complete theoretical formulations have not been developed. Mean values are taken over a sufficiently long interval of time for them to be completely independent of time.

Laminar flow stress

8. The viscosity of a liquid is a measure of its resistance to

shear or angular deformation, and results from the cohesion and momentum exchange between molecules in the liquid. This molecular exchange produces a shear or friction force between adjacent layers of the liquid and may be visualized as shown in Figure 1. Consider two parallel

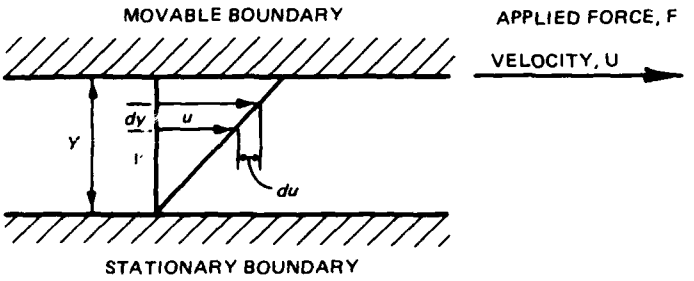

Figure 1. Liquid shear and velocity profile produced by parallel plate motion with velocity U

plates of area A* placed a small distance Y apart, with the space being filled with liquid. Assume the lower surface to be stationary, while the upper one is moved parallel to it with a velocity U by a force F . The particles of liquid in contact with the plates will adhere to them (the no-slip boundary condition), and if the distance Y is not too great or the velocity U too high, the velocity gradient between the plates will be a straight line. Each sheet of liquid slips a little relative to the next layer.

9. It can be shown experimentally that for a large number of liquids,

$$F/A \propto U/Y$$

From similar triangles, U/Y can be replaced by the velocity gradient du/dy . Introducing a constant of proportionality μ , the shearing stress τ between any two layers of liquid may be expressed as:

$$F/A = \tau = \mu\, U/Y = \mu\, du/dy \qquad (1)$$

---

* For convenience, symbols and unusual abbreviations are listed and defined in the Notation (Appendix A).

As developed by Daugherty and Franzini (1965), Equation 1 is Newton's equation of viscosity, and the constant of proportionality μ is the coefficient of viscosity, or dynamic viscosity. In this laminar flow, the motion is characterized by the thin layers of liquid slipping over one another without mixing other than from a very slow molecular exchange.

Turbulent flow stress

10. If the top plate of Figure 1 is moved at too great a velocity, disturbances or irregularities develop in the liquid and the motion ceases to be simply a linear increase in velocity with distance above the bottom. This turbulent flow is characterized by eddy motions where there is intense lateral mixing and is regarded as a motion where a complex secondary movement is superposed upon the primary flow pattern. This turbulence has random velocity fluctuations which are superposed on the average flow and can be described only in statistical quantities.

11. The eddies are able to transfer momentum normal to the plates at much greater rates than molecular transfer in laminar flow. This additional transfer is incorporated into an eddy viscosity A_y term, so that:

$$\tau = (\mu + A_y)\, d\bar{u}/dy \tag{2}$$

However, since the eddy viscosity is much greater than the dynamic viscosity, it is customary to drop the dynamic viscosity entirely, producing

$$\tau = A_y\, d\bar{u}/dy \tag{3}$$

Here the bar indicates average quantities, and a prime will indicate the turbulent fluctuation components (Komar 1976) so that:

$$u = \bar{u} + u' \ , \quad v = \bar{v} + v' \ , \quad w = \bar{w} + w' \tag{4}$$

The instantaneous velocity component is then equal to the sum of a mean velocity plus a fluctuating component, where by definition the average of the fluctuations is zero.

12. Eddy fluctuations are important in transferring momentum under turbulent flow. In Figure 2, consider liquid layers 1 and 2

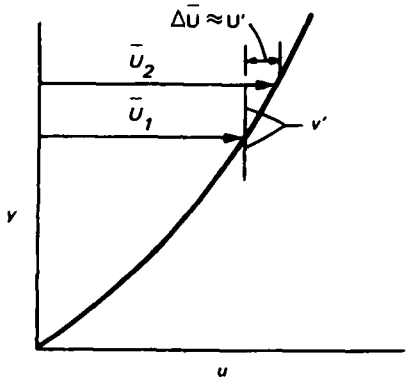

Figure 2. Eddy viscosity momentum exchange deviation from mean flow

moving with slightly different average velocities. If an eddy of lower velocity fluid were to fluctuate from level 1 into level 2, the drag of the faster moving surroundings would increase its momentum. The flux of material moving from level 1 to level 2 would be $\rho v'$. The flow direction momentum change would be this flux multiplied by u' , or on the average over a long period of time,

$$\tau = \rho \overline{u'v'} \tag{5}$$

where ρ is the density of the liquid. This is an effective resistance to motion and is known to be a significant shearing stress in turbulent flow. From Figure 2 it can be seen that the fluctuating velocity components are proportional to the mean values. Hence

$$\tau \propto \rho \bar{u}^2$$

It has also been found empirically that for turbulent motion the stress is proportional to the square of the average velocity.

13. It can be concluded, following Schlichting (1968), that the components of the mean velocity of turbulent flow satisfy the same equations of motion as those satisfied by laminar flow, except that the

laminar stresses must be increased by additional stresses. These additional stresses are known as apparent or Reynolds stresses of turbulent flow. In experimental work on turbulent flow it is usual to measure only the mean values of velocity (and pressure) because these are the quantities which can be measured most conveniently. The measurement of mean values is quite sufficient for most practical applications, although the turbulent fluctuation components can be obtained with more elaborate equipment, such as hot-wire anemometers.

Boundary layer conditions

14. The boundary conditions which must be satisfied by the mean velocity components are the same as those in ordinary laminar flow, i.e., they must all vanish at solid walls (the no-slip condition). In addition to vanishing at the walls, all turbulent components are very small in the immediate neighborhood of the wall. Hence, the only stresses that act near solid walls are the viscous stresses of laminar flow (since they do not vanish there). Since near the wall the Reynolds stresses are small compared with the viscous stresses, it follows that in turbulent flow there exists a very thin layer near the wall which behaves like one in laminar motion. This has come to be known as the laminar sublayer or viscous sublayer, since it is observed to be not entirely laminar but is accompanied by considerable irregular fluctuations (Figure 3). The viscous sublayer exists only for smooth boundary conditions.

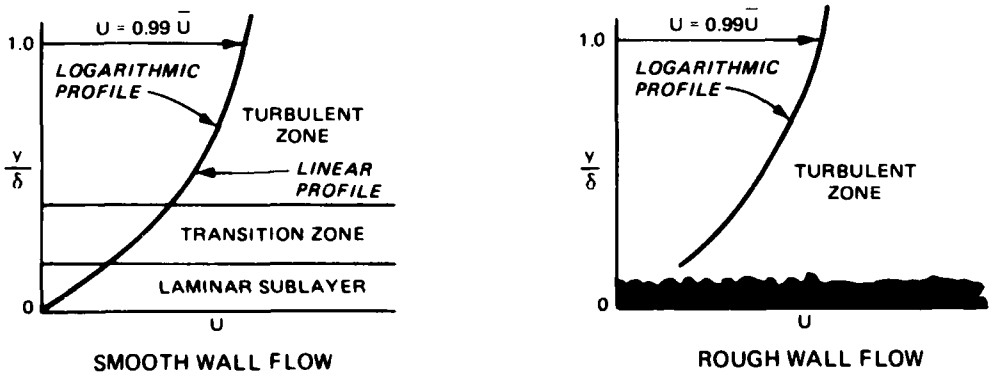

Figure 3. Zones within the boundary layers for smooth and rough boundaries

15. Above the viscous sublayer is found a second zone in which the viscous and turbulent transfers of momentum are comparable for a smooth boundary. Farther out into the boundary layer, turbulent transfer is found to dominate over viscous transfer. The thickness of the viscous sublayer is so small, in most cases, that it is impossible or very difficult to observe experimentally. Nevertheless, it is of decisive importance because it influences drag and shear stress.

16. When the boundary is rough the viscous sublayer will be disrupted so that the turbulence extends all the way to the wall. This is commonly the case where flow occurs over sand, and the size and form of the roughness elements become additional important parameters. Defining the frictional velocity as

$$u_* = (\tau/\rho)^{1/2} \tag{6}$$

and letting

$$\nu = \mu/\rho \tag{7}$$

the equation for the velocity profile over rough boundaries, according to Komar (1976), can be shown to approximate

$$\bar{u}/u_* = (1/k)\ (\ln y/k_s) + 8.5 \tag{8}$$

where

k = von Karman's constant (approximately 0.4 for many flows)

k_s = a measure of the roughness elements. In uniform sand, k_s is taken as the diameter of the sediment grains. When a sediment grain-size distribution is used, k_s is assumed by many researchers to be the sieve size of which 75 percent of the mixture by weight is finer.

Sediment Motion Threshold

17. When a liquid begins to flow over a bed of movable material, initially there is no motion of bed particles. A condition is ultimately

reached where a grain begins to move because the hydrodynamic forces exceed the stabilizing gravity forces acting on the particle. A sediment grain on the bed surface is subjected to a weight force and liquid forces (Figure 4) which give rise to shear stresses between the grains

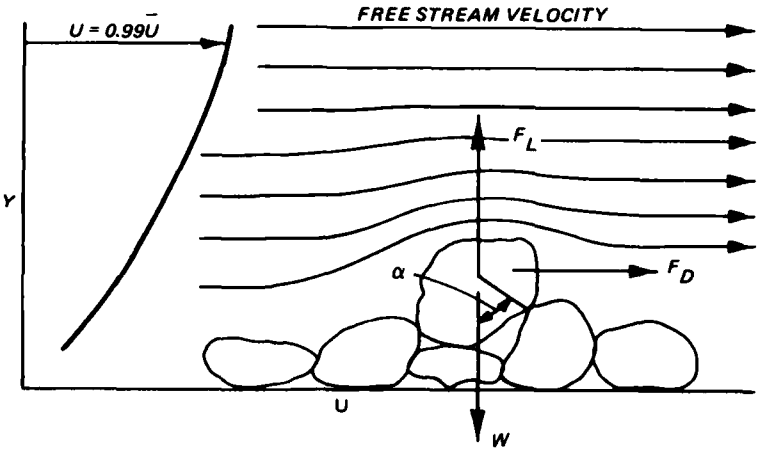

Figure 4. Body and hydrodynamic forces acting on a sediment grain in a liquid flow field

and the stationary bed, with the tangential components of the forces striving to maintain forward movement. As the velocity of flow increases, the shear stress on the particles increases until eddy formations develop and a wake is formed downstream of the particles. The drag force then becomes a combination of surface skin friction drag and form drag due to pressure differentials. The lift force is not ordinarily considered in the analysis because it can be effectively included inherently in the turbulent fluctuations. In turbulent flow both the lift and drag forces are fluctuating quantities in magnitude and direction. Two different approaches have been used in relating the pertinent parameters of liquid motion and sediment transport; the first approach considers the velocities of flow of the fluid, and the second method relates the shear stresses developed by the liquid on the sediment particles.

Sediment transport
initiation velocity

18. Theoretical considerations have not been entirely successful

in developing expressions for the velocity necessary to initiate sediment movement at the surface of a bed of transportable material. The drag and lift forces, when expressed in the usual manner, are:

$$F_D = 1/2\ C_D\ \rho\ A\ u_b^2\ ,\quad F_L = 1/2\ C_L\ \rho\ A\ u_b^2 \tag{9}$$

Here fully turbulent flow is assumed and the stresses (forces) are related to the square of the velocity, u_b , at the bed. These drag and lift forces are then equated to the tangential and normal components of the sediment particle weight. Unfortunately, the values of the drag and lift coefficients, C_D and C_L , respectively, are not well known. Furthermore, the projected area, A , of the particles depends upon the shape of the elements, and this incorporates additional uncertainties into the analysis. Experimental verification to obtain these empirical quantities has not been entirely successful, due in part to the inability to obtain good definition of the bottom velocity, u_b . Hence, the theoretical applications of the bottom velocity analysis are of limited use from a practical standpoint, and most researchers tend to use the average velocity of flow.

19. The classic work in relating the average velocity of flow to erosion, transportation, and deposition for varying size particles was performed by Hjulstrom (1935). An extensive analysis of data obtained from experiments with movable-bed material of uniform size shows sharp lines of demarcation between transport and sedimentation (Figure 5). The greater resistance to erosion of the smaller size particles is an indication of the significance of cohesion and adhesion forces.

20. Neill (1967) developed a design curve for scour of coarse, uniform bed material by applying the mean velocity criterion, yielding

$$\bar{u}_{cr}^2/(\rho_s/\rho - 1)gd = 2.5(d/D)^{-0.2} \tag{10}$$

where

u_{cr} = critical average velocity required to move a substantial number of surface bed particles

ρ_s = particle density

g = acceleration due to gravity

d = sediment particle diameter

D = depth of uniform flow

Because of the inability to relate the average velocity values to prototype situations where bottom topography varies significantly with time and space, many researchers have accepted the more satisfactory concept of the bottom shear stress as a scour criterion for establishing bed material movement.

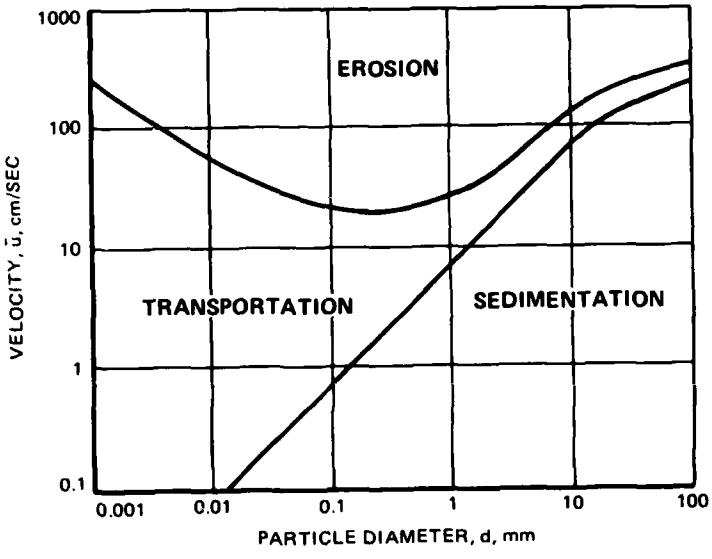

Figure 5. Hjulstrom's curve relating average velocity to grain size for erosion, transportation, and sedimentation (after Hjulstrom 1935)

Critical tractive force

21. For a control volume concept, the gravitational component in the direction of flow is balanced by the frictional resistance at the bed, and the resulting equality yields the bottom shear stress,

$$\tau_o = \gamma DS \tag{11}$$

where

γ = weight of the liquid per unit volume

S = slope of the hydraulic gradient producing the uniform flow

When incipient motion of the bed particles occurs, the resulting shear stress is considered to be the critical tractive force, τ_i . An analysis of the pertinent variables involved indicates a functional relation between the critical stress and the remaining variables,

$$\tau_i = \tau_i \ (\gamma, \ \gamma_s, \ \nu, \ \tau_o, \ \rho, \text{ and } d) \tag{12}$$

although the form of the relation is not readily apparent. Some researchers advanced the idea of expressing the turbulent flow conditions in terms of the friction or shear velocity, u_* , previously discerned. This permits the establishment of a reference dimensionless quantity incorporating both fluid properties and sediment size, and referred to as the shear Reynolds number, Re_* , where

$$Re_* = u_* d/\nu \tag{13}$$

22. Graf (1971) reports that Shields appears to have been the first in the field of sediment transport mechanics to have used this concept for the special case of uniform sand. Since that time, however, other researchers have experimented with a wide assortment of materials with densities varying from 1.06 to 7.90 g/cm^3. Their results are shown in Figure 6, which is a representation of the critical bottom shear stress as a function of the shear Reynolds number. Considering all the experimental data (which were obtained from different researchers and with quite different experimental arrangements) that went into developing this figure, the overall scatter should not be alarming. Other threshold curves that form the basis for predicting initial sediment motion, knowing some combination of sediment grain size and density or water velocity and stress, have been extrapolated from the Shields diagram; but this work for the initiation of sediment movement serves as a quite accurate and general criterion.

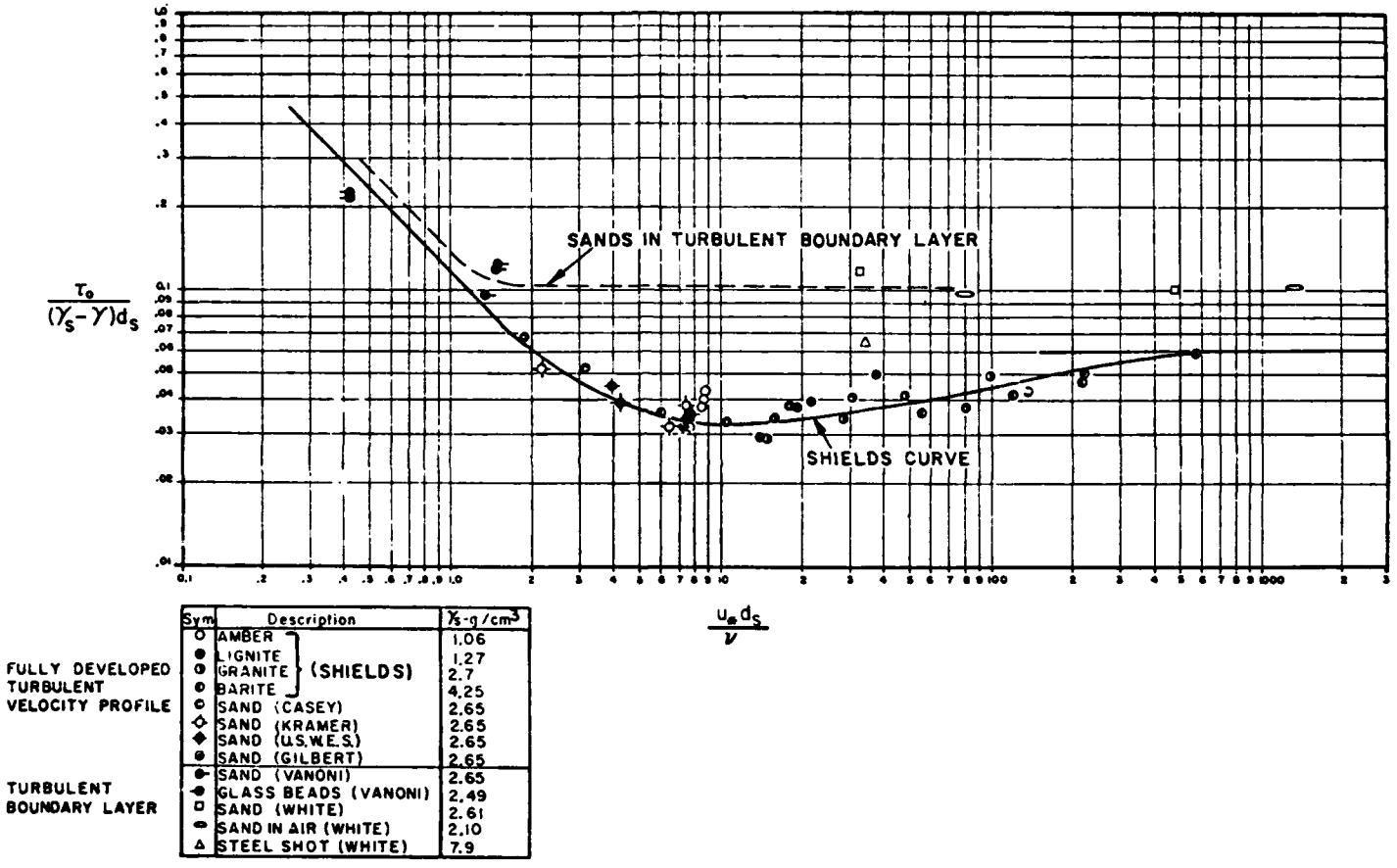

Sym	Description	γ_s-g/cm^3
○	AMBER	1.06
●	LIGNITE	1.27
○	GRANITE	2.7
●	BARITE	4.25
○	SAND (CASEY)	2.65
◇	SAND (KRAMER)	2.65
◆	SAND (U.S.W.E.S.)	2.65
⊕	SAND (GILBERT)	2.65
⊕	SAND (VANONI)	2.65
●	GLASS BEADS (VANONI)	2.49
□	SAND (WHITE)	2.61
⬭	SAND IN AIR (WHITE)	2.10
△	STEEL SHOT (WHITE)	7.9

Figure 6. Shields diagram relating tractive shear stress with shear Reynolds number for uniform sand, and comparisons with other materials by additional researchers (after Vanoni 1964)

Sediment Transport Mechanics

23. The control of alluvial streams for navigation and coastal sediment transport (including harbor shoaling) are probably the two most important classes of sediment transport problems to be encountered by hydraulic and/or coastal engineers. Sediment in streams may be transported either by rolling along the bed (bed load) or in suspension by the turbulent water motion (suspended load). There may be other transport mechanisms, such as dissolved particles; however, these are insignificant relative to the quantities transported by bed load or suspended load. These two types of sediment motion are usually considered separately with the total sediment load consisting of their sum; however, there really is no sharp well-defined line of demarcation between them, and individual particles may alternately be transported as bed load and suspended load. Discussions often ensue between researchers regarding the most appropriate means of discriminating between the two types of sediment transport. The classic approaches are based on separate analysis of the bed load in terms of the tractive force and of the suspended load in terms of turbulent transfer mechanisms. Analytical models have been developed for these separate processes and have been correlated using empirical relations.

Bed-load transport concepts

24. There are essentially three different approaches to the bed-load transport problem: (a) the duBoys analysis assumes that the bed moves in a layered laminar flow as a result of the tractive force of the flowing water; (b) the Schoklitsch investigations propose a discharge relation to explain bed movement; and (c) the Einstein model applies statistical considerations to the forces involved. All of the studies are similar in that, except for minor cases, the bed-load motion has been investigated in laboratory flumes instead of prototype situations, which are quite difficult, and all bed-load equations rely on experimental determination of their coefficients.

25. The duBoys-type analysis. The purpose of the duBoys equation is to estimate the amount of sediment that is being transported by

specific volumes of flow (implying a known tractive force on the bed) in concert with unique sand characteristics and channel geometry at the specific prototype location. The duBoys-type analysis assumes that layers of the bed slide over each other in such a way that the velocity of the elements decreases linearly with depth, becoming zero at the top of the layer which does not move because its frictional resistance has just balanced the shear force at that level. Here the resisting force is the product of the submerged weight of the bed sediments and its coefficient of friction. This type of approach has been the subject of much criticism, although the conceptual model is frequently used. Sediment characteristic parameters have been evaluated in the laboratory, and the resulting expression for transport per unit width of channel as developed by Straub (1942) is

$$q_s = \left(111{,}000/d_m^{3/4}\right) S^{1/2} (n/1.5)^3 u^3 \qquad (14)$$

where

d_m = mean diameter of the bed material

S = channel slope

n = Manning's roughness coefficient

u = average channel velocity

26. Kalinske (1947) recognized that the turbulence mechanism above the bed played an important role, and that the force on bed particles actually fluctuated as a result of the turbulent wake behind the particles. He reasoned that the maximum bed shear stress could be as much as three times that determined by simple computations, and that the actual drag force on a particle could be as much as twice the mean force on it. Based on the hydrodynamics of the problem, Rouse (1938) modified Kalinske's equation to a form which contains only easily available quantities,

$$q_s = 10\, \gamma_s\, \gamma^2\, g^{1/2}\, (DS)^{5/2} / (\gamma_s - \gamma)^2\, d \qquad (15)$$

where

γ = unit weight of the liquid

γ_s = unit weight of the solids

27. The Schoklitsch-type analysis. Theoretical considerations used in development of the Schoklitsch-type equations rely on a discharge relation to evaluate the amount of sediment that may be moving past a channel section. A critical discharge is determined by extrapolating experimental data to the point at which incipient sediment motion occurs. Also, actual bed-load measurements in prototype situations were made, and the following equation was developed:

$$q_{cr} = 0.26\ (\gamma_s/\gamma - 1)^{5/3}\ d^{3/2}\ S^{7/6} \tag{16}$$

where q_{cr} is the critical discharge. This value is related to the rate of bed-load weight per unit time and width as

$$q_s = 2{,}500\ S^{3/2}\ (q - q_{cr}) \tag{17}$$

where the values are in metric units.

28. Froude similarity criteria have been used as a guide in the establishment of an experimental program by Meyer-Peter and resulted in formulation of the following bed-load equation, in metric units,

$$q_s^{2/3} = (d/0.4)\ (q^{2/3}\ S/d - 17) \tag{18}$$

for sand. The strongest deviations of this equation from the experimental data occurred with sand of small grain diameters (less than 0.2 mm), where Froude's law may not strictly apply. The equation is probably limited to coarse materials because of these deviations. These original experiments have been extended to include particle mixtures, and the results enjoy great popularity, especially in Europe.

29. The Einstein-type analysis. The definition of a critical value for the initiation of sediment motion is difficult, at best; thus Einstein suggested that bed-load transport should be related to the

fluctuations of the velocity rather than to the average value of velocity or shear stress. He then developed a formula which relates the rate of bed-load transport with properties of the grain and of the flow causing the movement, and employed statistical reasoning to a much greater extent than previous investigators. The probability that any one particle is moving at a given time is related to its fall velocity, size, and specific weight, as well as to hydraulic properties of the flow. Einstein further assumed that the probability of erosion is the fraction of time during which, at any one location, the instantaneous lift exceeds the weight of the particle (Einstein 1950).

30. The Einstein analysis requires evaluation of a function which must be determined empirically, and he found that a logarithmic function would correlate fairly well with laboratory data. Rouse (1938) had previously suggested a simpler function which appears to fit the data equally well and thus the Einstein equation can be modified to

$$q_s = \frac{40\ \gamma^4\ D^3\ S^3\ F}{\rho^{1/2}\left[(\gamma_s - \gamma)^5\ d^3\right]^{1/2}} \tag{19}$$

where F is a dimensionless function such that

$$F = (2/3 + G)^{1/2} - G^{1/2} \tag{20}$$

and

$$G = \frac{36\ \mu^2\ g}{d^3\ \gamma(\gamma_s - \gamma)} \tag{21}$$

Suspended-load transport concepts

31. In many streams, the suspended load is equally as important as the bed load, particularly when the turbulent intensity is sufficient to cause a continual interchange with the bed particles. Particles in suspension (suspended load) tend continually to fall by gravity to the bed while turbulence tends to throw bed particles up into the flow area and to maintain them there. For equilibrium conditions to exist, these two conditions are just balanced at each level in the flow field. The

amount of sediment tending to fall through a unit horizontal area is the product of the fall velocity of the particle v_f and the sediment concentration C_s at that level. The transfer of sediment up from the bed and throughout the flow area is essentially a diffusivity process and is equal to the product of the diffusion coefficient ε and the gradient of concentration of the sediment at that elevation dC_s/dz .

$$v_f C_s + \varepsilon \, dC_s/dz = 0 \tag{22}$$

Equation 22 is the basic differential equation for suspended sediment and can be solved when certain assumptions are introduced.

32. The Lane-Kalinske (1941) method of solution is based on the assumption that the diffusion coefficient is a constant through the vertical section and is equal to the average value determined in terms of the von Karman turbulence constant and the friction velocity u_* . Hence, Equation 22 becomes

$$C_s/C_a = \left[(D/z - 1)/(D/a - 1)\right]^{v_f/0.4u_*} \tag{23}$$

For a given sediment, it is possible to determine the concentration C_s at any and all points in a vertical section if the concentration C_a is known at a single point a in the vertical. Comparison with prototype data indicates that results produced by Equation 23 are sufficiently accurate for practical purposes. However, it may be of limited usefulness since it applies only for a particular sediment size and to equilibrium conditions, and requires measurements of the concentration at some level, $z = a$.

33. In actual measurements of the suspended load of a stream, both the velocity and the sediment concentration at a level are necessary. The suspended sediment load is determined by sampling the water, filtering to remove the sediment, drying, and weighing the filtered material. The sample is collected in a specially designed bottle to avoid distortion of the streamlines of flow during collection of a representative sample of the sediment-laden water. The depth-integrating

samplers remove the necessity for averaging point values.

Total sediment-load concepts

34. The total sediment load of a stream is the sum of the bed load and suspended load (ignoring other relatively insignificant transport mechanisms). It is convenient to distinguish between these two methods of transport since they are measured by entirely different means and since the basic transport mechanisms are substantially different. Bed load moves in a rather thin layer, with the particles rolling or sliding. Above the bed layer, particles in suspended load are continuously supported by fluid turbulence. Bed load is measured by traps while suspended load is quantified from water samples of the sediment-fluid mixture.

35. Reasoning from the point of view of general physics, Bagnold (1966) states that the existence and maintenance of upward supporting stresses equal to the immersed weight of the solids provide the element necessary for initiating their transport. Dynamic transport rates should be directly related to the stream power available for performing their transport. Bagnold arrived at a relation for the total load which may be obtained if four parameters are known: (a) a bed-load efficiency factor; (b) a suspended-load efficiency factor; (c) the friction coefficient of the material; and (d) the average velocity of flow of the stream. Efficiency factors were evaluated from laboratory experiments.

36. Some other investigators feel no need exists for distinguishing bed load from suspended load, because the hydrodynamic forces are the same in either case. This procedure of considering the sediment load as a single entity was developed on the basis of model studies and fitting empirical information to theoretical curves. While it is reasonable that the total sediment load should be functionally related to the flow depth and velocity, channel slope, density of particles, and viscosity of fluid, there exists scatter in the data which may be the result of bed roughness uncertainty. The development of Garde and Albertson (1958)

$$q = \frac{1.08\, u^4\, n^3}{\nu^3\, d^{3/2}\, D} \tag{24}$$

uses Manning's roughness coefficient which probably does not account for ripple pattern or dune formation. A completely satisfactory solution of the problem of sediment transport has not been obtained, and the application of any currently available sediment formula should be made with careful engineering judgment.

PART III: SCOUR BY UNIDIRECTIONAL FLOW

37. Rivers and channels in alluvial material adjust their boundaries and experience changes in depth and planform in response to the dynamic hydraulic conditions to which they are subjected. Consequently, the sediment transport capacity of a stream changes since this phenomenon is a function of the flow parameters. When transport from an area is greater than the rate at which material is supplied to the region, scour results. When the transport capacity is less than the supply, deposition will occur. Thus, cycles of scour and fill as well as variable rates of scour and fill occur at any particular location, and the process is not amenable to simple mathematical analyses. Recourse is sometimes made to the use of physical hydraulic models with movable beds and the fitting of prototype observations to analytical treatments. Hence, all scour prediction formulas are empirical to some degree and are therefore somewhat limited in their application. The dynamic problem usually accepted as scour may be decomposed into three components: (a) natural scour, (b) contraction scour, and (c) local scour. Scour at bridge piers is a significant problem and encompasses all three of these separate actions.

38. Natural scour is the tendency of alluvial channels with movable boundaries to meander and shift their location with an accompanying change in bed elevation as a shift in thalweg develops. Usually, scour at one location is accompanied by deposition at another, as a reach of river consists of a series of contractions and expansions. Channel degradation is considered to be the process whereby a stream of flowing water has the potential to transport a sediment load, and if the transportable load is not already in the system, then scour or erosion will take place until the transport capacity of the stream is reached. Degradation may occur naturally as a result of changed hydraulic conditions, or it may be caused by man's activities such as flow augmentation or the reduction of sediment supplied to a reach by dam construction.

39. Contraction scour occurs over a relatively large area and is usually the result of man-made changes at specific locations. For

example, construction of a bridge waterway opening will constrict the floodplain flow, and the discharge must move laterally relative to the bridge opening. When the flow returns to the channel location, there may be general scouring of the entire opening or there may be severe scouring of the abutments. The scour potential can only be assessed by first predicting the flow pattern for the conditions that will exist during the life of the structure.

40. Local scour results from localized changes to the streamline flow patterns caused by obstructions placed in the flow field. Local scour occurs when the capacity of the flow to remove or transport bed material is greater than the rate at which material is being supplied to the region. In flows without continuous sediment supply, the shear stresses on the bed surface generally decrease as scour hole size increases, until a state is reached where the stresses are unable to transport additional material from the scour hole. For given hydraulic conditions, the size of the ultimate scour will be directly related to the characteristics of the bed material, and will require a finite time interval to reach full development.

41. Investigations into scour and erosion processes are a logical extension of the sediment transport studies previously elucidated. Many researchers have attempted to develop "simple" scour prediction formulas by collecting data over several limited ranges and determining the relation for each individual data set. This has produced a large number of sometimes conflicting formulas for the estimation of scour under specific circumstances. These scour prediction formulas can be grouped into two broad categories: (a) regime theory, which includes the natural scouring tendencies of channels to shift their boundaries in the absence of any constriction or artificial work of improvement, and contraction scouring as a result of large-scale construction which reduces the flow area; and (b) local scour, where secondary flow characteristics caused by alterations to the flow field cause intense lift and drag forces near structures. No single scour formula has won general acceptance, and the design of nonscouring foundations is performed largely by judgment and experience, since the assimilation of quantitative field

data during periods of actual scour is extremely difficult.

Regime Concept

42. Dimensions and shape of an alluvial channel are usually in some sort of equilibrium with the long-term pattern of discharges and sediment loads that the stream is required to transport. The concept of the channel adjusting its boundaries to accommodate changing discharges and sediment loads is the fundamental basis of regime theory. Flow in an actual river system is nonuniform, nonsteady, three-dimensional, and turbulent. It involves a complex system of curves, cross and spiral currents, converging and diverging flows, and turbulent eddy formations. According to Neill (1964), most of the erosive activity takes place during comparatively rare high river stages. However, the beds of many rivers return to substantially the same levels during each succeeding low-flow period. Thus it may be difficult to specify exactly what constitutes scour, since the riverbed tends to be an erratic or nonstationary datum.

General river scour

43. The classical concept that mean bed elevation over a stream reach was lowered by scour during the passage of a flood wave and then restored by filling during the waning flood phase has long been questioned. Systematic field measurements were performed by Foley (1975) which confirmed that alternative scour and fill occur at different sections of the stream reach simultaneously. It was found that mean bed scour or fill in a uniform channel is minor relative to local scour or fill caused by bed-form migration, and that maximum local scour and fill may occur on the waning stages of the flood wave. This work demonstrated that the major part of the scour and fill which occurs in a reach of an ephemeral sand-bed stream is produced by the development and passage of large-scale bed forms, primarily antidunes. This explains the source of material for fill and shows that during a flood a particular section of a stream may be experiencing either scour or fill, depending upon its location relative to the nearest migrating antidune. In fact,

any section may experience several cycles of scour and fill during the passage of a single flood wave. Steinman and Watson (1957) advanced the idea that the riverbed is fluidized to a finite depth during flood stages. This conclusion appears to be unsubstantiated and probably arose from observations of the passing antidune wave form and the local scouring around footings of structures.

44. Terzaghi and Peck (1948) reported scour depth figures for a number of bridge crossings, and advised that in the absence of additional guidance, the maximum depth of scour could be estimated as some multiple of the rise in water level. This multiple has been variously quoted as anywhere from 1 to 4, although the relation between scour depth and rise in stage is highly uncertain and depends greatly on the degree of constriction imposed by the bridge.

Constriction scour
(bridged waterways)

45. Because of the importance of bridged waterway safety, considerably more study and analysis of scour and erosion in this region have been performed than for the general scouring of stream reaches. Total scour that may occur at a constricted region consists of one or more separate kinds of erosion which may be additive. These include local scour near the piers and ends of abutments, the general erosion produced by the encroachment of embankments, and additional erosion due to the presence of bends or misalignments in the immediate vicinity of the bridge.

46. A diversity of approaches has been used by different investigators over the years to explain the mechanics of sediment transport and to predict the ultimate scour depth expected at a particular location under various flow conditions. All these investigations are empirical to the extent that data were collected for limited conditions, and the "fitting" procedure may not be extrapolated beyond the range of the experiment or for other variables. The prediction formulas do not necessarily include the same variables, although Hopkins, Vance, and Kasraie (1975) have shown that the formulas may be expressed in terms of three dimensionless variable groupings describing flow characteristics in

terms of velocity, obstruction dimensions, and properties of the bed material:

$$d_s/b = f(F_r, y/b, \text{sediment}) \tag{25}$$

where

d_s = maximum scour depth to be expected

b = obstruction width normal to the flow lines

F_r = Froude number, defined as

$$F_r = u/(g\ y)^{1/2} \tag{26}$$

The sediment characteristic is taken by various investigators to be either density, specific weight, or specific gravity.

47. Anderson (1974) has examined several empirical formulas in the technical literature, and has reduced them to similar equations of dimensionless parameters by the introduction of appropriate simplifications so that a direct comparison can be made regarding structure and form. He further shows that to a considerable degree, the size and depth of the scour hole depend on the strength of the cohesive bond of the material. Hence, if the bed material is coarse enough to be non-cohesive, then bed transport will occur into the scour hole; and the limiting depth will be less than if the material were cohesive with minimal bed-load transport.

48. Ahmad (1962) prediction equation. Laboratory experimental studies were conducted by Ahmad to investigate scour around spur dikes, and subsequent field studies of bridge crossings in Pakistan enabled him to develop the estimation of scour near bridge piers as

$$d_s/b = (y/b)\left(4.77\ F_r^{2/3} - 1\right) \tag{27}$$

The symbols have been previously defined. Here it is assumed that the bridge piers are sufficiently far apart so that interaction does not occur.

49. Blench (1969) prediction equation. A particle bed factor to account for a relatively wide range of sediment sizes was developed by Blench, and the relative scour equation was given as

$$d_s/b = 3.72\ (y/b)^{3/4}\ F_r^{1/2} - y/b \tag{28}$$

50. Breusers (1965) prediction equation. Based on physical model tests, Breusers deduced that

$$d_s/b = 1.4 \tag{29}$$

which indicates that on the average and for the range of values tested, the depth of the scour hole is determined entirely by the structure width and is independent of flow or bed material characteristics.

51. Chitale (1962) prediction equation. By conducting laboratory experiments on model bridges, Chitale concluded that the scour depth at the nose of the pier is related to the velocity of flow by a second degree expression of the Froude number.

$$d_s/b = (y/b)\left(-5.49\ F_r^2 + 6.65\ F_r - 0.51\right) \tag{30}$$

52. Inglis (1949) prediction equation. This study conducted in Poona, India, considered bed material ranging from 0.06 to 0.37 mm in diameter, and it was concluded that material size had little or no effect on the maximum depth of scour. After analyzing data from 17 prototype bridge installations, it was determined that the maximum scour depth was related to Lacey's regime depth by approximately a factor of 2.

$$d_s/b = \left[4.05\ (y/b)^{3/4}\ F_r^{1/2}\right] - y/b \tag{31}$$

53. Larras (1963) prediction equation. Larras analyzed data from both prototype river bridges and laboratory model studies of stable and unstable riverbeds. He concluded that the maximum scour depth is independent of the water depth and bed material size if the depth is at

least 40 times the size of the bed particles. The scour depth is a function of the maximum width of the pile, its shape, and flow direction.

$$d_s/b = 1.42\ K\ b^{-0.25} \tag{32}$$

The coefficient K depends on the pier shape and varies from 1.0 for cylindrical piles to 1.4 for rectangular piers aligned with the flow.

54. Laursen (1962) prediction equation. The work of Laursen has probably had a greater impact on the thinking of American researchers in the area of scour problems than that of any other individual. He approached the problem of scour around bridge piers by making use of the long contraction analysis. He reasoned that scour depth could be determined from the depth ratio of constricted to unconstricted sections and developed

$$b/y = (5.5)(d_s/y)\left[(1/r)(d_s/y) + 1\right]^{1/7} - 1 \tag{33}$$

The constant, r , was found to have a value of 11.5 for the best-fit condition. This equation represents an implicit relation between d_s/b and y/b .

55. Neill (1965) prediction equation. An analysis of prototype bridge data led Neill to conclude that scour around bridge piers was independent of the Froude number, and was dependent only on the depth of flow and the width of the flow obstruction

$$d_s/b = 1.5\ (y/b)^{0.3} \tag{34}$$

56. Shen et al. (1969) prediction equation. In a series of papers by this investigator into the mechanism of local scour, it was pointed out that the dominant feature of flow near the pier is the large-scale eddy structure, or system of vortices, which develops about the pier. The horseshoe vortex system is the mechanism for scour and is dependent on the pier Reynolds number; and scour properties can be determined from properties of the vortex system. Data from other

researchers were analyzed, and a least-squares best-fit was developed as follows:

$$d_s/b = 0.00073\ u^{2/3}\ b^{-1/3}\ \nu^{-2/3} \qquad (35)$$

57. Even a cursory review of these prediction equations reveals that each is based on those factors which appeared to be the most important to the researcher at the time. To obtain an indication of the manner in which the predicted scour depths vary for identical circumstances, the Highway Research Board (1970) applied the prediction formulas enumerated above to the illustrative example of water depth of 69 ft*, average velocity of flow of 2.0 fps, fine sand, and a rectangular pier 47 ft wide aligned with the flow. Predicted depths of scour by these different formulas were:

Equation	Predicted Scour ft	Equation	Predicted Scour ft
Ahmad	0.0	Larras	35.0
Blench	0.0	Laursen	63.0
Breusers	66.0	Neill	79.0
Chitale	0.0	Shen	1.5
Inglis	0.0		

The range of results produced by these prediction formulas vividly illustrates the designer's dilemma. Perhaps the only guide available to the practicing engineer is to compare the particular design situation with the circumstances under which a particular formula was developed in order to gain some insight into its probable usefulness.

Local Scour

58. Local scour is the erosion phenomenon that occurs in the immediate vicinity of hydraulic structures when the capacity of the flow to transport bed material is greater than the rate at which material is being supplied to the region. This implies an inherent distinction

---

* A table of factors for converting U. S. customary units of measurement to metric (SI) units is presented on page 4.

between two types of local scour: (a) clear-water scour and (b) sediment transport scour. During the active process, the difference between the case of scour in the presence of sediment transport and the case of clear-water scour is primarily a difference in rate of scour, or the time evolution of erosion.

Clear-water scour

59. Erosion that takes place below a large dam or reservoir is the classic example of clear-water scour, since the water released from the dam is essentially sediment-free. This flux conveyance system has the potential for transporting a large sediment load, and the stream will immediately begin to scour or erode the channel bed and side slopes in order to develop its transport capacity. As the finer materials are picked up and moved, a coarsening of the bed develops. This armoring with larger particles appearing on the bed surface causes the more intense scouring action to be transferred downstream.

60. The limit of clear-water scour is reached when the capacity to transport material out of the scour hole becomes zero, or when the boundary shear becomes equal to the critical tractive force on the bed material. This critical force is entirely a function of the bed material, while the boundary shear is related to the velocity of flow, the geometry of the locality, and the roughness of the surface. Hence, depth of clear-water scour is some functional relation of the geometry, velocity, and sediment characteristics.

61. The temporal variation of local scour below a dam or sill across a clear-water stream has been investigated experimentally by Cunha (1976), who develops an expression for the time evolution of the scour. It was found that both the friction velocity u_* and the fall velocity of the particles v_f are pertinent parameters in describing the process. Maximum scour depth is approached asymptotically as

$$d_s/y = 325\ (u_*/v_f)^{3.25}\ t^{0.16} \tag{36}$$

where

d_s = maximum ultimate scour depth that will occur

y = initial unscoured water depth

The maximum depth of scour at any instant of time was determined by Meulen and Vinje (1977) for a similar experimental arrangement, and it was determined that

$$d_{max}/y = (t/t_1)^{0.38} \tag{37}$$

where t_1 is defined as the time at which $d_{max} = y$. Scour growth appeared to have been caused primarily by vortices, since the deepest point of scour moved both longitudinally and laterally. The dependence of characteristic scouring time t_1 on flow conditions (i.e. velocity, material, and geometry) was further investigated; and it was concluded that the influences of these various factors on the rate of the scouring process can be described by the same general relation for both two- and three-dimensional local scour:

$$t_1 = 250 \left[(\rho_s - \rho)/\rho\right]^{1.7} y^2 (\alpha u - u_{cr})^{-4.3} \tag{38}$$

where u_{cr} is the flow velocity necessary for initiation of particle movement, and the coefficient α varies from 3 to 8, depending upon the particular geometry under consideration.

62. The tests described above were conducted in such a manner that material transport could only take place out of the scour hole (i.e. clear-water situation). In prototype situations, a dam across an alluvial stream will probably be releasing water that carries a high concentration of suspended material; and hence, scour hole development described by Equations 36, 37, and 38 may not occur at quite as rapid a rate as indicated. Also, scaling relations from model to prototype are not well established for scouring of sand-bed models. Neill (1964) has stated that although fixed-boundary models are widely used with great success in the design of hydraulic structures, loose-boundary models are still in their infancy and present great difficulties in scaling. Movable-bed models are extremely valuable for visualizing processes, gaining qualitative knowledge about sediment motion, and understanding relative effects of different test arrangements. However, there is

little agreement among hydraulic engineers regarding the proper methods of scaling scour depths from model to prototype, and the results of using different proposed methods vary widely.

63. In investigations of the similarity of prototype scour to sediment motion during model tests, Yalin (1959) showed that the Froude time scale (the time scale based on gravity being the dominate force balancing inertia) is valid only when the sand used in the model has a characteristic diameter of at least 1.8 mm and, furthermore, that the relative densities of bed material should be the same between model and prototype. Dietz (1976) further determined that scale effects produce a nonlinearity of a nature such that small model scour should be scaled up with a smaller ratio than large model scour. Scale factors for the scour depths are not identical with the geometric scale factor; and, scour depths measured in the model must be scaled up with a substantially smaller factor than the geometric scale.

64. Model tests conducted at the U. S. Army Engineer Waterways Experiment Station (WES) by Murphy (1971) have demonstrated advantages of preforming a scour hole below dams and reservoirs so the flow can expand and dissipate its excess energy in turbulence rather than in a direct attack on the channel bottom. This makes it possible to stabilize the channel with rock of an economical size since the construction can be accomplished in a dry situation, and the necessary equipment will already be at the construction site. Also, the preformed scour hole need not be as large as that which would naturally occur under existing prototype hydrodynamic conditions.

Sediment transport scour

65. Sediment transport scour is generally considered to be scour that occurs around structures erected in sediment-laden streams and especially structures erected in rivers which experience significant flood wave passage. The scour limit is reached when the capacity for transport of sediment out of the scour hole becomes equal to the supply of sediment into the hole. Two significant types of scour problems exist which are of great economic importance: (a) scour around vertical, cylindrical piling and (b) scour around highway embankments and

spur dikes at bridges. These two situations are strongly influenced by flow patterns, including vortices and separation generated by the obstructions. The process is heavily dependent on the flow field in the immediate vicinity of the obstruction, and thus knowledge of the redistribution of energy over the region is necessary for understanding the character of the scour.

66. Vertical cylindrical piling. When a vertical cylindrical piling is placed in a steady unidirectional flow field, velocities and accelerations are altered near the vicinity of the piling; and the resulting forces are sufficient to initiate sediment motion around the base of the structure. For potential flow (flow without a velocity gradient in the vertical plane), a stagnation line will occur on the upstream face of the piling. However, since all streamlines will have the same velocity, the stagnation pressure for all streamlines will be the same; and flow will occur in a horizontal plane around the piling.

67. In real fluids, potential flow theory is not applicable in the immediate neighborhood of boundaries; hence, a velocity gradient is generated and all streamlines have different velocities of approach. Thus, the stagnation pressure along the vertical face of the piling will vary with a higher pressure near the surface and decrease pressure downward. The resulting pressure gradients give rise to a vertical flow of fluid along the upstream face of the piling in a downward direction which interacts with flow around the piling to produce vortices and spiral flow, schematized in Figure 7. The streamlines are no longer in any horizontal plane but converge downward toward the bed, which leads to an increase in fluid velocities in the lower layers and to an increase in mean boundary shear. This appears to be an important mechanism of local scour around vertical cylindrical piling.

68. Due to large friction forces in the boundary layer, a fluid particle consumes so much of its kinetic energy moving around the cylinder that it cannot penetrate very far into the wake behind the cylinder; consequently, flow separation takes place as vortex motion is formed and moves downstream. This circumstance completely changes the flow field in the wake; and the pressure distribution suffers a radical

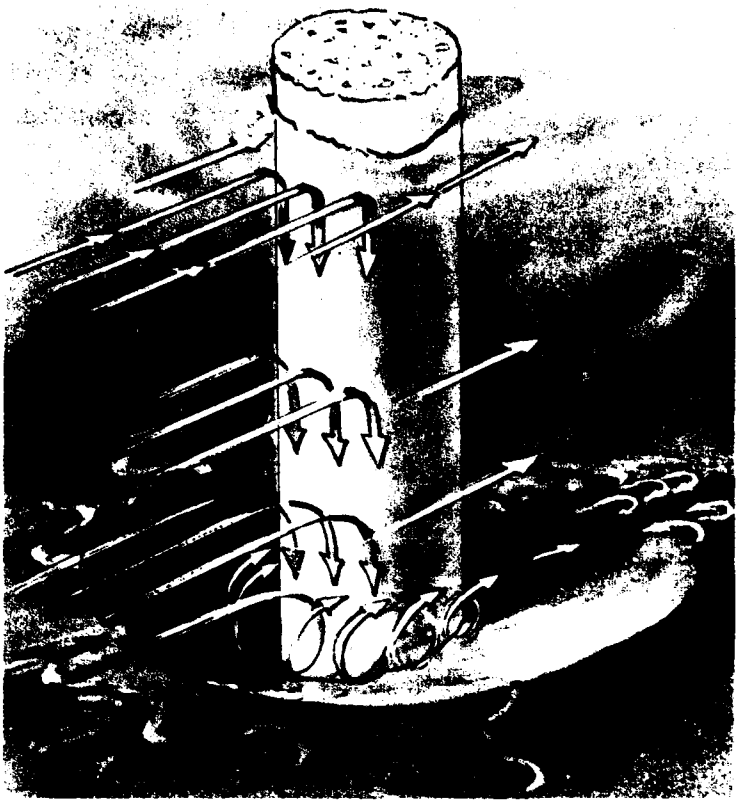

Figure 7. Unidirectional flow around a circular cylinder (after Highway Research Board 1970)

change as the eddy region behind the cylinder causes a large pressure drag on the body. A regular shedding pattern of vortices which move alternately clockwise and counterclockwise, known as the Karman vortex street, can be discerned. The separation which rolls up ahead of the base of the pile is known as the horseshoe vortex system and plays the most important role in the local scour process around the pile.

69. Some general conclusions have been agreed upon by several researchers from laboratory and field investigations, among which is the location and shape of the scour hole near a piling. For blunt piles, these holes are generally situated at the upstream side of the pile and have the form of an inverted cone with the slope of the sides equal to the angle of repose of the sediment. For streamlined piles, the location of the maximum scour is shifted downstream, and the scour hole

becomes much more shallow. The blunter the pile, the deeper the scour. The shape of the downstream side does not appear to be significant. The lateral spacing of the piles does not appear to be significant as long as scour holes do not physically overlap.

70. The influence of the approach velocity on the scour process is considered to be well known. As the free stream velocity increases from zero, scour will begin close to the pile when the average velocity of the flow field reaches a certain fraction of the critical velocity necessary to initiate motion in the absence of a structure (0.5 for circular cylinders). The scour depth then increases almost linearly with velocity until the average velocity becomes almost equal to the critical velocity. For values of velocity slightly greater than the critical, the depth of scour oscillates about a mean value (Chitale 1962); but for increased values of velocity, additional phenomena are introduced. An increased fraction of the sediments being transported goes into suspension, and a bed-form change may result. The depth of scour d_s varies as

$$d_s = b^{\alpha} \tag{39}$$

where

b = width of the pile

α = shape factor which varies from 0.62 to 1.00, depending upon the researcher and the pile shape

71. Hjorth (1975) has experimented with circular cylinders, and it was found that for velocities slightly higher than that necessary to cause incipient motion, sediment movement was most pronounced downstream of the cylinder. Fluid passing under the trailing vortices, into the low-pressure zone, scoured into the bed and transported sediment into the wake region. As flow velocity increased, the region of most intense motion shifted to the upstream part of the cylinder (Figure 8). The strength of the horseshoe vortex depended on the Reynolds number of the flow.

72. In order to predict scour processes expected to occur at a prototype bridge crossing Akashi Channel, Japan, Nakagawa and Suzuki

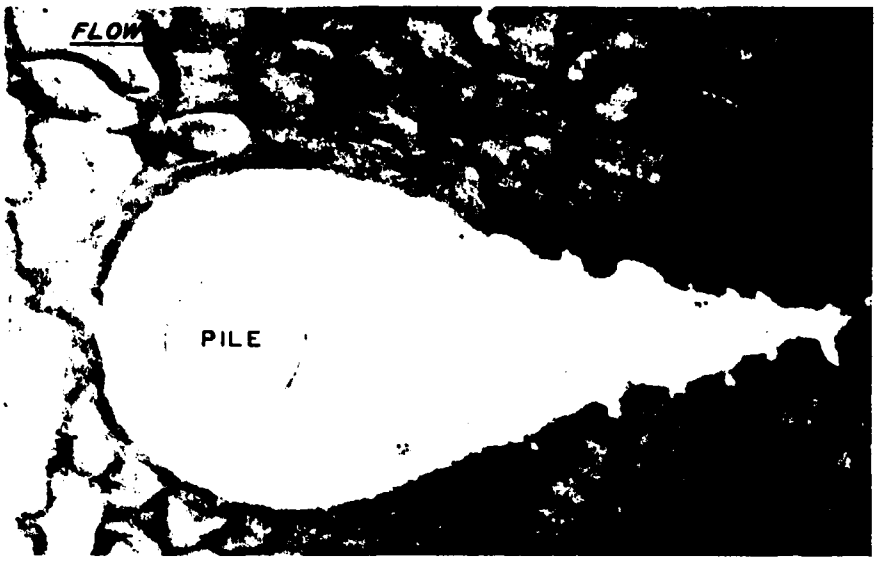

Figure 8. Scour around a vertical circular pile by unidirectional flow (after Hjorth 1975)

(1976) conducted similarity investigations by introducing a reference time defined as the time when the maximum scour depth becomes equal to the width of the bridge piers. The characteristics of this reference time were studied by systematic experiments for various scales of sand diameter, flow velocity, and pier width. Scour depth scale for the case in which the scale of sand diameter is distorted from the length scale of the pier also was investigated. Field tests were conducted by erecting a 9-m-diam vertical cylinder and comparing the results of these tests with a 1:150-scale model.

73. The problem situation investigated by Nakagawa and Suzuki (1976) was determined by strong tidal currents (about 4 m/sec). Two main piers of 40-m by 70-m rectangular cross section were to be constructed on a sand and gravel foundation. Because the periodicity of reversal of the flow process was of such long duration, it was determined that the experimental studies could be conducted with steady unidirectional flow conditions. One series of tests was conducted with steady flow in one direction, a second series consisted of the flow reversing periodically, and a third series of tests was conducted with

the piers rotated at specific angles to the steady and reversing flows.

74. The general shape of the scour hole which developed as a result of the unidirectional flow around the experimental piers is shown in Figure 9 for both the one-directional flow and for the periodic flow which reversed direction every 30 min. In the case of the one-directional flow, scour began at the upstream corners of the pier with an inverse cone shape which developed from the corners. The deposition area of the sediment shifted downstream with time. In the case of the reversing flow, the scour became deepest at the corners of the pier, and the scour and deposition were repeated according to normal and reverse flows, respectively. The maximum scour depth for the periodic flow became slightly smaller than that of the one-directional flow because of the sediment supply of the reverse flow.

75. Scour hole contour lines for the condition of the pier being rotated 30 deg with the direction of flow is shown in Figure 10. The diagonal corners became extremely scoured and their scour depths did not

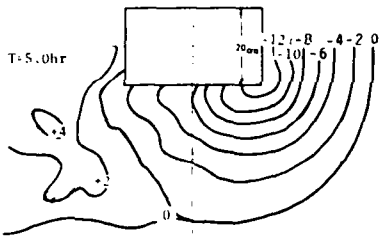

a. One-directional steady flow

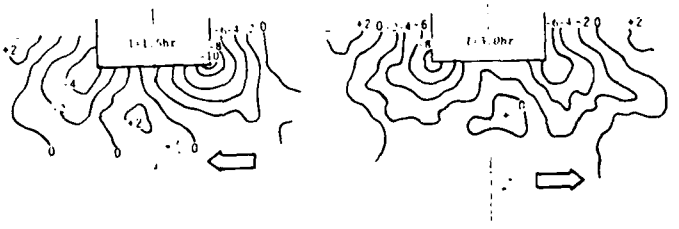

b. Reversing flow (period of reversal = 30 min)

Figure 9. Scour around a vertical rectangular pile by one-directional steady flow and by periodic reversing steady flow (after Nakagawa and Suzuki 1976)

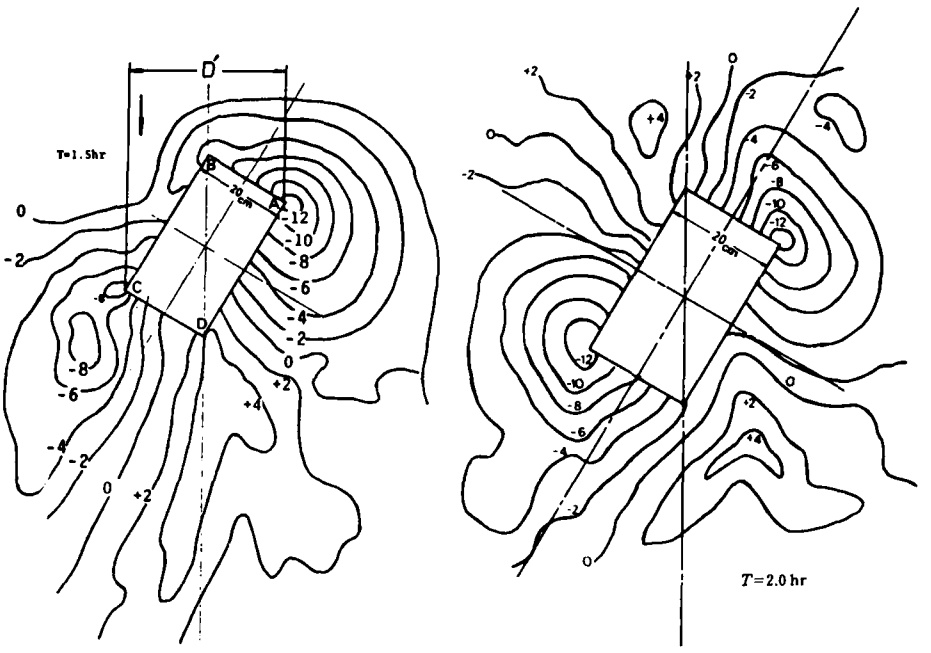

a. One-directional flow b. Reversing flow

Figure 10. Scour around a vertical rectangular pile by one-directional steady flow and by periodic reversing steady flow where the angle of rotation is 30 deg (after Nakagawa and Suzuki 1976)

become smaller even by the reverse flow. This was considerably different from the results obtained with no pier rotation. It was determined by analyzing the longitudinal and traverse profiles of the scour hole that the scour hole has a similarity with time variation, independent of grain size and pier scale.

76. The maximum scour depth d_s was found to change linearly with time t according to:

$$d_s/D = (t/t_r)^{0.22} \tag{40}$$

The reference time t_r, which is the time when $d_s = D$, is dependent on a grain diameter d, a width of pier D, and a mean flow velocity. When t_r has been determined, the time variation of the maximum scour depth can be expressed by Equation 40. The effect of the angle of

attack on the time variation of maximum scour depth is shown in Figure 11. The maximum scour depth becomes larger with the increase of the angle of attack. This is due to the increase of the apparent width of the pier with increase in angle of rotation.

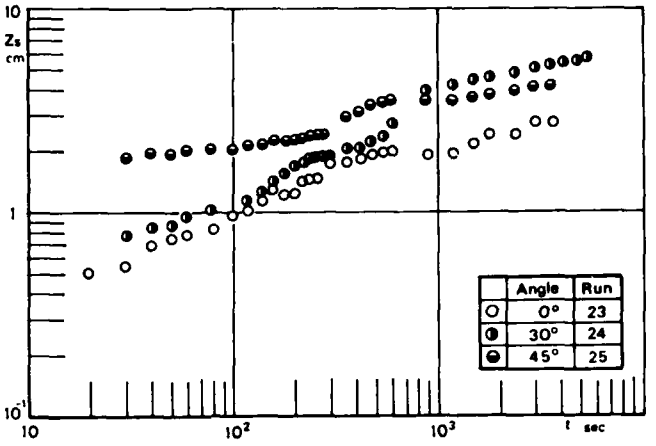

Figure 11. Time variation of maximum scour depths with different angles of attack (after Nakagawa and Suzuki 1976)

77. To obtain field data of scour depth at the location where the Akashi Channel bridge was to be constructed, a steel pile of 9-m diameter and 13.5-m length was installed in the channel. The maximum velocity of flow during the conduct of the tests was 3.5 m/sec. At the initial stage after installation, the scour depth increased rapidly; but after a few cycles of reversal of flow, the rate of scour increase was reduced so that after 100 days the scour depth was approximately 4.5 m. Scour geometry around the prototype test section is shown in Figure 12 after 100 days exposure to the natural scouring forces of the region.

78. A scour depth scale between model and prototype was investigated by Nakagawa and Suzuki (1976) by using a simple assumption when the length scale of the sand diameter is distorted from that of the flow geometry. The similarity condition for a uniform flow and that of the surface roughness should be satisfied on conditions that $u_*d/\nu > 70$ (Yalin 1971). When sand is used as a bed material for the model, this

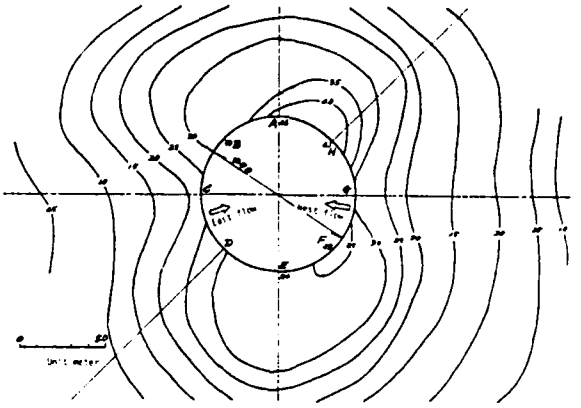

Figure 12. Scour geometry around a prototype test pile of 9-m diameter after 100 days exposure to scouring forces. Maximum velocity experienced = 3.5 m/sec, maximum scour depth = 4.5 m (after Nakagawa and Suzuki 1976)

condition is never satisfied; and if the sand diameter in the model is extremely small, it will be transported in suspension which is quite different from the motion in the prototype. When it is impractical for the horizontal scale ratio to be sufficiently large to avoid this problem, this scale effect can be overcome by choosing the scale ratio of the sand to be larger than that of the water depth such that:

$$n_{s/d} = 1/\lambda \tag{41}$$

where λ is a distortion factor of a sand scale to a flow depth scale. Under these conditions the scale ratio of the final scour depth, n_{d_s}, between a model and its prototype is expressed as:

$$n_{d_s} = n_r/\lambda^{1/2} \tag{42}$$

Experimental data displayed in Figure 13 show good agreement with the theoretical development except when λ is relatively small. When λ is small, d_s/d_o decreases with increase in the flow velocity, which

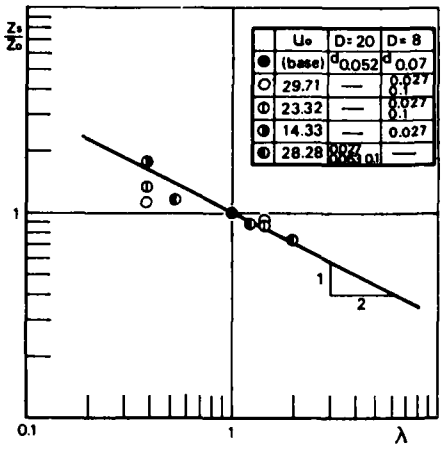

Figure 13. Relation between distortion ratio of sand to flow depth and relative scour depth, d_s/d_o (after Nakagawa and Suzuki 1976)

means that a time of sufficient length to reach the final scour depth must be allowed. When this time has elapsed, the scour depth ratio of a model to its prototype will be approximately given by Equation 42.

79. Embankments and spur dikes. When highways cross wide floodplains, embankments to support the highways are usually constructed to the river from both directions to decrease the amount of bridge necessary to span the river. These embankments severely restrict the cross-sectional area of flow for flood discharges. Flow patterns of the floodwaters are concentrated at the upstream corners of the embankments and result in a serious scour potential at the abutment (Figure 14). Physical model experiments by Laursen (1951) and Karaki (1959) have

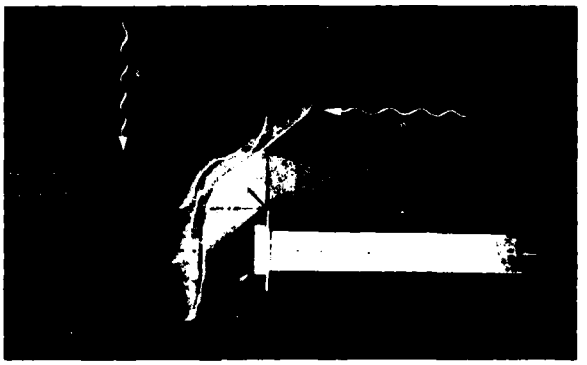

Figure 14. Relative scour depths at highway embankments (after Highway Research Board 1970)

yielded qualitative knowledge regarding this problem, although scaling limitations make it impossible to extrapolate these tests to prototype situations. However, an understanding of the basic problem provides insight which coupled with experience and engineering judgment can produce designs that minimize scour at embankments. Included in these designs are riprap protection, sheet-pile toe walls, and spur dike construction.

80. Usually, a spur dike is a nonpermeable earth embankment constructed near a bridge abutment to streamline the flow through the bridge opening. However, the dikes may be either permeable or impermeable and have been constructed of loose rock-fill timber cribs, open timber piling, or solid sheet piling. These dikes, projecting upstream from the embankment, seem to afford the optimum protection for both the embankment and for the adjacent piers. In addition to redirecting the flow parallel to the desired channel alignment, the spur dike minimizes scour at the embankment by providing a scour location at the end of the spur dike where excess kinetic energy of turbulent floodwaters can be dissipated (Figure 15). Effectiveness of a spur dike is qualitatively known to be a function of embankment geometry, flow over the floodplain, and size of bridge opening. Of all shapes tested, the elliptical shape with a 2.5 ratio of major to minor axes apparently provides the best overall results.

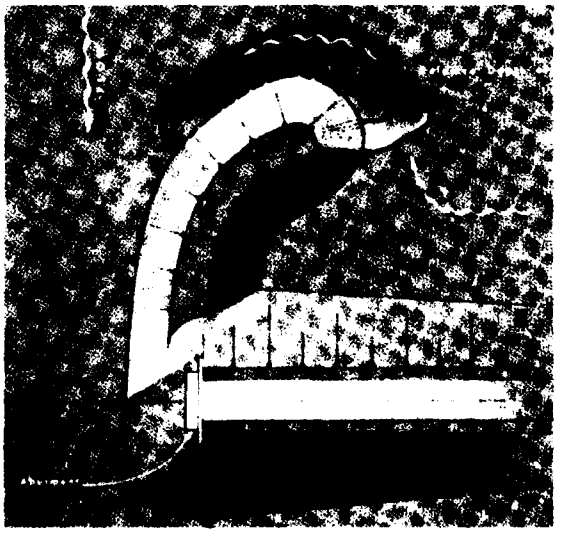

Figure 15. Spur dike construction at roadway embankment showing relocation of scour hole and relative scour depths (after Highway Research Board 1970)

81. Installation of a spur dike does not eliminate scour; it does, however, lessen the probability of severe erosion to the roadway embankment by relocating the scour upstream. The spur dike itself must be protected from erosion. This is usually accomplished by riprap placed on the upstream end of the dike.

PART IV: UNSTEADY OSCILLATORY FLOW (WAVE MOTION)

82. The ability of water waves to transport bottom sediments is related to the magnitude of the shear stress exerted by the water motion on the bed. Oscillatory fluid motion associated with surface gravity waves exerts shear stresses on the bottom that are often several times larger than shear stresses produced by unidirectional currents of the same magnitude. Thus the importance of wave motion in initiating and transporting sediments in a coastal environment is apparent. Shear stresses produced by wave motion may put sediments into suspension where they can be transported by currents of a magnitude insufficient to initiate sediment motion.

83. The mathematical description of wave motion is derived from the basic principles of conservation of mass and momentum. Conservation of mass is a statement of equality of the rate at which fluid enters and leaves a control volume. Conservation of momentum can be interpreted as an equilibrium of body and surface forces to inertia of a fluid element. Since viscous surface forces become important only in the boundary layer, the major portion of the fluid can be regarded as inviscid. The fluid is also considered to be homogeneous and incompressible; therefore a velocity potential exists, the gradient of which produces the velocity components of particle motion. Further nonlinearities exist in the dynamic free surface and bottom boundary conditions. These nonlinearities are usually eliminated by a linearization which is justified when wave height H is small relative to wave length L and water depth h. The first order approximation (linear solution) is relatively simple, and it provides a significant amount of information without unduly complicating the solution. Linear theory is applicable within a reasonable percent of uncertainty. It predicts several useful features of water waves over a range of conditions (H, L, and d) far exceeding the strict mathematical assumptions on which linearization was based. There are some features of wave motion, however, which are not well predicted by linear theory (i.e. wave breaking characteristics). Also, the linear solution indicates that water particle orbits are closed; i.e., no net

fluid motion is associated with a progressive small amplitude sinusoidal wave (Eagleson and Dean 1966).

84. Waves on the open ocean are known to have crests that are narrow and peaked, and troughs that are broad and flat. These characteristics can be described by a second order approximation (Stokes solution) in which corrective terms are added to the first order approximation. In Stokes wave theory, water particle orbits are no longer closed; and a net mass transport occurs in the direction of wave propagation. In shallow water neither the first nor higher order Stokes approximations are adequate for describing wave motion. Nonlinear Stokes theory is based on a series expansion in terms of H/L or the wave steepness; consequently, Stokes theory can be expected to be applicable for near-limit steepness waves in which the water depth is not important (i.e. large amplitude deepwater waves). Cnoidal theory, on the other hand, is based on a series expansion in terms of H/d or the relative depth; therefore, it can be expected to be applicable near depth-induced breaking wave conditions (i.e. shallow water). Cnoidal theory indicates that the wave tends to behave as a solitary wave in which the wave form is entirely above the still-water line. It should be realized that there is a zone for which neither Stokes nor cnoidal theory is satisfactory. This area is in intermediate water (i.e. $1/20 \lesssim d/L \lesssim 1/2$ (Sorensen 1978)). In the absence of other theories, Stokes theory is more applicable on the deeper portion and cnoidal theory is more applicable on the shallower portion of this interval. Other types of nonlinear theory may be more applicable in this interval (i.e. Boussinesq theory and other nonlinear wave theories (Whalin 1976)).

85. The inviscid assumption provides a solution having a finite value of velocity at the bottom for waves in intermediate or shallow water. Real fluids, on the other hand, require a no-slip boundary condition which implies significant shear stresses at the bottom. The portion of the fluid motion of interest from the standpoint of wave-sediment interaction is the flow in the immediate vicinity of the boundary. Within the boundary layer, the velocity decreases from the value predicted by potential theory to zero at the bed; and the thickness of

this layer depends on wave period. Maximum bottom shear stress is related to the square of the velocity by a wave friction factor which, for turbulent flow, is a function of the relative bottom roughness but not wave Reynolds number, and can be obtained from published friction factor diagrams, for example Jonsson (1965).

Wave Boundary Layer Flow

86. The principal characteristic of the oscillating boundary layer is that the motion is unsteady, being periodic in both time and space. In unidirectional riverflow, the boundary layer develops throughout the water column. For oscillatory waves, velocity changes direction before the boundary layer reaches the free surface. Hence, the flow never becomes fully developed and viscous effects are, for wind waves, limited to a region very near the bottom. Outside the boundary layer viscous effects are negligible, and potential theory is applicable. Within the thin boundary layer, velocity is primarily horizontal and decreases from its free stream value at the top of the boundary layer to zero at the boundary in the case of a smooth bottom. In the natural prototype situation, the bottom is usually composed of rough, movable materials; hence, the "no-slip" bottom boundary condition is relaxed as sediment is placed in motion by oscillatory flow. It is known a priori that oscillatory boundary layers are fully rough turbulent; unfortunately, details of the fluid motion within the boundary layer can be treated analytically only as long as flow remains laminar. Therefore, knowledge of flow fields in oscillatory turbulent boundary layers is deduced mainly from empirical laboratory studies. Wave boundary layers and their relation to sediment transport have been studied by Teleki (1972) and others.

87. Some investigators, including Kalkanis (1963) and Einstein (1972), have performed laboratory studies in which a horizontal bottom is oscillated harmonically under still water. This effectively restricts the study to a long wave condition as the vertical acceleration effects are not included. The horizontal acceleration because of the

long wave motion is small compared with local accelerations of the flow near particles due to turbulence. The velocity in the laminar boundary layer is described analytically, and it is hypothesized that the same considerations apply to turbulent boundary layers. While acceleration terms are different for these two cases (laminar versus turbulent boundary layers), these small discrepancies were incurred for the sake of a much simpler experimental apparatus. The mechanics of sediment suspension in the turbulent boundary layer under oscillatory water waves has also been simulated in a swing flume by Das (1971), but here again unnatural acceleration and forces were exerted on the particles as the wave orbital effects were not included.

Rough turbulent oscillatory boundary layers

88. The thickness of the boundary layer has historically been defined as the vertical distance above the bed to that elevation where the velocity is 99 percent of the free stream velocity, for both steady and unsteady flows (Figure 16). While a mathematical definition of the

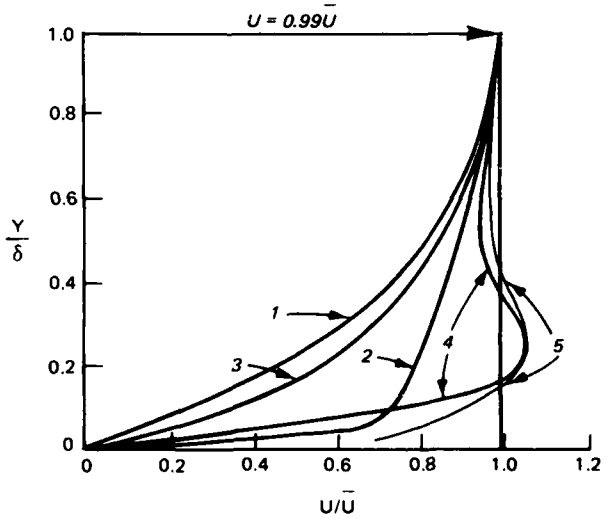

Figure 16. Typical velocity profiles in boundary layers: (a) steady laminar, (b) steady clear-water turbulent, (c) steady sediment-laden turbulent, (d) oscillatory laminar, and (e) oscillatory turbulent flow

thickness of the boundary layer does not exist, researchers have developed various definitions from assumptions regarding flow conditions in the three regimes near a smooth bottom, i.e., the laminar sublayer, the transition zone, and the turbulent layer. Schlichting (1968) has defined the oscillatory boundary layer thickness as $(2\nu/\omega)^{1/2}$ where ω is the frequency of oscillation. Jonsson (1965) considers this same thickness to extend from the bed to the elevation where the velocity first reaches its maximum value, which defines a much thinner layer than most other investigators. Proper evaluation of boundary layer thickness is important from the standpoint of a conceptual model to describe sediment movement, since shear stresses evolving from near-boundary flow are directly dependent on boundary layer velocities.

89. Many different methods have been used to formulate the boundary layer problem. Kalkanis (1963) assumed that the form of a laminar solution is preserved in the case of a turbulent wave boundary layer, and empirical coefficients were determined by experimentation and curve-fitting. Such a representation has been shown to be capable of interpretation in terms of an eddy viscosity. The studies of Horikawa and Watanabe (1968) have shown that a periodic eddy viscosity is present that is a function of depth, and Jonsson (1965) has determined values of the mean eddy viscosity which are an order of magnitude greater than those which were deduced by Kalkanis (1963). Davies and Wilkinson (1977) pointed out that a peculiar feature of the results of both Jonsson and Horikawa is that, at certain instants in the wave cycle, the calculations suggest that the eddy viscosity assumes a negative value. These negative values are explained by possible failure of their mathematical model over a rippled bed where vertical velocities, which were not included in the formulation, are present. These vertical velocities are associated with vortex formation in the lee of the ripples.

90. The formation of ripples appears to play a critical role in the problem of sediment transport in oscillatory flow. Since the potential flow problem for oscillatory flow over a rippled bed has not yet been solved analytically, it follows that the boundary layer

thickness over a rippled bed cannot be defined (even for laminar flow). Hence, the velocity profiles and bottom stress distribution over ripples are subject to considerable uncertainty. Ripples are seldom, if ever, stationary features of the bed; instead, they migrate about their mean position with a wavelength that is governed by the frequency ω and the diameter A of the particle orbit. Ripple wavelength may vary from a few inches to a few feet and constitute an effective roughness much different from the bed particle diameters. Height-to-wavelength ratio of bed particles (i.e. sand) is typically in the range of 0.1 to 0.2, and the ratio of ripple wavelength to the orbital diameter usually varies from 0.5 to 1.5. The dominant ripple is considered to be that for which the growth rate of a small disturbance is a maximum.

91. For sediment transport under oscillatory wave motion, it is the instantaneous velocity and bed shear stress that are of paramount importance because this type of sediment transport is a threshold phenomenon. Whether or not any particular theory correctly predicts the velocity precisely is dependent to a large extent on an understanding of the hydraulics of vortex shedding in the lee of bed roughness.

Friction factors for
oscillatory boundary layers

92. In steady flow it is known that shear stresses at the bottom are directly proportional to the square of the average velocity for turbulent flow. This analogy has been extended to oscillatory flows by Jonsson (1965 and 1978) to relate the maximum bottom shear stress and the maximum free stream velocity through a coefficient f_w, termed the wave friction factor, such that

$$\tau_{max} = (1/2)\ f_w\ \rho\ u_{max}^2 \tag{43}$$

For laminar boundary layers, the wave friction factor can be deduced as

$$f_w = 2/(RE)^{1/2} \tag{44}$$

where RE is the wave Reynolds number defined as

$$RE = (u_{max} A)/\nu \tag{45}$$

Here u_{max} is the maximum particle velocity at the bottom, and A is the orbital diameter, which now becomes the characteristic length scale of the viscous motion. According to Jonsson (1965), the flow remains laminar in the boundary layer only as long as RE is less than about 12,600. By this criterion, all prototype investigations will be turbulent.

93. The transition from laminar to turbulent flow also depends on the ratio of the orbital diameter A to the equivalent effective roughness of the bottom d_e. The wave friction factor concept has been used to present empirical data obtained by various investigators, by extending the analogy of steady-state friction factors for pipe flow as reflected in the Moody diagram. Jonsson (1965) found the wave friction factor f_w to be a function only of the relative roughness A/d_e for fully rough turbulent flow in the boundary layer. His wave friction factor diagram can be used through the application of Equation 40 to determine the maximum shear stress exerted by specific wave conditions if the value of the relative roughness is known. This maximum bottom shear stress associated with the wave motion is generally considerably larger than the shear stress from a steady current of the same magnitude. This emphasizes the importance of wave motion as an initiating agent which makes sediment available for transport by a current which would otherwise not be able to initiate sediment motion.

94. The wave friction factor diagram was first presented by Jonsson (1965), but it was based on very little data. Riedel, Kamphuis, and Brebner (1972) performed systematic experiments on both smooth and sand-roughened beds in an oscillating water tunnel to measure the maximum shear stress from which the wave friction factor was then computed. These data were sufficient to define the wave friction factor over the range of practical use and has been presented in Figure 17 in the same form as that of Jonsson (1965). The equivalent sand roughness for a

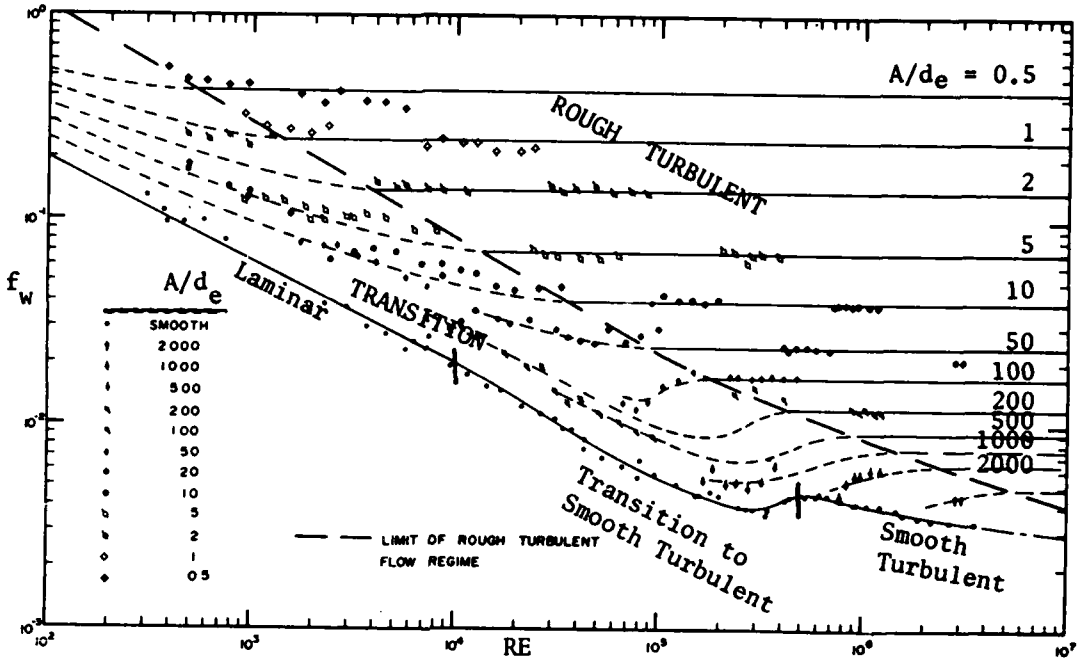

Figure 17. Experimental wave friction factors (after Riedel, Kamphuis, and Brebner 1972. By permission of American Society of Civil Engineers)

range of grain size particles was determined to be

Sand Size, d_{50}, mm	Effective Equivalent Sand Roughness, d_e, mm
0.37	1.41
1.65	8.43
3.13	15.80
9.80	51.50
50.00	139.00

95. Riedel, Kamphuis, and Brebner (1972) concluded that within the laminar range the agreement between theory and experiment was very good. The upper limit of the laminar range occurs for $RE \approx 10^4$ which corresponds approximately to the middle of the observed range of values of transition for wave flume tests. In the smooth turbulent range, the data points define a curve which lies approximately 25 percent below the predicted line. However, this difference is remarkably small considering the assumptions that were made in the derivation of the theoretical

expression. The lower limit of the smooth turbulent regime was found to be $RE = 6 \times 10^5$, which agrees quite well with the theory. For the rough turbulent flow regime, that most commonly found in nature, RE number is no longer important, and a least-squares fitting technique relates wave friction factor to roughness as follows:

$$1/\left(4.95\ f_w^{1/2}\right) + \log\left[1/\left(4\ f_w^{1/2}\right)\right] = 0.122 + \log\ (A/d_e) \qquad (46)$$

This expression is consistent with the assumption that a logarithmic velocity law exists near the bed. For $A/d_e > 25$, the orbital amplitudes are relatively large and unidirectional flow is approached; and the phase difference between the free stream velocity and the shear stress at the bed approaches zero. Hence, it was concluded that the assumption of a logarithmic velocity profile at the instant of maximum free stream velocity was reasonable.

96. The maximum value of the instantaneous bed shear stress under oscillatory wave motion has been utilized by Nielsen (1979) to evaluate the magnitude of the wave boundary layer friction factor f_w in terms of the periodic characteristics of the wave motion. The maximum value can be expressed as

$$t_{max} = \frac{1}{2}\ \rho\ f_w\ (a\omega)^2 \qquad (47)$$

where velocity of the water particle just outside the boundary layer is given by

$$u(t) = a\omega \sin \omega t \qquad (48)$$

with the wave amplitude defined as a and the wave frequency expressed as ω. Since t_{max} is proportional to the square of the water velocity, the variation of t with time can be considered as

$$t(t) = t_{max}\ |\sin \omega t|\ \sin \omega t \qquad (49)$$

97. For laminar flow the friction factor for wave motion is

$$f_w = 2\left(\nu/a^2\omega\right)^{1/2} \tag{50}$$

but for the more general turbulent cases, it was found convenient by Nielsen (1979) to use Swart's (1974) formula

$$f_w = \exp\left[5.213\left(\frac{d_e}{a}\right)^{0.194} - 5.977\right] \tag{51}$$

which is a good approximation to Jonsson's (1965) semiempirical expression. Equation 51 is applicable when the ratio of wave amplitude to roughness of the bed exceeds about 1.7. For smaller ratios, f_w has been found to remain constant at 0.28. Under these considerations, Equation 46 can be reexpressed as:

$$\frac{1}{4(f_w)^{1/2}} + \log \frac{1}{4(f_w)^{1/2}} = -0.08 + \log \frac{a}{d_e} \tag{52}$$

and is displayed in Figure 18.

98. The bed roughness has also been investigated by Nielsen (1979) and was found to be equal to the grain diameter when the bed is flat and well smoothed. When the bed is not so well smoothed, it was found to be reasonable to use

$$d_e = 2.5\ d \tag{53}$$

When the bed is covered by ripples, the total shear stress was found to be a function of both the ripple height n and the ripple length ℓ as

$$d_e = 25\ n^2/\ell \tag{54}$$

Threshold of Sediment Motion Under Wave Action

99. Considerable attention has been given to the threshold of

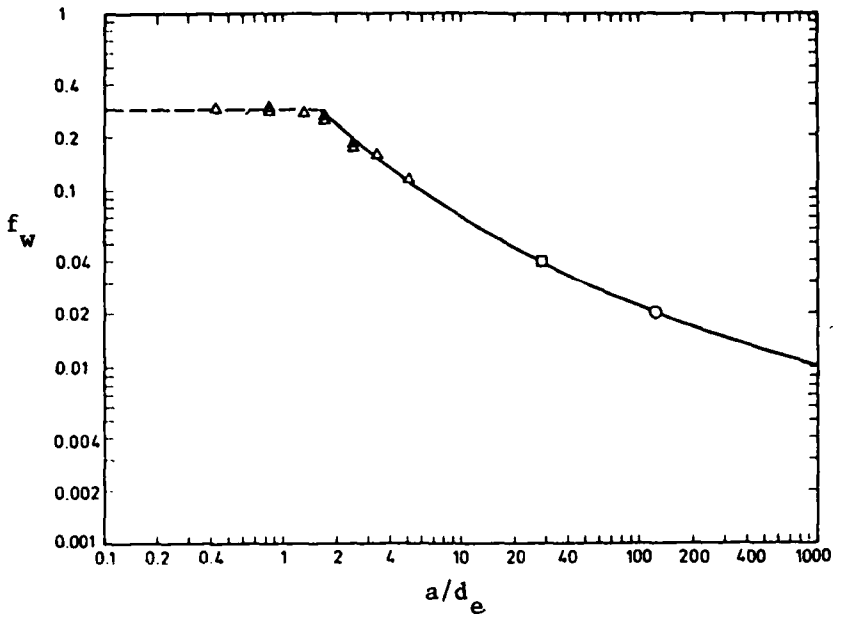

Figure 18. Wave friction factors as a function of work amplitude to bed roughness ratio (after Nielsen 1979)

sediment motion under unidirectional currents such as those found in rivers. Far less attention has been given to the threshold of sediment motion under oscillatory wind waves because of the greater measurement difficulty under the wave motion where currents are continuously varying and accelerations are important. Historically, the procedure has been to apply the curves of Hjulstrom (Figure 5) or Shields (Figure 6) for unidirectional flow to the case of the wave motion and to realize there might be some error since accelerating currents exert a greater shear stress than does a steady flow of the same magnitude.

100. Komar and Miller (1973) analyzed five sets of previously published data to determine the threshold of sediment motion under wave action. These included data by Bagnold (1946) and Manohar (1955), who oscillated a bed of sediment through still water within a tank. Besides investigating the threshold, these two studies generated ripple marks and vortex motions which seem to agree with wave channel and prototype observations. The Rance and Warren (1968) data were obtained in an

oscillating water tunnel using material as coarse as 4.8 cm. The advantage of using an oscillating bed or water tunnel is that prototype parameters can be obtained, such as period, velocities, and accelerations, although the forces resulting on the particles may not be precisely the same as those in a wave flume. Other data analyzed by Komar and Miller (1973) included that of Horikawa and Watanabe (1968), where wave heights up to 7 cm were generated with periods up to 2.19 sec. The last set of data was by Eagleson, Dean, and Peralta (1958), where the threshold of single isolated grains resting on otherwise fixed particles was investigated.

101. In the preliminary findings of this analysis, Komar and Miller (1973) concluded that application of the Shields function to define the threshold of sediment movement under oscillatory water waves could lead to considerable errors due to fundamental differences between the entrainment forces associated with an unsteady oscillatory flow and those associated with a steady unidirectional current. They displayed the experimental data of Bagnold (1946) in a diagram showing sediment grain diameter d as a function of the parameter

$$\theta_t = \frac{\rho\, u_{max}^2}{(\rho_s - \rho)\, g\, d} \tag{55}$$

Considerable scatter was found to exist which precipitated their preliminary conclusions. However, it should be emphasized that the function of Equation 55 is not the same as the Shields parameter of Figure 6.

102. Madsen and Grant (1975) and Komar and Miller (1974) independently investigated the 1973 conclusions of Komar and Miller and determined that the scatter exhibited by Bagnold's data in the first comparison was caused primarily by a difference between the parameters used for the comparison rather than by a basic difference between steady unidirectional and unsteady oscillatory flows. In fact, it was found that the data of Bagnold are in good agreement with the Shields function when plotted in a Shields diagram of bed particle Reynolds number as a function of the parameter

$$1/\psi = \frac{\tau_{max}}{(\rho_s - \rho)\ g\ d} \tag{56}$$

where τ_{max} is the maximum bottom shear stress of Equation 43. For boundary layer flows it has become customary, following Jonsson (1965), to relate the bottom shear stress to the near-bottom particle velocity through the friction factor f_w of Equation 43. The basic difference between the parameters θ_t and $1/\psi$ is the noninclusion of the friction factor in the θ_t parameter of Komar and Miller in 1973. Figure 19 is the more recent display of all the data by Komar and Miller (1974) in the form of the customary Shields diagram which includes the influence of the wave friction factor f_w. The data of Manohar (1955) plot somewhat above the Shields function, but the deviation is at most by a factor of 2, which is a deviation found even in experiments with steady unidirectional flows. Madsen and Grant (1975), therefore, concluded that the Shields function, with all its shortcomings, may serve as a relatively reliable and quite general criterion for the threshold of sediment movement under water waves.

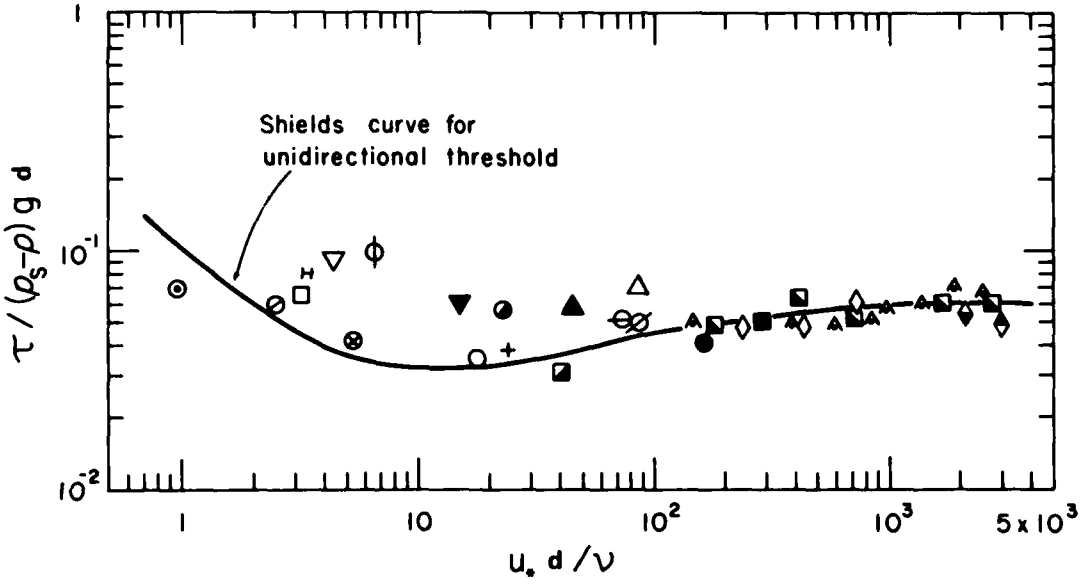

Figure 19. Comparison between the Shields curve for threshold under unidirectional currents and the threshold data for oscillatory wave motion (after Komar and Miller 1974. By permission of American Society of Civil Engineers)

103. Komar and Miller (1974) recognized that for oscillatory wave motion, the threshold of movement for a given grain diameter d and density ρ_s can be specified by a wave period T and orbital velocity at the near-bottom u_{max}. The best-fit expression for this relation is

$$\text{for } d < 0.05 \text{ cm:} \quad \rho\, u_{max}^2/(\rho_s - \rho)\, g\, d = 0.21\, (A/d)^{1/2} \tag{57}$$

$$\text{for } d > 0.05 \text{ cm:} \quad \rho\, u_{max}^2/(\rho_s - \rho)\, g\, d = 0.46\, \pi\, (A/d)^{1/4} \tag{58}$$

Equations 57 and 58 are displayed graphically in Figure 20. Since all data used in these developments came from laboratory experiments of various configurations, probably the most severe shortcoming of these results is the limited amount of prototype field data to verify these

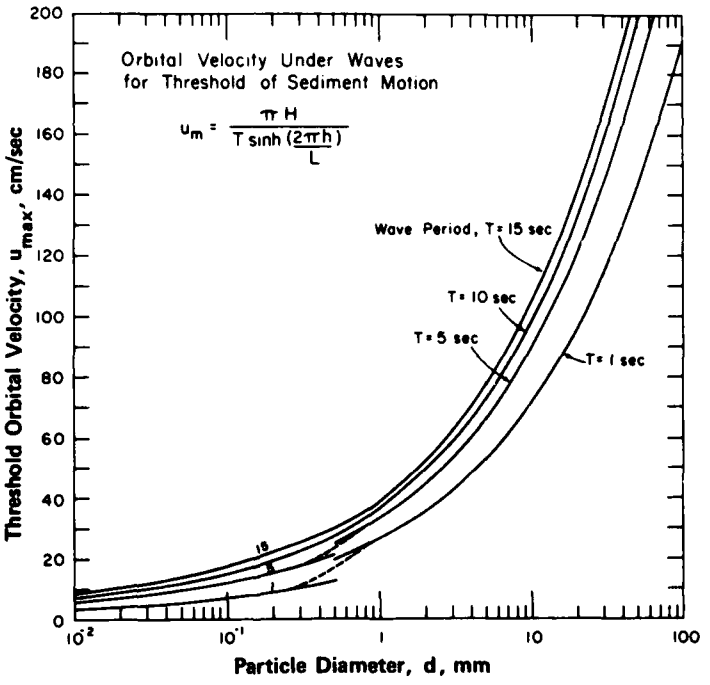

Figure 20. Near-bottom orbital velocity for threshold of sediment motion under oscillatory waves (after Komar and Miller 1974. By permission of American Society of Civil Engineers)

conclusions regarding the threshold of sediment motion under oscillatory waves. Interactions of wave trains of differing periods under natural conditions may generate instantaneously higher velocities, and sediment motion may occur at lower velocities than those implied in these analyses. Dingler and Inman (1976) studied ripples in fine sand in the field at La Jolla, California. They found that when the bottom is subjected to waves of variable height and of sufficient intensity that transition ripples occur following the passage of intermediate height waves, the larger waves will produce sheet flow and a flat bottom. As the wave conditions intensify, sediment begins to move and vortex ripples start to form. The ripples eventually reach an equilibrium configuration with a steepness of about 0.15.

104. Naheer (1979) developed an empirical relation to describe the conditions under which a rock embedded in the upper layer of a bed of similar rocks will start to move during passage of solitary waves. Rock (specific gravity 2.68) of two different diameters was tested (5.44 mm and 7.70 mm), and coal (specific gravity 1.28) of two different diameters (8.00 mm and 11.10 mm) also was investigated. The amount of motion of these four materials was measured in a wave flume and found to depend on a dimensionless shear stress similar to the Shields parameter. This slightly different parameter comprises the ratio of the hydrodynamic shear force exerted on the bed to the submerged weight of the particles. Extrapolating the curve passing through the experimental data to the point of zero motion yields the value of the dimensionless shear for which incipient motion occurs. Theoretical considerations were used to evaluate the shear stress under the waves, and the dimensionless shear was then transformed such that incipient motion could be described in terms of measurable quantities; i.e., the density and diameter of the particle, the density and depth of the water, and the wave height. Wave period has no meaning for solitary waves. The relation between these quantities can be expressed as follows:

$$\tau_{max} = \frac{K(H/y)^2(d/y)^{-0.37}}{2(\rho_s/\rho_w - 1)[1 + (H/y)]} \tag{59}$$

The empirical relation for the coefficient K is presented in Figure 21. In this figure, and in Equation 59, H is wave height, d is particle diameter, and y is still-water depth. The friction coefficient was found to be independent of Reynolds number.

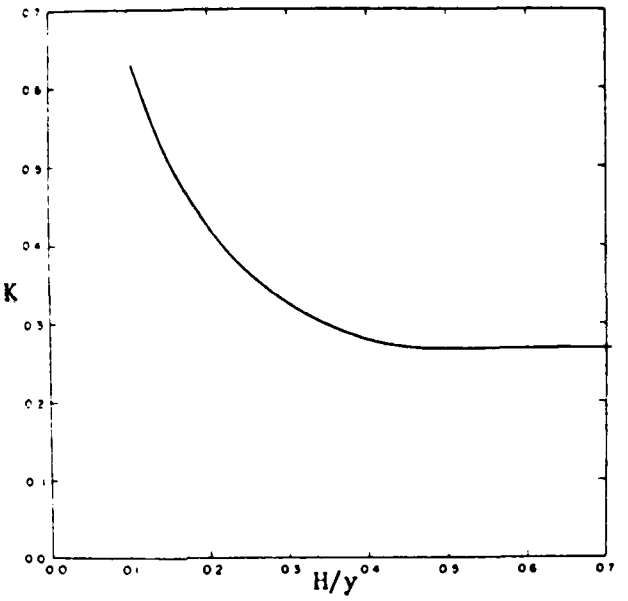

Figure 21. Empirical relation between K and H/y (after Naheer 1979)

Sediment Transport by Wave Motion

105. In steady unidirectional flow, once it is set in motion, sediment will be transported in the direction of flow. Thus in a steady current, sediment transport rate is related to flow characteristics and to the interrelationship between fluid and sediment properties. In oscillatory, unsteady flow sediment motion is much more complex, since the flow above the bed and hence the sediment transport continually varies in magnitude as well as direction. To the first-order approximation, the near-bottom fluid velocity associated with wave motion may be described by linear theory as a purely oscillatory motion. Thus, no net sediment transport is associated with the motion even if the threshold

velocity has been exceeded. However, water waves do not induce a purely sinusoidal flow near the bed. Nonlinear effects such as wave asymmetry and wave-induced mass transport currents disturb the equilibrium between the to-and-fro bottom motion, thus producing a net sediment transport. For finite amplitude waves, the wave profile is no longer symmetric about the mean free surface and wave crests become more peaked than wave troughs. Near-bottom velocities exhibit a larger forward velocity of shorter duration under the wave crests and a smaller backward velocity of longer duration under the troughs than that predicted by linear theory. Net sediment transport, then, is brought about by the small difference between large quantities of sediment moving forward and backward with the wave.

106. From the breaker zone shoreward, the complex flow patterns produced by turbulence associated with wave breaking and the return flow across the surf zone result in, at best, only a qualitative approach to sediment transport estimates. Quantitative estimates, which are only approximate at best, are based on field measurements of gross transport quantities. Seaward of the breaker zone, in relatively deep water, the sediment transport problem can be approached in a somewhat more theoretical manner. Laboratory and field observations indicate that sediment transport on the sea bottom offshore of the breaker zone is of two different types (bed load and suspended load as in unidirectional flow). The mechanism for both types of motion is the oscillatory flow near the bed induced by the wave propagation.

Bed-load transport by wave motion

107. It has been hypothesized for some time that a basic similarity exists between the motion of river sediment (unidirectional movement) and that of coastal sediment (oscillatory movement). This does not imply that the laws governing the two phenomena are exactly the same, nor that the theories of riverflow are directly applicable to wave motion. It does imply, however, that some fundamental concepts used in the derivation of one theory may be applied as a basis for derivation of the other. The Einstein (1950) analysis for sediment transport in rivers has been applied to wave-induced sediment transport. This

analysis supposes a thin moving layer between the suspended load and the fixed bed, which has come to be known as bed load. The reasoning is that very close to the bed, the scale of turbulence is so small that the eddies are the same order of magnitude as the particles and thus are unable to move the particles away from the bed. The bed layer in motion is considered to have a thickness of about two grain diameters, an estimate based on observation.

108. Kalkanis (1963) developed a semiempirical approach to the determination of bed load under wave action based on an application of Einstein's bed-load concept for unidirectional riverflow. The approach has been modified to account for the unsteady oscillations of forces and accelerations and correlated with results of certain critical experiments. Abou-Seida (1965) extended the work of Kalkanis by conducting additional experimental efforts to better define the shape of the intensity of flow and intensity of transport functions by using actual wave flume tests instead of the oscillating bed previously employed. He also introduced modifications necessary to the Kalkanis approach in order to have a general solution for the sediment transport of coarse particles as well as fine sediment. It was found that shape of sediment particles is much less important than particle size. It is therefore possible to describe the sediment by its size analysis and its fall velocity v_f. Both these researchers (Abou-Seida and Kalkanis) used plane beds in their experiments.

109. The only other known data on bed-load sediment transport rates under oscillatory waves is that provided by Manohar (1955) who undertook a study of bed-form geometry and migration using a slightly different oscillating plate. The oscillations of the sediment-carrying plate were not purely sinusoidal as asymmetric motion was achieved by changing the radian frequency. Sediment motion occurred only during the forward motion of a test, and knowledge about sediment transport rates in the presence of a rippled bed form was discernible.

110. Madsen and Grant (1976) reanalyzed the data of Kalkanis (1963) and Abou-Seida (1965) by nondimensionalizing the bed-load sediment transport rates by the fall velocity v_f and the diameter d of

an equivalent spherical sediment grain. Since the experiments analyzed were performed for an initially flat bed, the equivalent sand roughness of the boundary was taken as the sediment grain size. From knowledge of the oscillatory motions of the plate and applying Jonsson's (1965) wave friction factor, the value of the maximum boundary shear stress could be computed by Equation 43. These data are displayed in Figure 22

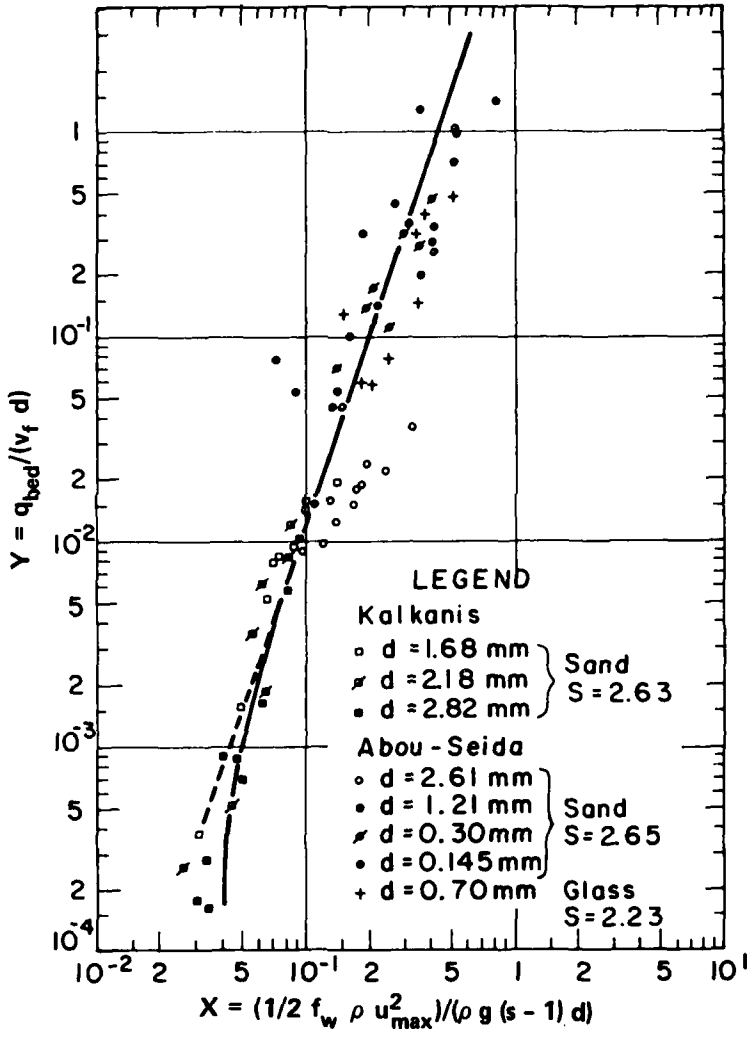

Figure 22. Empirical relation for bed-load transport by waves on a plane bed (after Madsen and Grant 1976. By permission of American Society of Civil Engineers)

and indicate a rather well-defined functional relation between the two parameters of the type

$$Y \propto X^3$$

The constant of proportionality was evaluated by taking the instantaneous values of the sediment transport function and the instantaneous value of the Shields parameter under the basic assumption that the response time of the rate of sediment transport is short relative to the time it takes for the Shields parameter to change appreciably. Ultimately, the solution was obtained as

$$Y = 12.5\ X^3 \tag{60}$$

111. The data from Manohar (1955) were treated in a similar manner by Madsen and Grant (1976) but were displayed separately because of the rippled bed that developed in some of the experiments. This display is presented in Figure 23. The bed remained flat in some of the tests since the ripples formed only for a certain range of values of the transporting force. For small values of shear stress, the sediment transport was insufficient to cause development of bed forms whereas the sediment transport was so intense at high shear stress values that bed forms were completely washed away.

112. While there is apparently no general agreement among nearshore prototype investigators regarding the vertical extent of the bed-load layer, Downing (1977) suggested that the bed layer extends about 10 grain diameters above the bed of stationary material. Above this level, the grains are transported by suspension mechanisms. Three approaches presently can be undertaken to determine the rate of bed-load movement in the field based on this criterion: (a) bed-load traps, (b) tracer studies, and (c) bed-form migration studies.

113. Bed-load traps. The bed-load trap has been used extensively in the laboratory but less frequently in the field. The device consists of a receptacle with an opening or grating configured so that moving grains in the vicinity of the device decelerate and fall into a collector. In the field the traps used by Cook and Gorsline (1972) were

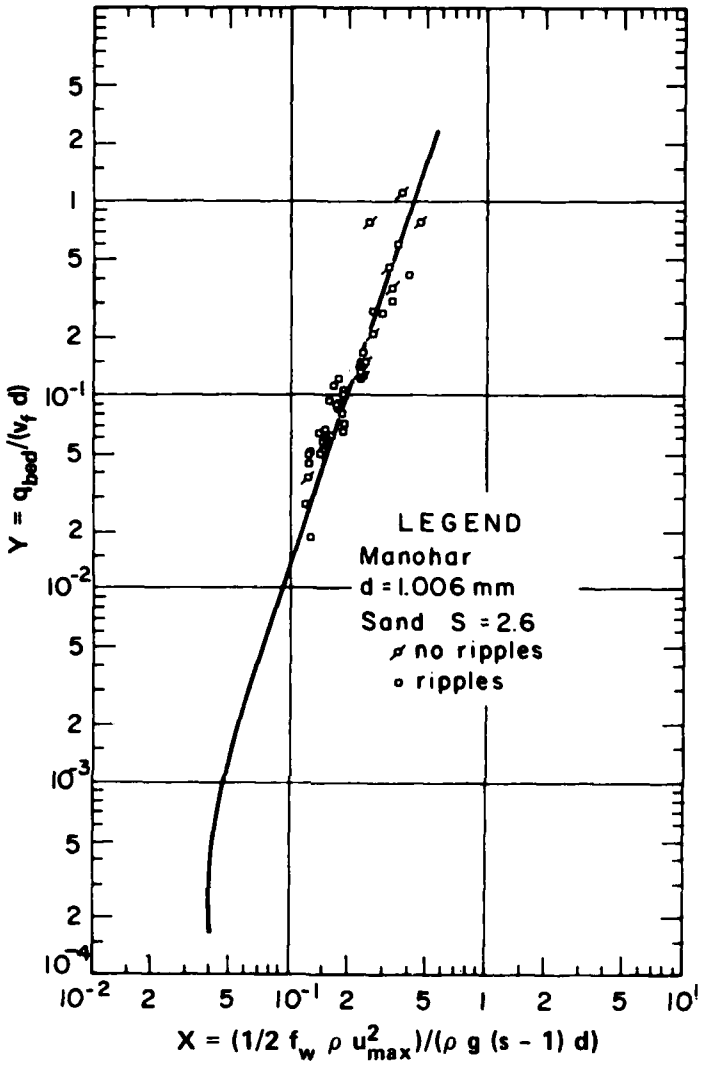

Figure 23. Empirical relation for bed-load transport by waves on a plane or rippled bed (after Madsen and Grant 1976. By permission of American Society of Civil Engineers)

planted by divers and consisted of two configurations so that grains moving onshore and offshore could be separated. Typical field sampling times ranged from 1 to 4 hr.

114. Tracer studies. Unanimity does not exist among researchers regarding the proportion of bed load that is measured by tracers;

however, all tracer investigations require the same basic assumptions: the labeled grains have dynamic characteristics identical with those of the bed material, transport occurs in a mobile layer of constant thickness, and the areal distribution of labeled grains on the surface is identical with the tracer distribution in the entire volume of the mobile layer. Radioisotopic and fluorescent materials are predominantly used at the present time, and either a space integration method (Lagrangian) or a time integration method (Eulerian) can be used. There are two major advantages with radioactive labeling of tracer materials. Unlike fluorescent tagged sand, radioactive sand is rapidly detectable in situ. Also, submersible detectors are capable of surveying a large study area almost synoptically, and thus a larger proportion of the dispersal area can be sampled.

115. Bed-form migration studies. Field evidence by Dingler and Inman (1976) indicates that ripples under shoaling gravity waves migrate in the direction of wave propagation, i.e. onshore. However, previous flume experiments by Inman and Bowen (1963) suggest that ripples under waves superposed on even small currents flowing in the direction of wave propagation can migrate in the direction opposite to wave propagation. It is apparent that the process of sediment transport near a rippled bed under the influence of both oscillatory waves and a current is not totally understood. Since ripples and sheet flow can coexist under a wide range of conditions, time series data of bed-form topography should not necessarily be considered overly reliable for the prediction of bed-load transport rates.

Suspended load transport by wave motion

116. In unidirectional fully developed turbulent flow in rivers, the steady-state, one-dimensional mass balance equation between the downward flux of material due to gravity and the upward flux due to turbulent exchange, together with the linear turbulent shear stress distribution and logarithmic velocity profile, are used to describe the distribution of suspended sediment. However, in an oscillating flow field under the action of surface gravity waves, the mechanics of

suspension are far more complex. The turbulent shear stress is periodic in time and space, and homogeneity does not exist in the turbulence since entrainment is intermittent due to the oscillatory nature of the flow in the presence of vortex shedding. The intensity of the vertical turbulent velocity fluctuations decays with distance above the bed and, therefore, the suspension is confined to a relatively narrow zone. The diffusion coefficients are dependent on the Reynolds stresses; and outside the boundary layer where the turbulent fluctuations are uncorrelated, the excursion length of the vertical component of velocity fluctuations governs the suspension mechanisms.

117. Laboratory experiments have been performed by Das (1971) and MacDonald (1973) to develop, from an empirical approach, a method for predicting the distribution of suspended sediment concentration based on the hydraulic flow conditions; i.e. surface wave amplitude and period, water depth, sediment characteristics, and bottom roughness. As in Kalkanis' bed-load function, the approach to the suspended load analysis was based on principles advanced by Einstein for suspended load transport in unidirectional flow. Laboratory and field observations by MacDonald (1973) indicate that suspension of sediment occurs to heights considerably above the boundary layer in an area where the shear stresses due to the oscillating motion are extremely small and difficult to measure. MacDonald (1973) concluded that any sediment exchange coefficient hypothesized for the boundary layer would not provide a means of estimating the exchange coefficient above the boundary layer. Therefore, a sediment exchange coefficient should be conceived which is not based on a shear stress distribution. Offshore from the breaker zone, where near-bottom velocities are the same order of magnitude as the fall velocity of the particles, a momentum exchange coefficient probably does not give a good estimate of the sediment exchange coefficient. Hence, velocity fluctuations should be used in analyzing the upward turbulent flux and the downward gravitational flux of sediment, concentration distributions for various flow conditions must be measured, and sediment exchange coefficients can be determined.

118. The transfer of sediment in the vertical direction from a

region of high concentration to a region of low concentration through a unit section area is $(-1/2\ \ell_e\ v\ \partial C/\partial y)$ where ℓ_e is the mixing length for the sediment exchange, v denotes the exchange discharge through the unit area due to vertical velocity fluctuations, and C is the concentration of suspended sediment with settling velocity v_f at elevation Y. There also exists a continuous settling of particles through the unit area at a rate of $(C\ v_f)$. The equilibrium condition is

$$(C\ v_f) + (1/2\ \ell_e\ v\ \partial C/\partial y) = 0 \tag{61}$$

From the results of the specialized laboratory experiments, empirical values of the necessary parameters were determined by MacDonald (1973).

$$1/2\ \ell_e = \left[-v_f/(M\ s_o)\right]\exp(10.57\ Y) \tag{62}$$

where

$$M = 11.53\ U_o - 18.45 \tag{63}$$

and

$$s_o = 0.0885\ U_o + 0.0557 \tag{64}$$

U_o is the average velocity of flow in the laboratory flume. It was found that the concentration distribution in oscillating flow could be expressed

$$C/C_o = \exp(M\ Y) \tag{65}$$

The base concentration C_o had been previously determined by Kalkanis (1963) as

$$C_o = (0.618\ q_{bed})/(2\ d\ u_{max}) \tag{66}$$

and q_{bed} can be determined from Figure 22.

119. Suspended solids in either the laboratory or field situation

can be measured directly by mechanical sampling devices or indirectly with sensing instrumentation based on a variety of physical principles.

120. Mechanical sampling devices. Mechanical samplers currently used in the nearshore environment are of the point integrating and instantaneous types. Both types take a bulk volume sample; the latter does so rapidly (in less than a few seconds) while the former samples at a fixed point over an extended time period (greater than 10 sec). Suspended material has a wide range of dynamic characteristics, and much uncertainty exists regarding sampler efficiency. Some mechanical samplers must be operated by divers, but according to Downing (1977) the University of Washington has developed a sampler that takes a core of the otherwise undisturbed suspension by thrusting a rigid cylinder around the sample volume, and this instrument has been used in both the surf and swash zone. However, the support frame and closure mechanism are prohibitively large, and thus the sampler cannot be used near current meters. Most surf zone suspended sediment data have been acquired with point-integrating samplers. Laboratory studies have indicated that the efficiency of samplers which draw a volume of suspension through a nozzle is greatly affected by the angle between the nozzle axis and the mean flow direction. Vial traps appear to be a useful means of obtaining time-averaged vertical profiles of suspended sediment concentration. Since the efficiency of these devices has not been accurately determined at various levels of turbulence intensity, it may not be clear what percent of the suspended load is actually being measured.

121. Indirect sensing devices. Photoelectric transmission meters and electrical-resistance particle counters have been used in many flume studies of sediment suspension under waves. An integrated light scatter-transmission meter has been developed by the Scripps Institution of Oceanography (Downing 1977), and has been calibrated in a turbidity tank and deployed in the field for preliminary testing. Because of its rugged construction and compact geometry, the instrument appears to produce minimal distortion of the velocity field. The major deficiency of both scatter and transmission type electro-optical instruments is their inability to distinguish between the many types of suspended particles

encountered in nearshore waters. Hence, quantitative results are uncertain at this time, although a variety of instrument systems are currently in use by the medical profession that operate in the ultrasonic frequency range and are potentially applicable to the suspended sediment measurement problem.

122. Field investigation. Suspended sediment concentration was measured in 235 breaking waves on undeveloped beaches near Price Inlet, South Carolina, by Kana (1978 and 1979) using portable in situ bulk water samplers. The purpose of the study was to determine what factors control the distribution of suspended sediment in the breaker zone. As many as 10 instantaneous 2-litre water volumes were obtained in each wave for a total of 1500 samples. Concentrations of suspended sediment were determined at fixed intervals of 10, 30, 60, and 100 cm above the bed for various surf zone positions relative to the breakpoint. The majority of waves sampled during 22 days in June and July 1977 were relatively long-crested, smooth, spilling-to-plunging in form, with breaker heights ranging from 20 to 150 cm. The beaches sampled were gently sloping (mean beach slope = 0.015), fine-grained (mean grain size = 0.18 mm), and densely compacted with an absence of small-scale bed forms.

123. Suspended sediment in the breaker zone was found to be composed of two fractions: a continuous wash load mode above 60 cm from the bed, and an intermittent mode of coarse bed material entrained to lower levels during certain wave conditions. Mean concentration decreased exponentially above the bed to approximately the 60-cm elevation, then maintained a generally constant level up to the water surface. Suspended sediment concentration at the study sites ranged over three orders of magnitude up to approximately 10 grams per liter.

124. The principal factor controlling suspended sediment concentration at a point in the breaker zone is the breaker type according to Kana (1978). Plunging waves typically entrained one order of magnitude more sediment than spilling breakers. Breaker type for these data could be reasonably quantified as a continuous variable on the basis of relative wave height, d_b/H_b . Plunging waves near Price Inlet occurred at

$d_b/H_b < 0.89$, whereas spilling waves generally broke at $d_b/H_b > 1.10$. Mean concentration increased with decreasing d_b/H_b according to:

$$\text{Log}_{10}(SS_{10}) = 17.4 - 1.7\ (d_b/H_b) \tag{67}$$

where SS_{10} indicates suspended sediment concentration at 10 cm above the bed. This theorized model accounted for almost 60 percent of the variation in mean concentration by d_b/H_b .

125. Secondary controlling factors of concentration also included distance relative to the wave breakpoint, beach slope, and wave height. Mean suspended sediment in the breaker zone reached a maximum several metres landward of the breaker line, peaking more sharply in plunging than in spilling waves. For the range of slopes in the study (0.004 to 0.040), mean concentration increased according to:

$$\text{Log}_{10}(SS_{10}) = 0.22 + 14.5\ m \tag{68}$$

where m is the beach slope.

126. The relation between wave height and concentration depended on breaker type. There appeared to be little or no dependency of concentration on wave height for spilling waves. However, for plunging waves, suspended sediment concentration at a point decreased with increasing wave height.

127. For the Kana (1978) data collected under moderate swell conditions, suspended sediment concentration was independent of wave period, longshore current velocity, wind velocity, and any breaker-type parameter involving wave steepness H_b/L_o . Kana's (1978) conclusions were that although the amount of variation in mean concentration accounted for only up to 65 percent, these data support the notion that sediment suspension in the surf zone is statistically predictable. The importance of breaker type on concentration suggests that transport of sand in the surf zone is less dependent on wave height and wave steepness than on relative wave height d_b/H_b .

Onshore-offshore movement

128. Johnson (1949), and other investigators, have long recognized two distinct classifications of beach profiles: (a) summer profiles with wide, flat beaches and (b) winter profiles with narrow, steep beaches. It was found that incident deepwater wave steepness was the principal factor in determining which type of equilibrium profile would be attained. When $H_o/L_o < 0.025$, material is carried in the onshore direction, flattening out the offshore region and building up the region near and beyond the breaker. When $H_o/L_o > 0.025$, material moves in the offshore direction, removing sand from the breaker region and depositing it in the offshore area.

129. Prototype field studies have been performed by Nordstrom and Inman (1975) where the principal objective was to measure beach profiles along a straight beach with uncomplicated offshore bathymetry that is exposed to ocean waves from all offshore directions. Emphasis was placed upon the accurate measurement of beach profiles in order to determine changes in profile configuration caused by wave action. Profiles were measured from the beach backshore seaward to a depth of about 18 m at monthly intervals for a period of 23 months. Additional measurements were made following storms and periods of high waves in order to document the extent of profile modification associated with storms and/or high waves. Comparison of the profiles from month to month and seasonally was made to determine the erosional and depositional parts of the profile and the volumes of sand involved in onshore-offshore transport.

130. Conclusions reached from these field studies off the coast of southern California include the fact that all significant changes in beach profile configuration can be related to the incident waves, tides, and local storms with strong onshore winds. Formation of a summer profile configuration is the result of a progressive onshore migration of sand from depths of less than 33 m that accretes on the beach face. The summer beach profile is characterized by a pronounced berm crest that is produced by the progressive accretion of sand starting as a bar at depths of 1 m. The summer beach profile at this particular location did

not fully develop until October when the berm crest was prograded the farthest seaward and beach face slope was the steepest. The change from summer to winter profile began to occur in November. At the time of high waves and tides, the summer profile berm crest was easily overtopped by wave runup and the upper foreshore quickly eroded. Most of the sand transported offshore during the winter seasonal change was removed from the beach face during the few days when high waves and tides were coincident. This sand which was transported offshore was deposited in depths of from 3 to 9 m. There was no detectable sand level change at depths greater than about 14 m.

PART V: SCOUR BY WAVE ACTION

131. Coastal and offshore structures are susceptible to continual attack by waves and closely related current action. Many failures of these structures, such as piling, seawalls and revetments, or undersea pipelines, occur as a result of excessive local scour. When an object is placed on the sea floor, the dynamic equilibrium is disturbed, local velocities increase, and additional turbulence and vortices are generated so that the flow locally obtains a greater transport capacity. Unless protected, materials around the foundations of these structures are susceptible to scour and transport by currents, thus undermining the integrity of the overall structure. This erosive action of both oscillatory waves and unidirectional currents in the coastal zone has long plagued engineers concerned with the planning, design, construction, operation, and maintenance of marine structures. Foundation scour has significantly affected the economics and service life of many coastal structures.

132. Damage and repairs to three fundamentally different types of coastal structures along the coast of North Carolina have been documented by Machemehl (1979). The Herbert C. Bonner Bridge (designed and constructed under the supervision of the North Carolina State Highway Department) spans the mile-wide unimproved Oregon Inlet which connects the Atlantic Ocean with Pamlico Sound. The combined effect of ocean waves and tidal currents caused scour depth on the order of 8 ft to occur around the piles supporting the bridge, and settlement of the bridge resulted which necessitated major repairs to the bridge. The Cape Hatteras groin field (designed and constructed by the U. S. Naval Facilities Engineering Command) on the shoreline of Hatteras Island has been a persistent problem for many years. The concrete and steel sheet pile groins have deteriorated as a result of very deep scour pockets, and major repairs are required to bring the groins to a functional level. Revetment along the shoreline of Fort Fisher State Historic Site (joint effort by State of North Carolina and U. S. Army Corps of Engineers) has experienced one of the highest rates of erosion known

to exist along this coastline. Wave action has caused substantial settlement and deterioration of the revetment, and extensive erosion of the shoreline has resulted.

133. One of the major problem areas addressed by this research effort is that of erosion at the outer end of jetties where, under flood flow conditions, the tidal current components can be advancing at 90 deg to the orbital motion produced by the wave kinematics. The resulting flow field is complex and has not been investigated either experimentally or analytically. Most scour-related laboratory investigations and field studies have been concerned with scour and erosion around piles, massive nearshore structures such as breakwaters or seawalls, or around pipelines on the sea floor.

Scour Around Vertical Piles

134. A laboratory experimental study was conducted by Abou-Seida (1963) to investigate scour patterns around some idealized structures of various geometric shapes under certain flow conditions. The structures tested included: (a) 2-in.-diam circular pile, (b) 2-in. square pile, (c) submerged 2-in.-diam hemisphere, and (d) a thin vertical plate 2 in. long placed at right angle to the direction of flow. Different experimental runs were carried out under the hydraulic conditions of: (a) a discharge large enough to cause an initial motion of bed material, (b) long and short waves with sufficient velocity at the bottom to cause an initial oscillatory motion of sand particles, and (c) a combination of these two cases, i.e., waves superposed upon a streamflow in the direction of wave propagation.

135. The observations and conclusions of Abou-Seida (1963) included the fact that under wave action alone, the flow pattern around a structure changed periodically with time, eddies formed on both sides of the piles (upstream and downstream), and thus the exact flow conditions around the structure cannot be described mathematically. The mean velocity of flow of the unidirectional current was 1.096 fps, while the maximum bottom velocity of the two waves tested was 0.15 and 0.24 fps,

respectively. It appears the steady current had a strength of from four to six times that of the wave field, and this probably accounts for the observations that scour due to the waves was much less than that due to the current alone. It was also observed that the scour was less severe in the case of long waves than with short waves. The researcher accounted for this as being the effect of the acceleration field which is larger in the case of short waves than with long waves.

136. When waves were superposed upon the streamflow, the current pattern in the vicinity of the structure was very complex. The position of the vortices changed with time, and the interaction between the vortices induced by the current at the leeward side of the structure and those induced by the oscillatory motion of the water particles seemed to reduce the scouring action of the current. It appeared that the latter eddies played a role of disturbing the scouring energy of the first ones and thus reduced the concentrated action of the vortices. The volume of scour in this case was also less than in the case of the current alone. Results of this series of tests are shown in Figure 24. The shape of the scour hole became more like that of a saucer than an inverted cone which had been produced by the unidirectional flow.

137. Field studies have been performed by Palmer (1969) to relate oceanographic parameters to the rate and magnitude of scour developed around natural and artificial obstructions to oscillatory wave-induced motions on the sea floor. The study was conducted at various sites along the coast of southern California in water depths up to 80 ft. Conclusions were based primarily upon time-lapse and real-time motion picture photography of the scour phenomena. A schematic view of the general hydrodynamic situation in the vicinity of an obstruction is shown in Figure 25 and indicates the pattern of secondary flows, or turbulence, which accounts for the removal of granular materials through the scour process. The main scouring force is the primary vortex that develops in front of the pile. Since the fluid velocity increases with increasing height above the bed, a pressure gradient is established and the result is flow downward along the upstream side of the pile. Erosion associated with the primary vortex created a flat floor within the

a. A circular pile

c. A hemisphere

b. A square pile

d. A flat plate

Figure 24. Equilibrium bed configuration due to short waves superposed on a unidirectional streamflow of magnitude U = 1.096 fps , u_{max} = 0.15 fps (after Abou-Seida 1963)

scour hole adjacent to the walls of the obstruction.

138. Secondary turbulence associated with the separation vortex formed a weak counter-vortex near the rim of the leading edge of the scour hole. Fluid at the sides of the pile accelerates to pass around the pile, and this flow maintains the transport of grains thrown into suspension by the primary vortex. Laboratory measurements reveal that the velocity in this region is about twice that of the ambient flow velocity over the sea floor. The pressure gradient at the rear of the

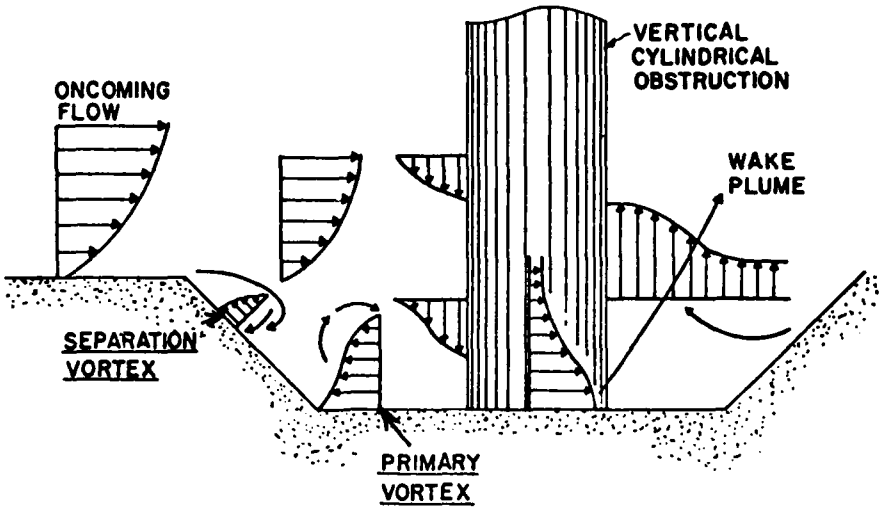

Figure 25. Schematic diagram of wave motion effects on a vertical pile, and the associated fields of turbulence (after Palmer 1969. By permission of American Society of Civil Engineers)

pile is the reverse of that developed at the upstream side. Here the pressure gradient decreases with increasing height above the bed, and this imbalance tends to lift grains out of the scour hole in a turbulent wake. Scour equilibrium is achieved for given oceanographic parameters when the volume of material removed by the vortex turbulence is matched by the volume of material introduced into the scour hole through bed and suspended loads.

139. The progressive growth of the scour hole to ultimate conditions occurred in a manner such that the bottom of the hole expanded outward at a rate equal to approximately one-half that of the scour hole rim. This continued until a critical distance of about one-half the diameter of the obstruction had been attained by the bottom of the hole, at which time the primary vortex system remained static and the rim continued to increase in circumference through slumping of the bed material.

140. Among the conclusions reached by Palmer (1969) was that the shape of the object had a significant effect on sediment transport rates early in the history of the scour, but eventually the overall object diameter became the dominant factor. Objects with a blunt or flat

surface exposed to flow will initially scour more rapidly than streamlined objects. The upper 10 percent of wave velocities measured in these field tests on the sea floor ranged from 24 to 61 cm/sec. It appeared that for this range, the scour hole diameter is independent of both velocity and grain size. Individual elements of pile clusters are initially scoured as individual obstructions; but after the scour holes coalesce, the scour hole for the cluster approaches that of a single element having a diameter of the cluster.

141. The scour around a circular pile due exclusively to wave motion was investigated experimentally in the laboratory by Wells and Sorensen (1970). They found that the critical velocity of the wave necessary to cause incipient motion was lower than that for steady-state flow, but that the ratio of the maximum velocity on the pile boundary to the free stream velocity was less than the value of 2.0 predicted by potential flow theory. The ultimate scour depth was directly related to the pile Reynolds number, and the scour pattern that resulted was primarily influenced by the pile and wave characteristics. A representative sample of their scour pattern results is presented in Figure 26.

142. Wells and Sorensen (1970) and Breusers (1972) emphasize that to predict scour depths for prototype situations from laboratory experiments was presumptuous at the time of their studies. Both geometric and dynamic similitude must exist between model and prototype for predictive equations to apply, and these requirements were far from being met under described conditions. However, from the results of these investigations, it was conjectured that the maximum scour observable in the prototype would be approximately equal to one pile diameter, which for a typical offshore drilling platform would be about 5 ft.

143. Other laboratory experiments have been performed by Machemehl and Abad (1975) to study scour around piles where surface gravity waves are superposed on a steady current flowing in the direction of the waves. They concluded that the increase of the water particle velocity in the immediate vicinity of the foundation, as the streamlines approached and divided around the pile under different conditions of wave and current velocities, was the most significant

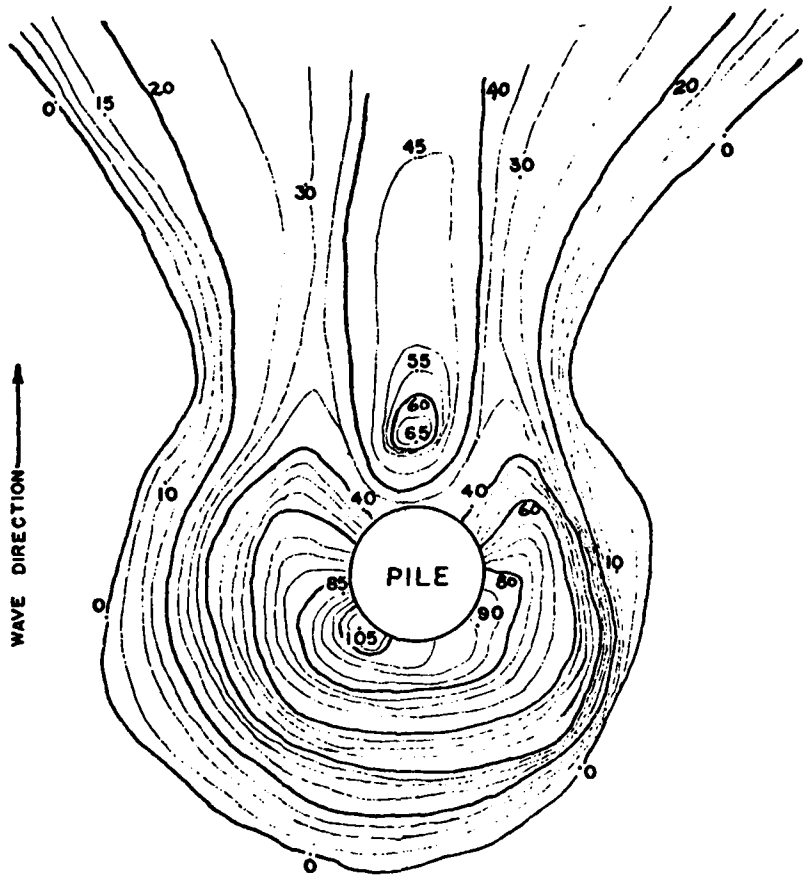

Figure 26. Scour pattern resulting from wave motion around a circular pile. Contours are feet × 1000 (after Wells and Sorensen 1970)

scouring mechanism. This phenomenon combined with the diving velocity component at the nose of the pile and the rising component at the tail, as well as with the vortex systems and eddies. The addition of oscillatory waves to the unidirectional current flow field expedited the rate of the scouring process, although the ultimate size of the scour hole appeared to be approximately the same with or without the test waves being present. The scour produced under the influence of long waves occurred at a faster rate than that produced with short waves. This may not be entirely consistent with the limited test results of Abou-Seida (1963). The greatest scour occurred at the horseshoe periphery forward of the pile, and this was attributed to the

increased velocity referred to as the horseshoe vortex.

Scour in Front of Seawalls and Around Breakwaters

144. Seawalls and breakwaters are usually built to protect a portion of a beach from scour and erosion caused by the continual breaking of waves directly on or in front of the beach face. In order to properly locate the protective structure, an estimation of the beach profile that will exist after construction of the structure is necessary and can be determined to a first approximation by experience and general guidelines. The scour that is expected to occur at the toe of such structures will develop a trough with dimensions based on the type of structure, the nature of the wave attack, and properties of the foundation. Where rubble-mound structures are concerned, the scour may be allowed for by overbuilding the structure to account for settlement into the scour hole, a stone blanket may be placed for some distance seaward of the structure toe to prevent formation of the scour hole, or excess stone may be placed on the toe to fill the anticipated scour trough. The U. S. Army Engineer Coastal Engineering Research Center (CERC) (1975) estimates that as a general guideline in a wave climate only, the maximum depth of scour in front of a structure below the unscoured natural bed is about equal to the height of the maximum unbroken wave that can be supported by the original water depth at the toe of the structure.

145. Chesnutt and Schiller (1971) simulated the scour due to wave action in front of seawalls in laboratory experiments, and in their literature review found that Russell and Inglis (1953) had studied scour in front of a vertical wall by generating a constant wave height. This required the wave period and, therefore, the wavelength to be varied as the depth varied. The ultimate scour depth was found to be about one wave height below mean low water; but because of the peculiar experimental situation involved, the results are difficult to extrapolate to more general situations. Chesnutt and Schiller (1971) discovered that the relative position of a seawall (its location between natural shoreline and the breaker line), which changes with each change in

wavelength, is as critical as the wave height in determining the amount of scour that occurs.

146. Sawaragi (1966), in his investigations of scour at the toe of permeable structures, found a relation between the void ratio of the structure, the coefficient of reflection, and depth of scour. Herbich and Ko (1968) extended the work of Sawaragi (1966) and developed a mathematical model for determining the ultimate depth of scour S as

$$S = (d - a/2)\left\{(1 - C_r)\, u_{max}\left[3/4\, C_D\, \rho\, \frac{\cot \Phi}{d_{50}\,(\gamma_s - \gamma)}\right]^{1/2} - 1\right\} \tag{69}$$

where

$$a = H_i + H_r \tag{70}$$

and

$$C_r = H_r/H_i \tag{71}$$

where

C_D = drag coefficient of a spherical particle

Φ = bed material angle of repose

H_i = incident wave height

H_r = measured reflected wave height from the structure

All experiments performed indicated there is an asymptotic limit to scour depth. Scour depth increases very rapidly during the first few hours; subsequently the erosive process slows and finally reaches a state of "ultimate" erosion.

147. Scour in front of 30-, 60-, and 90-deg seawalls was studied by Sato, Tanaka, and Irie (1968), for both normal and storm beach profiles, using several grain sizes. After an equilibrium beach profile had been established, a seawall was introduced into a model; and five types of scour were observed and the mechanism producing each type was defined. They found that maximum scour depth would probably be no greater than the deepwater wave height which produced the scour. Also, the reflected wave was found to be a significant parameter in addition to the still-water depth. Along breakwaters or jetties, the toe of the

structures was scoured severely where the structure crossed the longshore bar, and at the tip of the structure. In a field situation, agitation due to waves breaking on the structure and the wave-induced currents around the structure play an important role in the scouring process.

148. Caisson-type structures exposed to wave action were experimentally investigated by Donnelly and Boivin (1968), and they determined that the most vulnerable part, from the standpoint of foundation erosion, is at joints between abutting caissons. For direct wave attacks, the velocity through the open joint can be estimated approximately as

$$V = 1.25\ (2\ \pi\ H/T)(1/\sinh\ 2\pi d/L) \tag{72}$$

Unless the material in the joint is coarse enough to resist this scouring velocity, erosion problems will likely occur. In practice, joints between abutting caissons should be effectively sealed if erosion problems are to be avoided. To seal the joints, two key placements are necessary: (a) one on the seaward side of the structure and (b) one on the harbor side. The height of the granular fill required to prevent erosion is

$$h = 2\ H/\cosh\ 2\pi d/L \tag{73}$$

For coarser types of gravel fill with suitable filters, the height given by Equation 73 can be reduced by up to 30 percent.

149. Recently, the construction of permeable detached breakwater systems of concrete blocks has become widely practiced as a countermeasure against beach erosion in Japan. Most of these breakwaters function effectively; however, there are occasional reports of erosion caused by local scour and wave-induced currents around the breakwaters. Experiments were conducted by Hotta and Marui (1976) to investigate characteristics of the local scour; and it was found that local scour and beach change exist simultaneously. That is, the local scour is superposed upon larger scale changes in bathymetry and there is a complicated interaction. A lightweight concrete aggregate with specific

gravity of 1.65 was used in their movable-bed studies, and it was found that the maximum scour depth varied from 0.6 to 1.0 times the initial wave height for different wave characteristics. The scouring depths were found to be greatest at X/X_b = 38 percent where X_b is the distance from the shoreline to the point where the wave breaks.

150. On the basis of laboratory experimental studies, Song and Schiller (1973) developed a semilogarithmic regression model that predicts relative scour depth S/H_o as a function of relative seawall distance X/X_b and deepwater standing wave steepness H_s/L_s and is given as

$$S/H_o = 1.94 + 0.57 \ln(X/X_b) + 0.72 \ln(H_s/L_s) \quad (74)$$

This expression is displayed in Figure 27, where it can be observed that for larger values of deepwater standing wave steepness, the relative scour depth is dependent upon the seawall position; but for small values

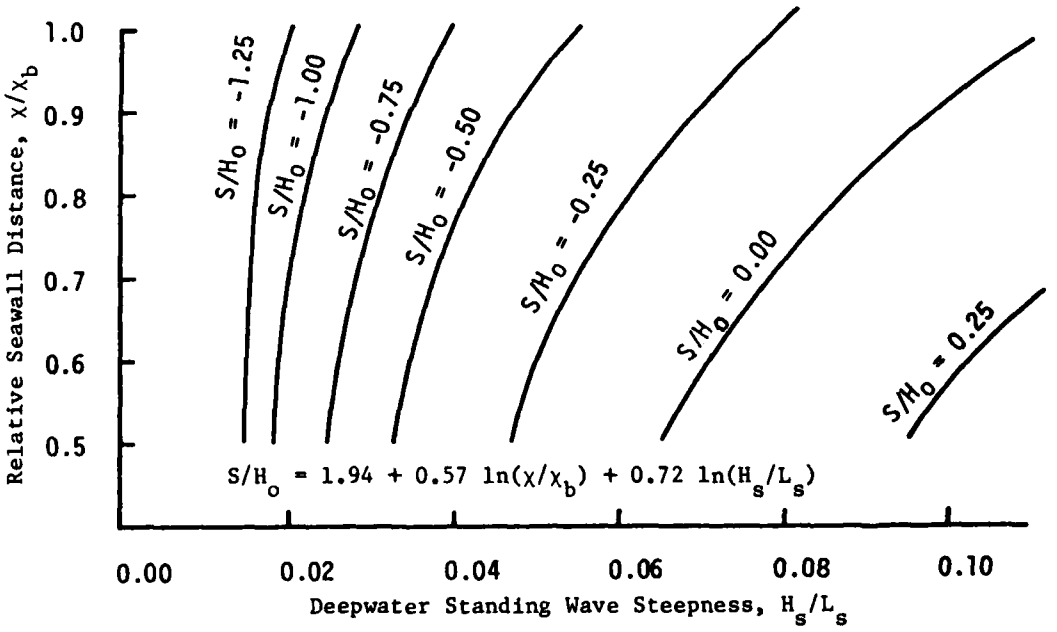

Figure 27. Variation of relative scour depth with relative seawall distance and deepwater standing wave steepness. Semilogarithmic multiple regression analysis, correlation coefficient (r^2) = 0.84 (after Song and Schiller 1973)

of deepwater standing wave steepness, the relative scour depth is nearly independent of seawall location.

Scour Around Pipelines

151. Oil and gas from offshore production platforms are often transported by pipeline lying on or imbedded in the sea floor. Another widespread application of pipelines in the coastal zone involves the disposal of municipal and industrial waste in deep water of both lakes and oceans. The size, number, and application of these offshore pipelines are steadily increasing, and at the same time the incidence of reported pipeline failures is also increasing. One basic reason for many of the failures is inadequate cover over the pipe, which may indicate that the depth of burial was insufficient, the type of burial material may have been inferior to the bed material, or the compaction of the cover material may have been inadequate. Other failures have occurred because the pipeline actually floated up to the surface as the cover material liquefied, or because the pipeline sank deeper into the liquefaction. Localized scour problems can occur when water seeping through a leaking joint washes the surrounding material away and a small hole is created under the pipe. Underflow caused by crosscurrents may then enlarge this hole laterally until the pipeline loses its support and collapses. Also, currents along the pipe will be disturbed by the joints, and the vortices thus created may erode the bed in the neighborhood of the joints.

152. From studies of unidirectional flow over pipelines lying on the bed, exposed, and placed perpendicular to the flow, certain fundamental characteristics of the flow can be ascertained. The approach flow can be considered to have a vertical velocity variation corresponding to the boundary over a rough plate. The effect of the pressure field induced by the presence of the pipe is to decrease the approach flow velocities near the bed. At some point, the adverse pressure gradient becomes strong enough to cause separation of the approach flow. The location of this point of separation varies with inherent velocity

and pressure fluctuations. Downstream from the pipe, the flow reattaches to the boundary at some point which also fluctuates about some average position.

153. A characteristic flow feature is the development of three vortices: (a) under the upstream separation surface, (b) downstream but near the pipe, and (c) farther downstream under the surface of separation. The distance from the pipe to the upstream line of separation is approximately equal to the height of the pipe crest over the general bed surface. The distance from the pipe to the downstream reattachment line is approximately six times the height of the pipe crest. The upstream vortex is supposed to be nearly circular, according to Hjorth (1975), while the downstream primary vortex has a length-to-width ratio of about five. Experiments by this researcher indicated that the mean pressure drop over the pipe is about $1/2\ \rho\ U^2$ for an uncovered pipe resting on the bottom, and about $2/5\ \rho\ U^2$ for a pipe halfway buried into the bed.

154. In addition to experiencing the aforementioned effects, an offshore pipeline must have sufficient horizontal and vertical stability against all imposed forces. The gravitational forces include the weight of the pipe and of the materials being transported inside the pipe. The environmental forces are quite complex and variable and include those due to storm or hurricane waves, vortex shedding, seismic loads, and foundation strength. Since forces due to waves may be considerable, particularly in shallow water, one solution is to place the pipeline in an excavated trench and cover with suitable material up to the original beach profile. The depth of the required cover depends on many variables, including the wave climate, the sediment size, and the liquefaction potential. When passing through the surf zone, the buried pipeline should be below the storm or winter profile. In the North Sea, migrating sand dunes with heights of 7 ft have been observed; hence, the depth of burial is not an insignificant matter. The drag forces induced by waves on buried pipelines are not large compared with partially or completely exposed pipes. Figure 28 indicates schematically the coefficient of drag C_D on pipes of various exposure.

155. An extensive laboratory study has been conducted by

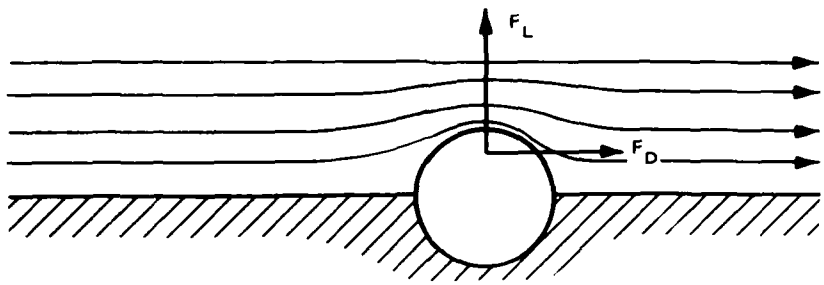

PARTIAL SCOURING UNDER REAR SECTION
$C_D \simeq 0.25$

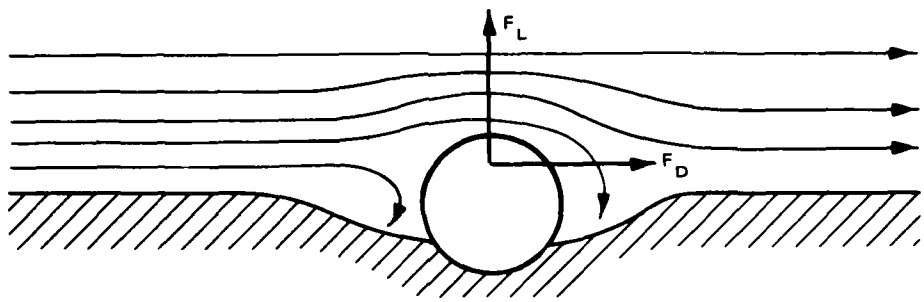

PARTIAL SCOURING UNDER FORE AND REAR SECTIONS
$C_D \simeq 0.50$

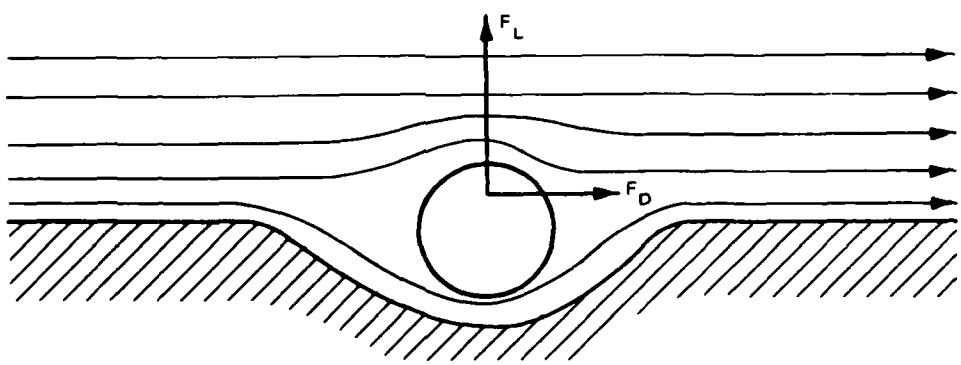

COMPLETE SCOURING UNDER PIPE LINE
$C_D \simeq 1.00$

Figure 28. Effects of partial covering on drag coefficients on underwater pipelines

Herbich (1976) to evaluate the development of underwater bars and scour patterns with the model pipeline buried at various depths below the ocean bottom. The objective of the study was to determine, through physical modeling, the effect of storm waves on buried pipelines approaching the shoreline. Scour depth and scour patterns were evaluated in a two-dimensional wave tank. Three-dimensional effects were also studied in a larger wave basin. Preliminary results indicate that local scour may be quite significant when waves approach at an angle to the pipe. The notation used by Herbich (1976) in this study is shown in Figure 29.

156. The experimental studies of Herbich (1976) were conducted to assess the required depth of burial for a pipeline through the surf zone. Two-dimensional beach profiles were allowed to come to equilibrium in a 2-ft-wide tank, with initial slopes of 1:10, 1:20, and 1:30. Deepwater wavelength was stable throughout a given test and was quite suitable as the independent variable in the regression analysis. The composite ratio of the water depths at the nearshore trough h_t to the water depths over the offshore bar h_c is presented in Figure 30 for the three different beach slopes used in this study. The effect of deepwater wavelength L_o on maximum depth of scour at the nearshore trough T_{max} is shown in Figure 31.

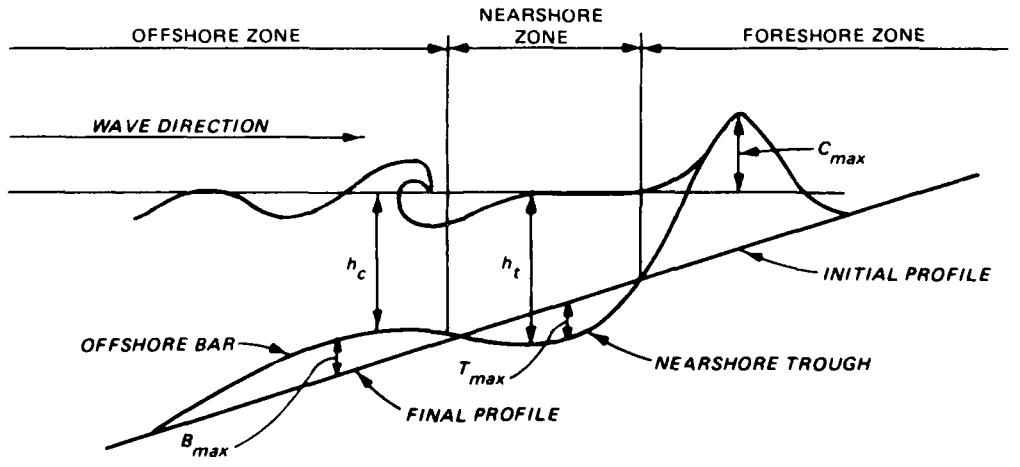

Figure 29. Notation used by Herbich (1976)

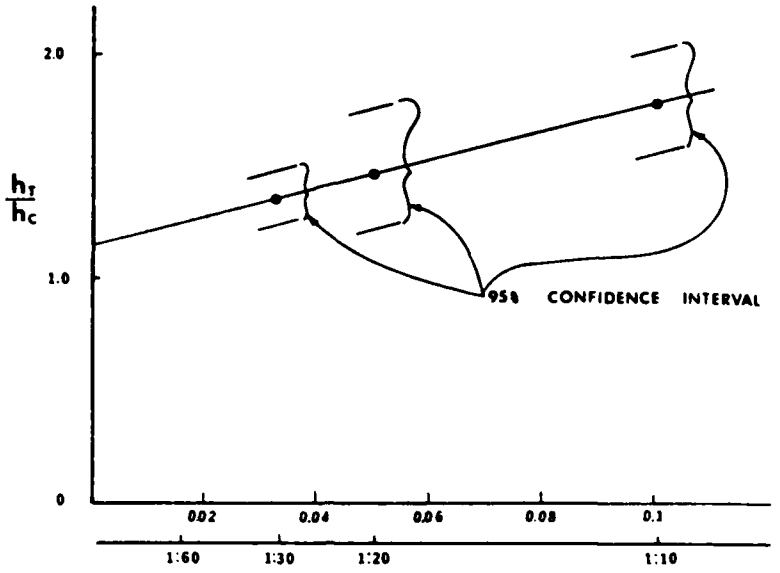

Figure 30. Effect of beach slope on equilibrium water depth over offshore bar and at nearshore trough (after Herbich 1976. By permission of American Society of Civil Engineers)

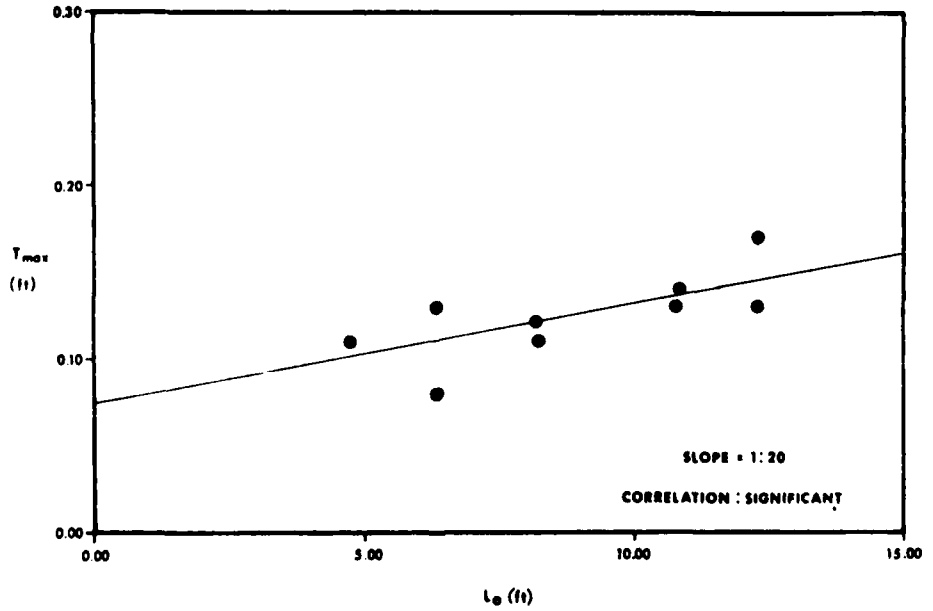

Figure 31. Variation of maximum depth of water over nearshore trough with deepwater wavelength (after Herbich 1976. By permission of American Society of Civil Engineers)

157. Qualitative agreement between this laboratory study and natural beaches was demonstrated by comparison with field profiles of Sabine Pass, Texas. A horizontal scale ratio of 1 to 25 and a vertical scale ratio of 1 to 8 were found to approximate the field data quite well. This produced a physical model scale-distortion factor of approximately 3 to 1.

AD-A088 893 ARMY ENGINEER WATERWAYS EXPERIMENT STATION VICKSBURG--ETC F/G 8 3
EROSION CONTROL OF SCOUR DURING CONSTRUCTION: REPORT 2. LITERAT-- TC(U)
AUG 80 L Z HALES
UNCLASSIFIED WES/TR/HL-80-3-2 NL

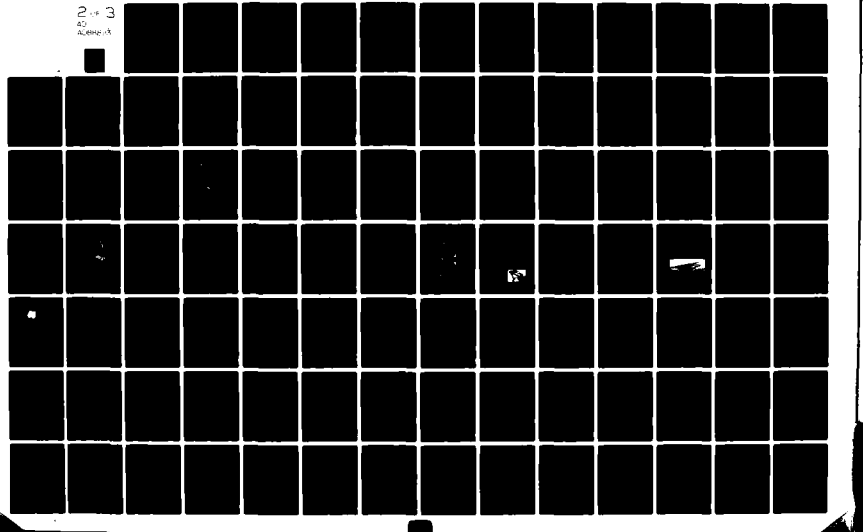

PART VI: COMBINED CURRENT AND WAVE MOTION

158. When surface gravity waves propagate from a region of otherwise still water into a region of streaming water, certain changes occur in their characteristics. It is an easily observed fact that waves which are traveling in the same direction as a current experience an increase in length and celerity and a decrease in height. Waves that propagate in a direction opposed to a current increase in height and decrease in length and celerity until a limiting steepness occurs which depends both on the initial wave characteristics and the strength of the opposing current. At this point the waves break and a large portion of the wave energy is dissipated in the turbulence associated with the breaking.

159. An understanding of the phenomenon connected with the interaction of currents and waves is important for several reasons. Nearshore currents affect the characteristics of shallow-water waves when the waves approach shore; thus, their capacity to cause damage as their energy is expended on coastal structures is altered. In considering beach stability and the potential for scour by waves around coastal structures, a design engineer should have knowledge of the ultimate wave conditions to be expected. At tidal entrances to estuaries, the current will alternately oppose and flow with the waves as the waves propagate toward and through the inlets, and this directly affects wave steepness.

160. Coastal inlets in a natural state are subjected to opposing forces that alternately try to close or enlarge the inlet. Since it is desirable that the inlet location and geometry remain fixed, decisions are frequently made that corrective engineering works be undertaken to ensure the stability of a tidal inlet on an erodible coast. To prevent the lateral movement of a coastal inlet, jetties are often constructed that extend seaward from the shore and become essential to the operation of a dependable inlet for navigation purposes. When both a jetty system and maintenance dredging of a navigation channel through the tidal inlet are required, the characteristics of the surface gravity waves being propagated toward the inlet can be significantly altered by the tidal

currents passing through the inlet (either ebb or flood).

161. The pattern of the buildup of the nonuniform tidal current on the flood stage from the region of low velocity offshore to its maximum value at the inlet throat is distinctly different from the decay of the ebb current as it is discharged into the ocean. The ebb flow emanates from the inlet as a jet and can create a strong current at a point some considerable distance offshore. For the flood situation, the driving force is the ocean tide which is uniform at all points in the near vicinity of the inlet. Therefore, fluid particles are traveling toward the inlet from a lateral as well as a longitudinal direction. This implies that those particles traveling around the tip of the jetties from a lateral direction are passing perpendicular to the orbital motion produced by the wave form. This particular phenomenon has not been investigated analytically although the potential exists for severe scour holes to develop near the seaward end of jetties.

Effect of Tidal Currents on Wave Characteristics

162. From a historical standpoint, the classic analysis of the effect of tidal currents upon surface gravity waves was presented by Unna (1942). He showed that the reduction in length when waves meet an adverse current entails reduction in their celerity and the speed of their energy propagation through the water. Unna assumed that the period of the waves with reference to a fixed point in space is constant, and developed an expression for the wave celerity as:

$$\frac{C_1}{C} = \frac{1}{2} \tanh \frac{2\pi d}{L} \left(1 \pm \sqrt{1 + \frac{4U}{C} \coth \frac{2\pi d}{L}}\right) \tag{75}$$

where

C_1 = celerity of the wave in the presence of a current of intensity U

C = celerity of the wave in the absence of any current velocity

When $U = -1/4\ C$ in deep water, the group celerity, C_g, is zero, and the waves must break however small their initial steepness. Unna

assumed without justification that the wave energy is propagated at its group celerity plus the velocity of the current, and that no interaction between the current and the wave motion occurs. On the contrary, it was shown later by Longuet-Higgins and Stewart (1960) and Lundgren (1962) working independently that the current does additional work on the waves at a rate equal to the product of the rate-of-strain of the current, $\partial U/\partial x$, and a so-called "wave thrust" or "radiation stress," S_x , defined as:

$$S_x = E\left(\frac{2C_g}{C} - \frac{1}{2}\right) \tag{76}$$

$$E = \frac{1}{2}\rho g a^2 \tag{77}$$

E is the energy density of the wave of amplitude a .

163. The concept of "wave thrust" was developed by Lundgren (1962) as a result of the application of the equation of momentum to a control volume containing waves and currents. The idea of Lundgren offered immediate and straightforward explanations of various important phenomena such as wave-induced currents and surf beats, the mechanisms of which had not previously been properly understood. He developed an expression for a coupling term between waves and currents which is analogous to the Reynolds stress. The concept was termed "radiation stress" by Longuet-Higgins and Stewart (1964).

164. Changes in the form of short gravity waves on long waves and currents were studied theoretically by Longuet-Higgins and Stewart (1960). In order to interpret physically the conclusions of their work, consider from a general point of view the transfer of energy by surface waves on a steady uniform current. In a nonviscous fluid, the rate of transfer of energy across a vertical plane x = constant, per unit distance in the y-direction is:

$$R_x = \overline{\int_{-d}^{\eta} \left[p + \frac{1}{2}\rho\,(u')^2 + \rho g z\right] u\, dz} \tag{78}$$

where the overbar indicates a temporal average.

$$u' = U + u \tag{79}$$

where

R_x = rate of energy transfer in x-direction

d = fluid depth below mean water

η = distance from the mean waterline to the free surface

p = pressure intensity at a point in the fluid

ρ = density of the fluid

u' = combined velocity due to the wave motion and stream velocity

g = gravitational constant

z = vertical direction

U = (U,0,0) denotes the mean stream velocity

When the integration and the averaging are carried out, it is easily shown that to order a^2 the mean rate of energy transfer across the plane x = constant is:

$$\overline{R_x} = E(C_g + U) + S_x U + \frac{3}{2}\frac{EU^2}{C} + \frac{1}{2}\rho d U^3 \tag{80}$$

where S_x is defined by Equation 76.

165. The first term on the right side of Equation 80, $E(C_g + U)$, represents simply the transfer of wave energy by the group velocity plus the stream velocity. Since the motion is irrotational, there is, owing to the mass-transport velocity, a net momentum E/C in the direction of wave propagation; and the last two terms together represent the mean stream velocity modified by the presence of the mass transport. The intermediate term, $S_x U$, represents a significant coupling between the waves and the current, and is analogous to the Reynolds stresses of turbulent flow theory. Thus, S_x is an additional stress, due to the wave motion, per unit length across a plane normal to the direction of wave propagation. It is composed of the integrated Reynolds stress plus the stress due to the relation between surface elevation and pressure, reduced by the effect of the presence of the waves on the average pressure in the body of the fluid.

166. Longuet-Higgins and Stewart (1960) considered a system of waves superposed on a current that varies gradually in the direction of wave propagation, and in which the variation in surface current is made up by a vertical upwelling or downwelling. The modifications that the currents produce in the wave form were calculated by a perturbation method. It was found that while the variation in the wave number, k_o, is given by the expected formula:

$$\frac{1}{k_o}\frac{\partial k_o}{\partial x} = -\frac{1}{C + 2U}\frac{\partial U}{\partial x} \tag{81}$$

the variation in the wave amplitude, on the other hand, is given by:

$$\frac{1}{a}\frac{\partial a}{\partial x} = -\frac{2C + 3U}{(C + 2U)^2}\frac{\partial U}{\partial x} \tag{82}$$

which is a higher rate of change than if there were no interaction between the wave and the currents. It was shown that the last result is consistent with the assumption that the equation governing the growth of wave energy, E, is:

$$\frac{\partial}{\partial x}E(C_g + U) + S_x\frac{\partial U}{\partial x} = 0 \tag{83}$$

In addition to the transport of energy by the group velocity and stream velocity, the current does work on the waves at a rate $S_x\frac{\partial U}{\partial x}$ per unit distance.

167. In a second example, Longuet-Higgins and Stewart (1960) consider a situation in which the increase in surface current is made up by a horizontal inflow from the sides. The results are strikingly different. Although the variation in wave number is the same as the first example, the variation in amplitude is now given by:

$$\frac{1}{a}\frac{\partial a}{\partial x} = -\frac{C + U}{(C + 2U)^2}\frac{\partial U}{\partial x} \tag{84}$$

168. Theoretical results of a general study were presented by Jonsson (1970) in which the interaction between a steady current and

surface gravity waves was investigated. Assuming irrotational flow and a second order Stokes wave motion, the study presented a graphical method for the computation of the wavelength in a current field. The concept of the mean energy level for a periodic wave motion and the calculation procedure for the "current-wave setdown" were developed.

169. These studies were generalized by Huang et al. (1972) to include nonuniform currents and a random gravity wave field. The Kitaigorodskii-Pierson-Moskowitz frequency spectrum was used as the basic spectral form for zero current condition. Modified spectral functions in both wave number and frequency spaces under the influence of the current were found by using energy conservation and kinematic wave conservation laws. As a result of the current-wave interaction, the magnitude and the location of the energy peak in the spectrum were altered. Since the phase speed of gravity waves is a monotonically decreasing function of wave number and frequency, the influence of the current was predominant at the higher wave number range.

170. Dalrymple (1974) theoretically investigated water waves propagating on a bilinear shear current flowing in the direction of the waves. The theory was developed first for small amplitude waves and then extended to any arbitrary order by a numerical perturbation technique for symmetric waves. Due to the lack of laboratory or field data for the empirical verification of either form of the bilinear shear current theory, analytic validity was used to verify the theories for various wave conditions.

171. An experimental study was conducted by van Hoften and Karaki (1976) to study wave amplitude attenuation along a laboratory wave channel and to compare the wave dissipation with and without flow. The waves were found to be altered by a combination of the interaction of the shear gradient, the normal turbulence, and the wave orbital velocities. The effect was to extract energy from the waves resulting in an increased wave attenuation. The flow itself was altered by the superposed waves. The induced orbital wave velocities distorted the mean velocity profile increasing the gradient near the bed. Turbulence energy was produced near the surface and diffused downward where it

was dissipated on the bottom by an increase in apparent boundary shear stress.

172. Results of an experimental study of wind waves generated on currents in a wind-wave channel were presented by Kato and Tsuruya (1978). The water current had the effect of changing the substantial (effective) fetch length, with an adverse current increasing the effective fetch and a favorable current decreasing it. The concept of the equivalent fetch length was developed. By using the equivalent fetch instead of the actual fetch, it was shown that the significant wave height measured under various current conditions can be represented by nondimensional fetch relations.

Sediment Transport by Waves and Currents

173. The transport of noncohesive sediments under the simultaneous action of waves and currents takes place along natural beaches and elsewhere when waves become superposed upon currents. The currents may be wave-induced, wind-driven, tidal, stream, or river or may originate from some other lesser known cause.

Longshore movement

174. Because of refraction, waves usually break at a fairly small angle to a beach. The mass of water piling up in the surf zone generates a wave-induced current that flows along the beach and is known as the longshore or littoral current. This longshore current, though relatively mild, is capable of transporting vast quantities of sediments that are tossed into suspension by the turbulence associated with wave-breaking. In addition, the water mass produced by the breaking process rushes up the beach face at a slight angle, and then down the beach face in such a manner that there is a zigzag path to the particles of water on the beach. Sand particles traverse the same sort of pattern along the beach face (Johnson and Eagleson 1966). Hence, the total longshore drift of sand consists of the general drift due to the longshore current in the breaker zone and the zigzag path on the foreshore due to wave uprush and backwash (or runup and rundown).

175. Longshore currents flow parallel to shore, accumulating in volume as more mass is introduced by additional breaking waves, until regions of return flow through the breaker zone are encountered (either rip currents or underflow return currents). The existence of these currents is necessary, otherwise the longshore current would become infinitely large. Longshore currents typically have mean values on the order of 1 fps, and observed speeds of 3 fps are quite unusual. Although low in magnitude, longshore currents are quite significant in beach processes because they flow along the shore for extended periods of time. The longshore current velocity appears to be quite sensitive to breaker angle α_b (which the wave crests make with the shoreline) and somewhat sensitive to breaker height H_b . An estimation of the magnitude of a longshore current may be obtained from the modified Longuet-Higgins (1970) expression

$$V_{ls} = 20.7\ m \left(g\ H_b\right)^{1/2} \sin 2\alpha_b \tag{85}$$

where

V_{ls} = velocity of the longshore current

m = beach slope

176. Longshore current and longshore sediment models have been developed by Ostendorf and Madsen (1979) and have been calibrated against both laboratory and prototype field data. The longshore current model can be considered as a modification of the original model of Longuet-Higgins (1970), while the longshore sediment model is a surf zone application of previous work by Madsen and Grant (1976) on nonbreaking wave-induced sediment transport. Calibration yielded physically plausible behavior for the model parameters. Laboratory (fixed bed and movable bed) and field tests show an accuracy of about 20 percent for the longshore current model. While the longshore sediment model fit the laboratory data to an accuracy of about 20 percent, it overpredicted the field data by a factor of 5. In view of these findings, the longshore sediment transport model of Ostendorf and Madsen (1979) should only be considered as an order of magnitude estimator of longshore sediment transport.

177. Most investigators have attempted a correlation between wave characteristics and measured longshore transport rate. Intuitively, the rate at which a transport process takes place should be related to the total power available for transporting material. Accordingly, the procedure that has evolved is to determine the alongshore component of wave power, or energy flux, in the surf zone. The alongshore energy flux is approximated under the assumptions of conservation of energy in shoaling waves and application of Airy wave theory. Based on these assumptions, the energy flux at the breaker zone is

$$P_{ls} = [(\rho\ g)/16]\left(H_b^2\ C_g\ \sin 2\alpha_b\right) \tag{86}$$

P_{ls} is the alongshore component of wave energy flux per unit length of beach and C_g is the group velocity, or the velocity of propagation of wave energy (i.e., $C_g = C$, the wave celerity in shallow water). If the energy density at breaking can be approximated by linear theory,

$$E = 8\ H_b^2 \tag{87}$$

and if the wave speed at breaking can be approximated by solitary theory,

$$C_g = C \simeq (2\ g\ H_b)^{1/2} \tag{88}$$

Equation 86 can now be expressed in terms of the wave breaking characteristics of breaker height H_b and breaker angle α_b as

$$P_{ls} = 32.1\ H_b^{5/2}\ \sin 2\alpha_b \tag{89}$$

following the development of CERC (1975).

178. A number of empirical equations have been advanced since the early 1950's that relate the longshore component of wave energy flux, Equation 89, with measured values of volumetric longshore transport.

The CERC expression, based entirely on 23 field observations and no laboratory data, is

$$Q_{ls} = 7{,}500\ P_{ls} \tag{90}$$

where Q_{ls} is longshore transport in cubic yards per year. The coefficient, 7,500 in Equation 90, is about 83 percent larger than the corresponding coefficient which appeared in an earlier edition, because the earlier correlation was based on fewer field observations and on a tremendous number of laboratory observations. It was determined that the small-scale laboratory data completely overwhelmed the small number of field observations; hence, it was deemed desirable to eliminate laboratory results and supplement the existing field data with more recent prototype observations. Equation 90 is displayed graphically in Figure 32, which shows the field data giving rise to the expression.

Evaluation of longshore transport formulas

179. The total longshore sediment transport can be estimated with the CERC formula at locations with fairly uniform bathymetry. The application of other formulas is not widespread because they lack direct verification from either prototype or model conditions. Van de Graaff and van Overeem (1979) compared the results of other sediment transport formulas with the results of the CERC formula. This comparison was simply a substitute for a comparison with actual prototype data. Resio (1978) developed a technique explicitly formulated to use two-dimensional spectra for calculations of longshore drift rates. This work suggests that the spectral process of wave breaking as waves propagate into shallow water and the energy losses due to bottom friction can play an important role in reducing and redistributing drift rates during a storm.

180. Many of the sediment transport formulas used in coastal engineering work were developed from formulas derived in river sedimentation computations, especially those of European descent. These formulas can only be applied when the wave effect is properly included.

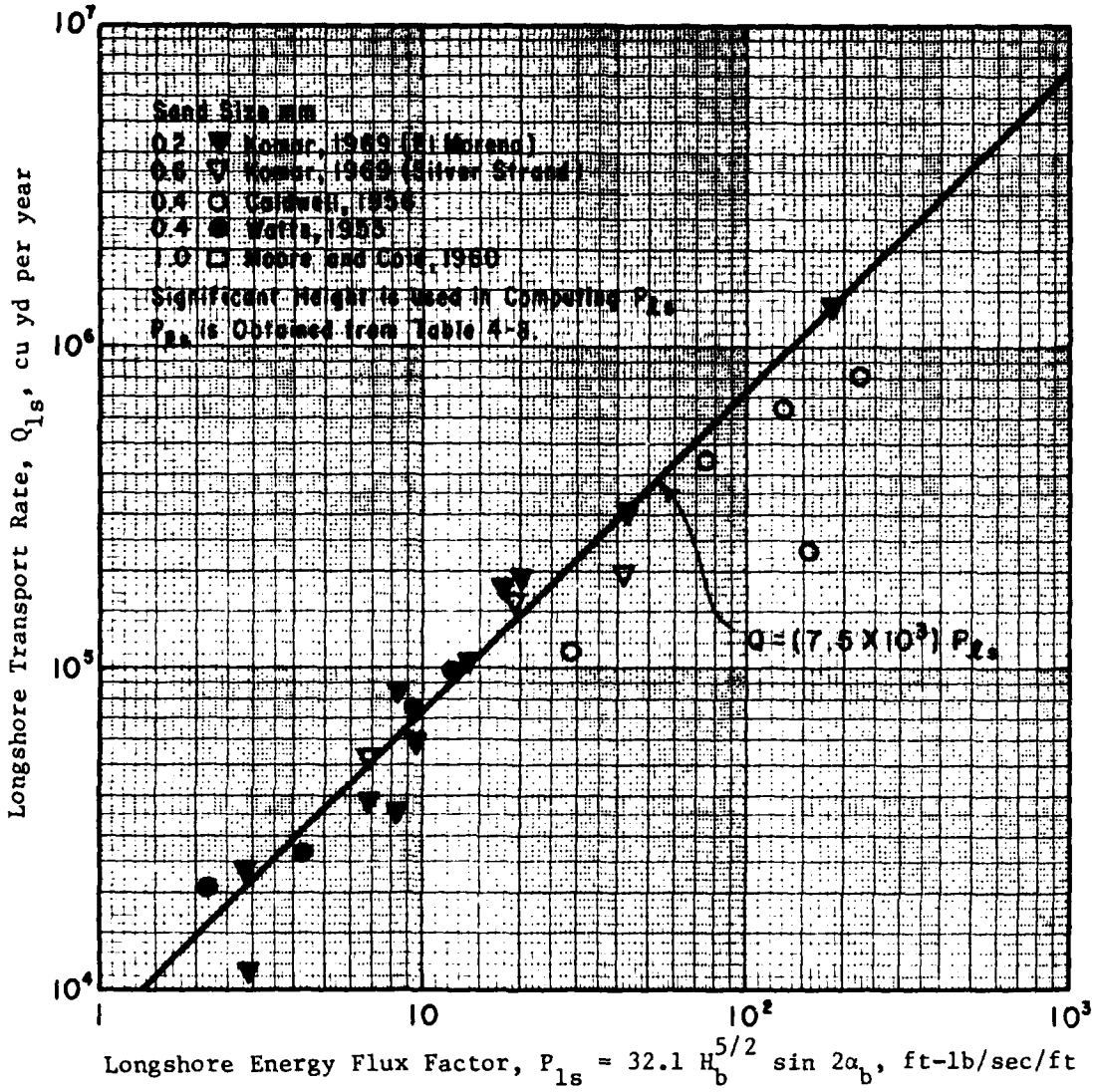

Figure 32. Prototype field data for development of longshore transport relation (after CERC 1975)

Four different expressions (Bijker, Engelund-Hansen, Ackers-White, and SWANBY) were evaluated for a range of values of bed material particle diameters, beach slope, bed roughness, breaker height, and breaker angle.

181. Bijker formula (1971). Starting from the Kalinske-Frijlink formula which predicts the transport near the bottom, Bijker suggested a formula for the bed load in the coastal environment as:

$$q_{bed} = 5d_{50} \frac{v}{C} g^{1/2} \exp\left\{\frac{-0.27\Delta d_{50}\rho g}{\ell\, \tau_c\left[1 + \frac{1}{2}\left(\epsilon \frac{u_o}{v}\right)^2\right]}\right\} \quad (91)$$

where

d_{50} = particle diameter (50 percent by weight exceeded in size)

v = mean current velocity

C = Chezy coefficient

g = acceleration due to gravity

Δ = relative apparent density of the bed material defined by

$$\Delta = (\rho_s - \rho)/\rho \quad (92)$$

where

ρ_s = mass density of bed material

ρ = mass density of water

ℓ = ripple factor

$$\ell = (C/C_{90})^{1.5} \quad (93)$$

where

C_{90} = Chezy coefficient based on the d_{90} particle diameter (10 percent by weight exceeded in size)

ϵ = Bijker's parameter

$$\epsilon = C(f_w/2g)^{1/2} \quad (94)$$

where

f_w = Jonsson's wave friction factor

τ_c = bottom shear stress due to current

u_o = maximum orbital velocity at the bed

This bed load is assumed to take place in a layer with thickness equal to the bed roughness.

182. The suspended load was formulated by Bijker (1971) based on Einstein's concept as

$$q_{sus} = 1.83\, q_{bed} \left[I_1 \ln(33h/r) + I_2 \right] \tag{95}$$

where

q_{sus} = suspended load

h = local water depth

r = bed roughness

I_1, I_2 = Einstein's integrals

$$I_1 = \frac{0.216(r/h)^{(z_*-1)}}{(1 - r/h)^{z_*}} \int_{r/h}^{1} \left(\frac{1 - y}{y} \right)^{z_*} dy \tag{96}$$

$$I_2 = \frac{0.216(r/h)^{(z_*-1)}}{(1 - r/h)^{z_*}} \int_{r/h}^{1} \left(\frac{1 - y}{y} \right)^{z_*} \ln y \, dy \tag{97}$$

$$z_* = v_f / k v_{*wc} \tag{98}$$

where v_f is the sediment particle fall velocity and k is von Karman's coefficient.

$$v_{*wc} = v_{*c} \left[1 + 1/2 \, (\varepsilon u_o / v)^2 \right]^{1/2} \tag{99}$$

where v_{*c} is the shear stress velocity due to the current. Ultimately,

$$Q_{Bi} = q_{bed} + q_{sus} \tag{100}$$

183. Engelund-Hansen formula (1967). The initial starting point for this development is the contention that grains are eroded from the upstream side of dunes and deposited on the downstream side. Consequently, along a finite section the total sediment load is elevated a height comparable to the dune height. This process can be described roughly by means of a simple energy expression where the gain in potential energy is equal to the work done by the drag forces on the moving particles in the same time interval. Furthermore, the average migration

velocity of the particles was assumed to be proportional to the friction velocity. When developed for a coastal environment, and using the presently defined symbols, the Engelund-Hansen formula can be expressed as:

$$Q_{EH} = \frac{0.05 v C \tau_c^2 \left[1 + \frac{1}{2}\left(\varepsilon \frac{u_o}{v}\right)^2\right]^2}{\rho^2 g^{5/2} \Delta^2 d_{50}} \tag{101}$$

184. Ackers-White formula (1973). Ackers and White assumed a substantial difference in the mode of transport of coarse and fine grains, as they stated that the fine sediments travel largely in suspension and that the rate of transport depends on the total shear on the bed. The expression is:

$$Q_{AW} = v \frac{1}{(1 - p)} d_{35} \left(\frac{v}{v_{*c}}\right)^n \frac{C_{D_{gr}}}{A^m} \left(F_c - A\right)^m \tag{102}$$

where

v = mean current velocity

p = porosity of sediment material

d_{35} = particle diameter (65 percent by weight exceeded in size)

$$n = 1 - 0.2432 \ln (D_{gr}) \tag{103}$$

$$D_{gr} = d_{35} \left(g \Delta / \nu^2\right)^{1/3} \tag{104}$$

where ν is the kinematic viscosity of water

$$C_{D_{gr}} = \exp\left(2.86 \ln D_{gr} - 0.4343 \ln D_{gr}\right)^2 - 8.128 \tag{105}$$

$$A = 0.23/D_{gr}^{1/2} + 0.14 \tag{106}$$

$$m = 9.66/D_{gr} + 1.34 \tag{107}$$

$$F_c = \frac{v\left(\frac{v_{*c}}{v}\right)^n C_D^n}{C_D\, g^{n/2}\, (\Delta d_{35})^{1/2}} \tag{108}$$

$$C_D = 18 \log (10h/d_{35}) \tag{109}$$

185. SWANBY formula. Swart (1976) and the Delft Hydraulics Laboratory assumed that the increasing effect of waves on sediment transport rate as computed with the Ackers-White formula could be handled by replacing v_{*c} with v_{*wc}, where

$$v_{*wc} = v_{*c}\left[1 + 1/2\, \left(\varepsilon\, u_o/v\right)^2\right]^{1/2} \tag{110}$$

This approach has been termed the SWANBY method, and the ultimate result is:

$$Q_{SW} = v\, \frac{1}{(1 - p)}\, d_{35} \left\{ \frac{v\left[1 + 1/2\, \left(\varepsilon' \frac{u_o}{v}\right)^2\right]^{1/2}}{v\left[1 + 1/2\, \left(\varepsilon \frac{u_o}{v}\right)^2\right]^{1/2}} \right\}^n \tag{111}$$

$$\times \frac{C_{D_{gr}}}{A^m} \left\langle \frac{v\left[1 + 1/2\, \left(\varepsilon' \frac{u_o}{v}\right)^2\right]^{1/2} \left\{ \frac{v_{*c}\left[1 + 1/2\, \left(\varepsilon \frac{u_o}{v}\right)^2\right]^{1/2}}{v\left[1 + 1/2\, \left(\varepsilon' \frac{u_o}{v}\right)^2\right]^{1/2}} \right\}^n}{C_D\, g^{n/2}\, (\Delta d_{35})^{1/2}}\; C_D^n - A \right\rangle^m$$

$$\varepsilon' = C_D\left(f_w'/2g\right)^{1/2} \tag{112}$$

and the other symbols have been previously defined.

186. Longshore transport computations were performed by van de Graaff and van Overeem (1979) for various values of the parameters of breaker wave height, period, angle, and of the associated parameters of bed material size, roughness, and beach slope. The CERC formula is sensitive to only the first three parameters which define the wave characteristics. The results of these computations are plotted versus the ratio of transport with sediment transport formula to transport with CERC formula. Figure 33 displays the effect of bed material and bed roughness on this ratio, Figure 34 shows the effect of

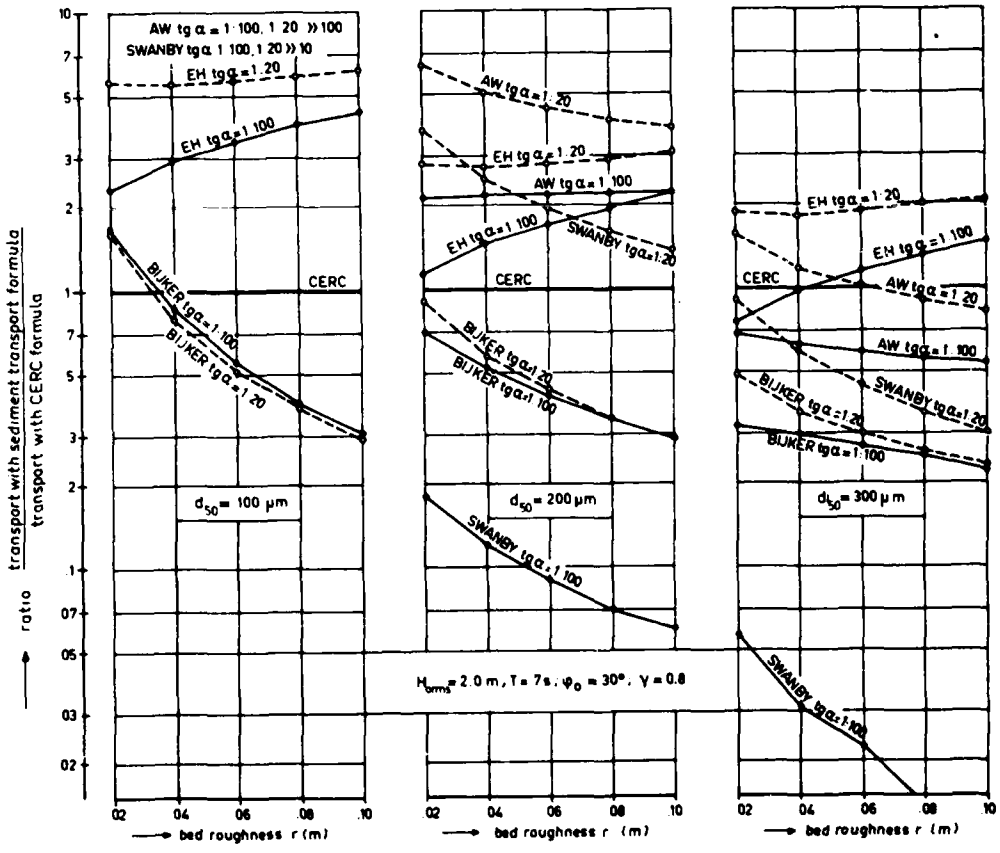

Figure 33. Effect of bed material and bed roughness on sediment transport (after van de Graaff and van Overeem 1979)

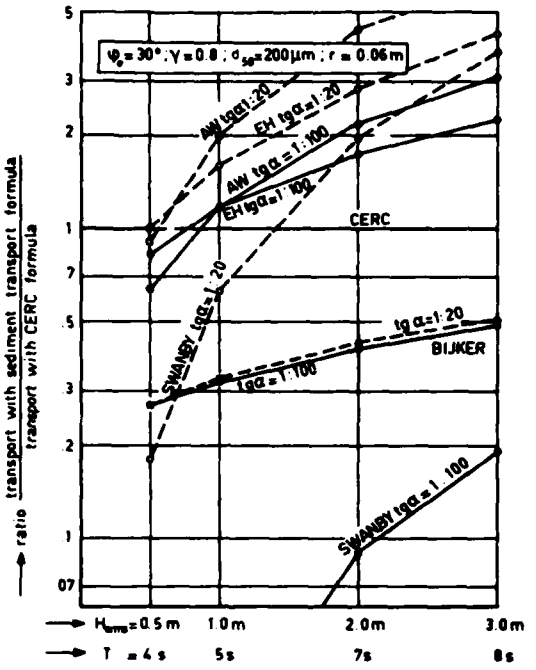

Figure 34. Effect of wave height on sediment transport (after van de Graaff and van Overeem 1979)

wave-height variation on the ratio, and Figure 35 provides an indication of the effect of breaker angle on the transport ratio.

187. Due to the lack of prototype transport measurements in the vertical direction, a direct verification of the various proposed sediment transport formulas is impossible. Hence, the comparison method of van de Graaff and van Overeem (1979) was developed in which relative comparisons were made by varying different parameters. It was determined that the Bijker formula comes closer, in general, to the results of the computations with the CERC formula than the other compared formulas and is far better than the SWANBY formula. Furthermore, the Bijker formula is rather insensitive to effects of particle diameter, bottom slope, and bed roughness. A possible fairly large error in the estimation of the actual conditions results in only a slight error in the computed sediment transport for the conditions compared in the investigations of van de Graaff and van Overeem (1979).

188. Resio procedure. The purpose of the investigation by Resio (1978) was to examine how results from a numerical wave hindcast study could be incorporated into predictions of longshore transport rates.

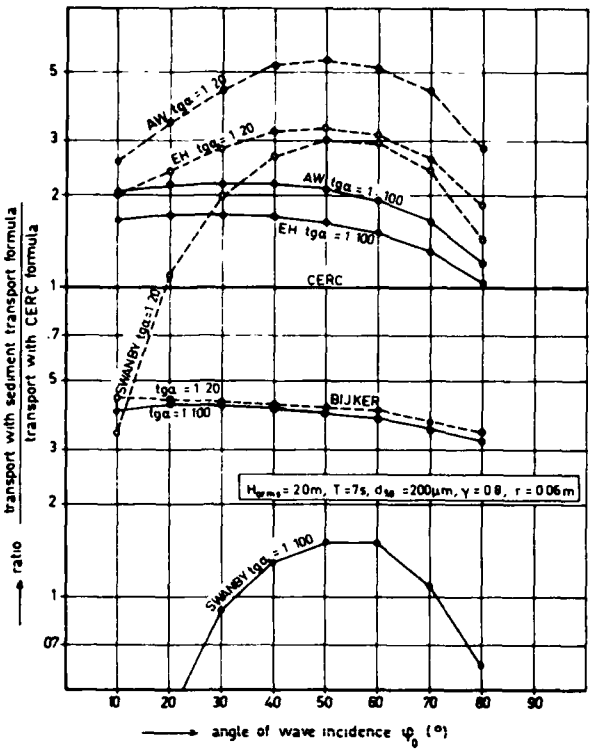

Figure 35. Effect of wave breaker angle on sediment transport (after van de Graaff and van Overeem 1979)

When the wave climate which is represented in the form of a spectrum is combined with the empirical relation for immersed weight and wave characteristics by Komar (1971), the wave spectrum can be decomposed into a one-dimensional energy spectrum. This permits an examination of the effects on the longshore component of wave power due to variations in the distribution of wave energy in frequency and in direction independently. For long-crested waves (all waves propagating in a common direction) the spectral width has little, if any, effect on the amount of material transported. This can be viewed as a property of the shallow-water assumption. For a short-crested wave system, extensive measurements by Longuet-Higgins (1962) have determined the representation of the angular distribution of wave energy in locally generated sea. These data were analyzed by Resio (1978); and it was found that as the angular

distribution of energy becomes broader, the longshore drift rate will decrease. The width of the angular distribution of wave energy plays a critical role in determining the longshore drift rate for mean wave approach angles up to about 50 deg.

Distribution across the surf zone

189. The longshore current and littoral process in the surf zone has been investigated by Thornton (1970) to determine the velocity distribution across the surf, and later by Thornton (1972) to evaluate the distribution of sediment. By applying energy principles, it was determined that a different expression was necessary for both current and sediment inside and outside the breaker zone. The mean sediment transport of sand outside the breaker zone, per unit time per unit width, in the longshore direction is

$$q_{lso} = \left[B\ (V_{lso}/u_{max})^{1/2}(u_{max}\ \tau_{max})\right]/\left[g - (g\ \rho)/\rho_s\right] \qquad (113)$$

where q_{lso} = unit longshore transport outside the breaker zone, τ_{max} can be evaluated from Equation 43, B is a coefficient of proportionality which is not well defined at this time, and V_{lso} is longshore velocity outside the surf zone which can be evaluated from the expression

$$V_{lso} = \left[(\pi\ L)/(\rho\ g\ f_w\ H)\right]\left[\cosh\ (2\pi y)/T\right]\left[\partial/\partial x(E\ C_g/C\ \sin\ 2\alpha)\right] \qquad (114)$$

Inside the breaker zone, the mean sediment transport of sand per unit time per unit width in the longshore direction is

$$q_{lsi} = \left\{B_s\ (V_{lsi}/u_{max})^{1/2}\left[\partial/\partial x(E\ C_g)\right]\right\}/\left[g - (g\ \rho)/\rho_s\right] \qquad (115)$$

where

$$V_{lsi} = (0.60)(0.78\pi/f_w)\ C_b\ \sin\ \alpha_b\ \cos\ \alpha_b\ y/D_b\ \partial y/\partial x \qquad (116)$$

Here the subscript b represents breaking conditions and f_w is Jonsson's wave friction factor. A different proportionality constant

B_s is necessary inside the breaker zone from that outside the breakers B.

190. Field experiments were conducted by Thornton (1972) in order to evaluate the constants of proportionalities B and B_s by sampling locations across the surf zone. The experiments were conducted intermittently over a five-year period, and the method of measuring the various parameters changed, evolving to a relatively sophisticated level. The B and B_s values were determined from a best-fit between theory and experiment and varied for each individual experiment. Inman and Bowen (1963) have attempted to quantify these coefficients by performing flume experiments on sand transport by waves and currents but were not entirely successful. Hence, Equations 113 through 116 should be used only as a qualitative predictive relation for the distribution of sediment across the surf zone. Results of a typical experiment at one prototype location are presented in Figure 36.

191. The purpose of the wave and superposed current experiments of Inman and Bowen (1963) was to simulate conditions prevailing along natural beaches. It has been shown that in two-dimensional wave motion (flume studies) the wave-induced drift velocity is downwave near the surface and bed but upwave in the center. However, real beach studies have revealed that the drift velocity is onshore at all depths, with the system being kept in equilibrium by the rip currents spaced along the beach. The current velocities superposed were of the same order of magnitude as the wave-induced drift velocities. It was found that the water moving over a ripple crest during the forward semiorbit generated a vortex in the lee of the ripple. As the water decelerated, the system became unstable and the vortex, no longer restrained, dispersed rapidly. It was lifted up over the ripple by the combination of its own vorticity and the initial acceleration of the backward semiorbit. This process removed sediment from above the downwave face of the ripple and dispersed it as a cloudy suspension moving upwave. During the second half of the orbit, a vortex was generated upwave from the ripple and then dispersed, its sediment content being thrown into suspension downwave from the ripple. Material was thus placed in suspension with some

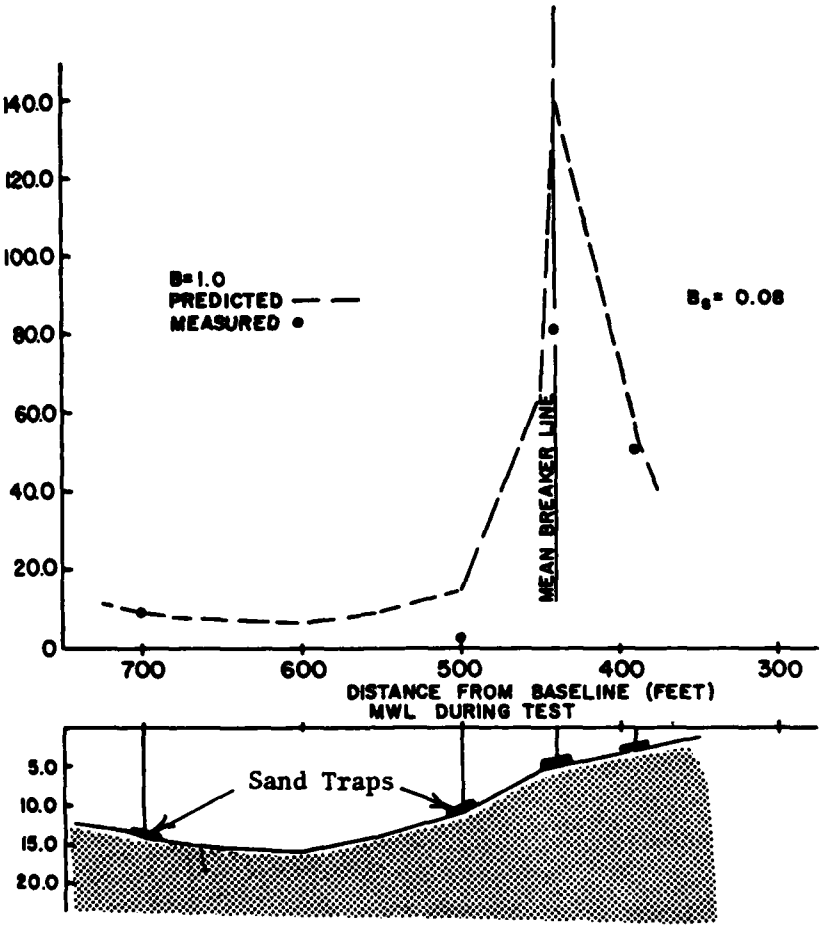

Figure 36. Distribution of longshore sediment transport across the surf zone (after Thornton 1972. By permission of American Society of Civil Engineers)

initial velocity at two distinct periods during an orbit. If the motion were otherwise symmetrical, the drift velocity would be the factor determining the direction and magnitude of the sediment transport.

192. The effect of the superposition of a small current on the wave field was to further reduce the symmetry of the system by increasing the effective orbital velocity downwave and decreasing it upwave. This resulted in a flattening of the upwave face of the ripple and the steepening of the downwave face. The vortex generated on the downwave face then became by far the stronger, and hence, much of the material

placed in suspension had an upwave initial velocity. The general effect was to substantially increase the rate of sediment transport in a downwave direction.

193. Because of the great difficulty in obtaining the required information in the breaker and swash zone, only minimal consideration has been given to the distribution of the longshore sand transport across the surf zone, except for Thornton (1972), Komar (1975), and Sawaragi and Deguchi (1978). Some sand tracer experiments have given an indication of the distribution, but not a quantitative measure. Komar (1975) treated the distribution from a theoretical standpoint and calibrated his analytical model in such a way that it agrees with the available data. When summed across the width of the surf and breaker zones, the sand transport distribution yields the correct total sand transport according to field measurements. These longshore current velocity and sand transport rate distributions are shown in Figure 37.

194. Sawaragi and Deguchi (1978) developed a specialized piece of equipment to separately record the distributions of longshore and onshore-offshore sediment transport rates in the surf zone. The

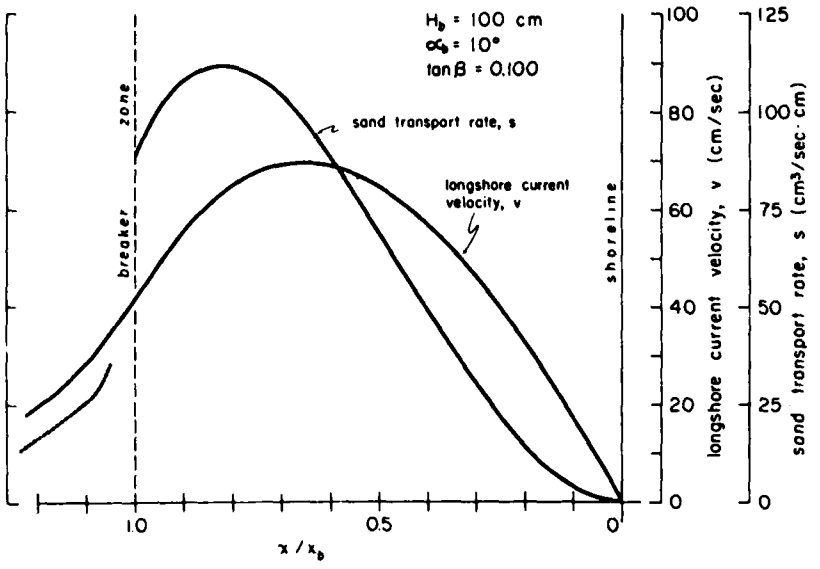

Figure 37. Distribution of longshore current velocity and sand transport rate across the surf zone (after Komar 1975. By permission of American Society of Civil Engineers)

distributions of each component of the sediment transport rate along a line normal to the shore across the surf zone were measured by using this apparatus in the field as well as in a laboratory model. The distribution of the longshore sediment transport rate as bed load showed a steep profile compared with the distribution of the longshore current, and the maximum longshore sediment transport occurred at the point between the breaking location of the incident waves and the location where the velocity of the longshore current showed the maximum value, also shown qualitatively in Figure 37 of Komar (1975). The maximum onshore-offshore sediment transport took place at about the same place as the longshore sediment transport maximum. However, the distribution of the onshore-offshore sediment transport rate showed more complicated profiles than that of the longshore sediment transport rate; the direction of the onshore-offshore sediment transport at any location changes with wave characteristics and beach slope from offshore direction to onshore direction. The locations where the maximum longshore and onshore-offshore sediment transport take place are mainly controlled by the sediment size relative to the wave height. Results of laboratory experimental tests are shown in Figure 38, which displays the longshore sediment transport distribution in part (a) and the onshore-offshore components in part (b). Figure 39, for two different ratios of

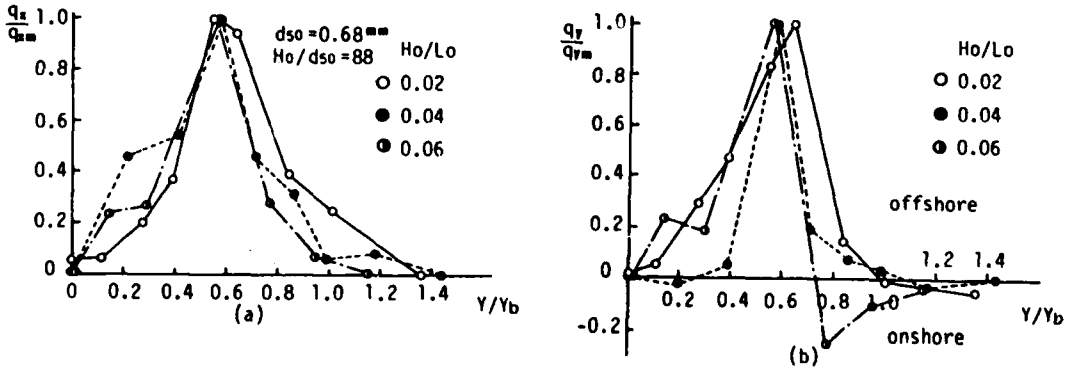

Longshore Onshore-offshore

Figure 38. Distribution of longshore and onshore-offshore sediment transport across the surf zone (after Sawaragi and Deguchi 1978. By permission of American Society of Civil Engineers)

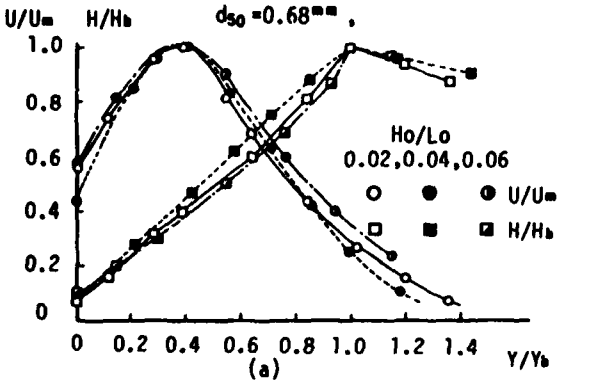

H_o/d_{50} = 88

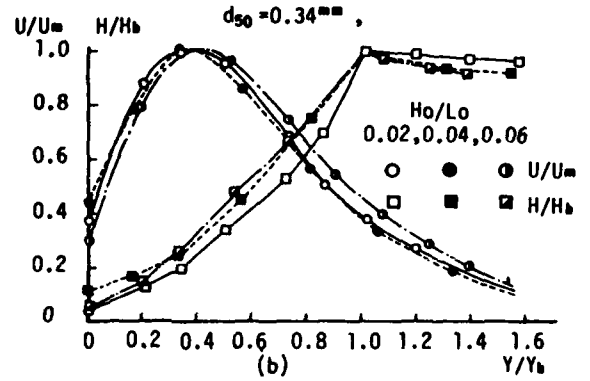

H_o/d_{50} = 176

Figure 39. Distributions of longshore currents and wave heights across the surf zone for two different sediments and H_o/d_{50} ratios (after Sawaragi and Deguchi 1978. By permission of American Society of Civil Engineers)

H_o/d_{50} , shows the distributions of longshore current velocities and wave heights across the surf zone.

195. A model for sand transport along beaches under the influence of wave action was developed by Walton and Chiu (1979) based on the surf zone radiation stress work of Longuet-Higgins (1970). The excess momentum flux of the water waves was used as the driving force to generate the water current, and an energetics approach was then applied to

develop the sand transport created by the water currents. The bed load and suspended load were considered separately in this model which is an outgrowth of the energetics approach to riverine sand transport adhered to by Bagnold (1966).. The expression for littoral sand transport is linear (in breaking wave angle) for suspended-sediment transport, and nonlinear (in breaking wave angle) for bed-load transport. The model was compared by Walton and Chiu (1979) with existing laboratory data and was found to fit within a constant. The model predicted reasonable values for total load transport; however, since the instrumentation used in the data collection did not perfectly differentiate the bed-load portion from the suspended-load portion, the individual bed-load and suspended-load sand transport could not be verified independently.

PART VII: SCOUR BY COMBINED CURRENT AND WAVE ACTION

196. Scour and erosion that occur around most open-ocean structures are results of a combination of current and wave action, to a greater or lesser degree. On a straight section of coastline protected by groins or breakwaters, scour generally results from particles being tossed into suspension by wave action and then being transported from the region by wave-induced currents; hence, these phenomena are all-inclusively considered to be the result of scour by wave action. On the other hand, in regions where strong currents (other than wave-induced) exist and where large expanses of open water allow the generation of surface gravity waves, scour effects that result are considered to be caused by a combination current and wave interaction. Dominant examples of this situation are jetties stabilizing a river mouth on the coast, or jetties protecting a navigation channel through a tidal inlet into an estuary. In either case, strong currents (riverflow or tidal) exist that act as a scouring mechanism in themselves, in addition to being a transporting vehicle for removing material placed into suspension by wave effects.

197. Objectives considered in the design of a jetty system at a tidal inlet include, among others, the minimization of: (a) undesirable wave action on navigation, (b) artificial channel maintenance dredging, and (c) adverse effects on shoreline modifications caused by the interception of littoral sediment movement. Jetties assist in channel maintenance by directing ebb tidal currents such that their natural scouring potential is enhanced. Jetties also aid channel maintenance by intercepting longshore sediment transport due to wave action; hence, many jetties are impermeable, extending from the beach to an offshore depth where sediment movement is minimal.

Masonboro Inlet, North Carolina

198. Masonboro Inlet, a natural inlet through the coastal barrier beach of North Carolina, is located in the southern portion of the State, 8 miles northeast of Wilmington, North Carolina. It appears that the inlet has been open continuously since 1733, although it has migrated

extensively. Improvements for the inlet, authorized in 1949, included two jetties, an ocean entrance channel between the jetties, and interior navigation channels to the Atlantic Intracoastal Waterway. Due to funding constraints, it was proposed to construct the north jetty initially since it was on the updrift side of the inlet (Sager and Seabergh 1977). The improvement plan consisted of the north jetty with a low interior weir, a deposition basin adjacent to the north jetty, and reestablishment of the navigation channel. The jetty was constructed using concrete sheet piles for the shoreward portion (the weir section) from +12 ft beach elevation to the existing -5 ft mlw, a distance of about 1,700 ft, and quarrystone from -5 ft mlw to -12 ft mlw, a distance of 1,700 ft. It was anticipated that sand moving southward along the beach and over the weir would be trapped in the deposition basin dredged between the jetty and the northern limit of the navigation channel.

199. A year and a half after construction of the jetty the existing channel had migrated northward through the deposition basin and against the north jetty. In addition, extensive material which had apparently scoured from near the north jetty had been deposited on the large shoal on the south side of the inlet (Figure 40). Hydraulic model tests were performed at WES (Seabergh 1979) to investigate the effects of closure of one of the channels that exit through Masonboro Inlet. These tests indicated that one of the interior channels (Shinn Creek) directs ebb flow oceanward perpendicular to the coast. The initial scour that occurred along the outer portion of the north jetty soon after it was constructed was the result of this strong ebb tidal current. The continuing scour was aided by wave effects that contributed to shifting the entrance channel alongside the jetty.

200. An analysis of the hydraulic regime at Masonboro Inlet by Kieslich and Mason (1975) had concluded that construction of a single jetty resulted in migration of the seaward portion of the thalweg toward the jetty; this would have happened regardless of the inlet-bay orientation or position of the jetty relative to direction of net longshore sediment transport. Although this migration was probably strongly influenced by predominance of the ebb tidal current, qualitative observations

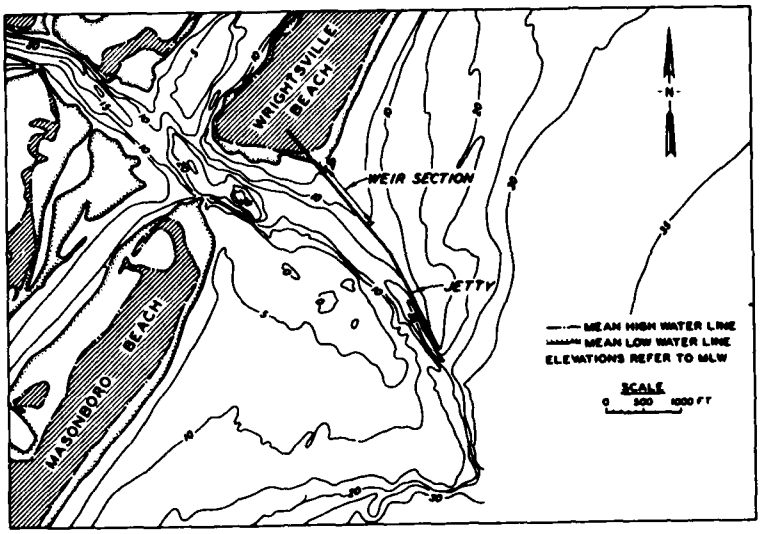

Figure 40. Masonboro Inlet, North Carolina, hydrographic survey for 1969 showing channel location after scouring adjacent to north jetty (after Seabergh 1979)

indicate that wave processes were also significant. Transport of littoral material to the inlet along adjacent beaches and deposition on the south shoal were results of combined tidal current and wave effects.

Galveston Bay and Harbor Entrance Channel, Texas

201. In the early 1960's, severe problems began to develop at the entrance channel to the Galveston Bay and Harbor. The original layout of the channel included a sharp turn located at approximately the inner end of the jetty, and this caused difficulty for large ships and tankers to negotiate at or near the strength of the tidal currents. The navigation channel had gradually migrated alongside the north jetty and the extremely deep water immediately adjacent to the jetty was causing concern that during a severe storm, a section of the jetty might slough into the channel as scour due to combined tidal current and wave action might completely undermine the structure.

202. Physical hydraulic model tests were conducted at WES (Simmons and Boland 1969) to develop plans for relocating and stabilizing the navigation channel between the jetties on an alignment and at a depth

suitable for the safe passage of supertankers, and to determine means for protecting the north jetty from the undermining action of scour by tidal currents and wave effects (Figure 41). A movable-bed model was used to reproduce the critical area under study. An analysis of the scaled-down forces available to move sediment in the model indicated that the movable bed should be molded of crushed coal. This material was of proper weight to permit movement and deposition in the model by the model hydraulic forces in a manner similar to the movement of prototype bed material by prototype hydraulic forces.

203. The objectives of the original model study were to determine a means for protecting the north jetty from being undermined by tidal currents and wave action effects. One of the plans tested in the model was constructed in the prototype. An analysis of pertinent data by Letter and McAnally (1977) 6 years after construction of the plan indicates that the model: (a) correctly predicted that the channel realignment and dredged-material disposal would halt undermining of the north jetty by tidal current scour; (b) correctly predicted a seaward shift in the channel shoaling volume distribution but overpredicted the magnitude of the shift--this overprediction was due to the erroneous scour prediction for the inner bar channel; and (c) correctly predicted that maintenance dredging volumes for the approach channel would increase. It was concluded that the model satisfied most qualitative objectives but failed to precisely meet some quantitative objectives.

Destin East Pass, Florida

204. Significant problems occurred during construction of the weir jetty system at Destin East Pass, Florida. While part of the problem can be attributed to construction problems, a major portion of the causes of the failure of the structure can be directly related to scour and erosion by combined tidal currents and wave action (Figure 42). The weir design specifications required the erection of concrete sheet piles driven 8 ft into the foundation and stabilized by massive timber wales that were bolted together. Construction problems began to occur when it appeared some of the connecting bolts were not threaded enough

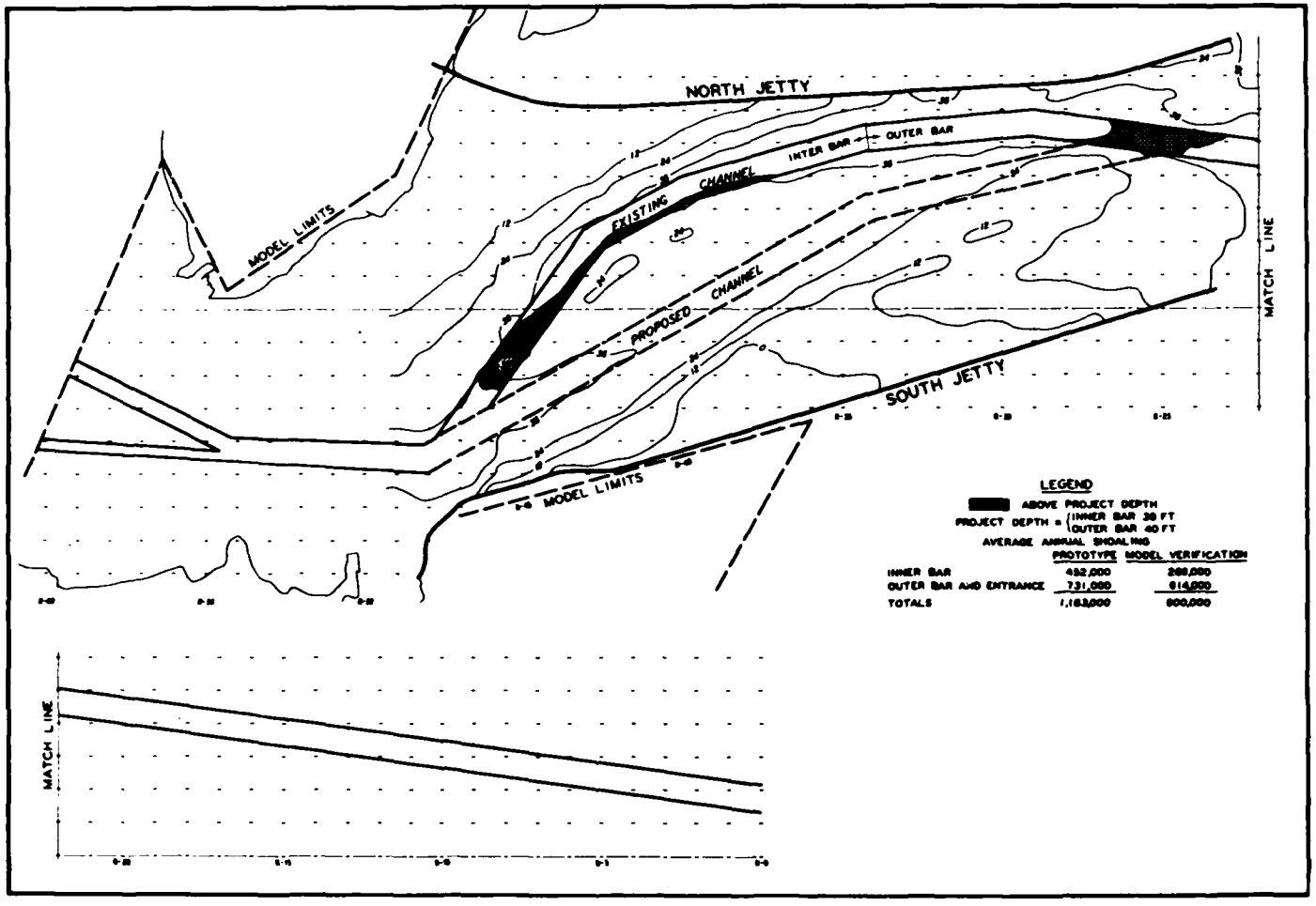

Figure 41. Galveston Bay and Harbor entrance channel, prototype existing channel condition before construction of proposed channel relocation (after Simmons and Boland 1969)

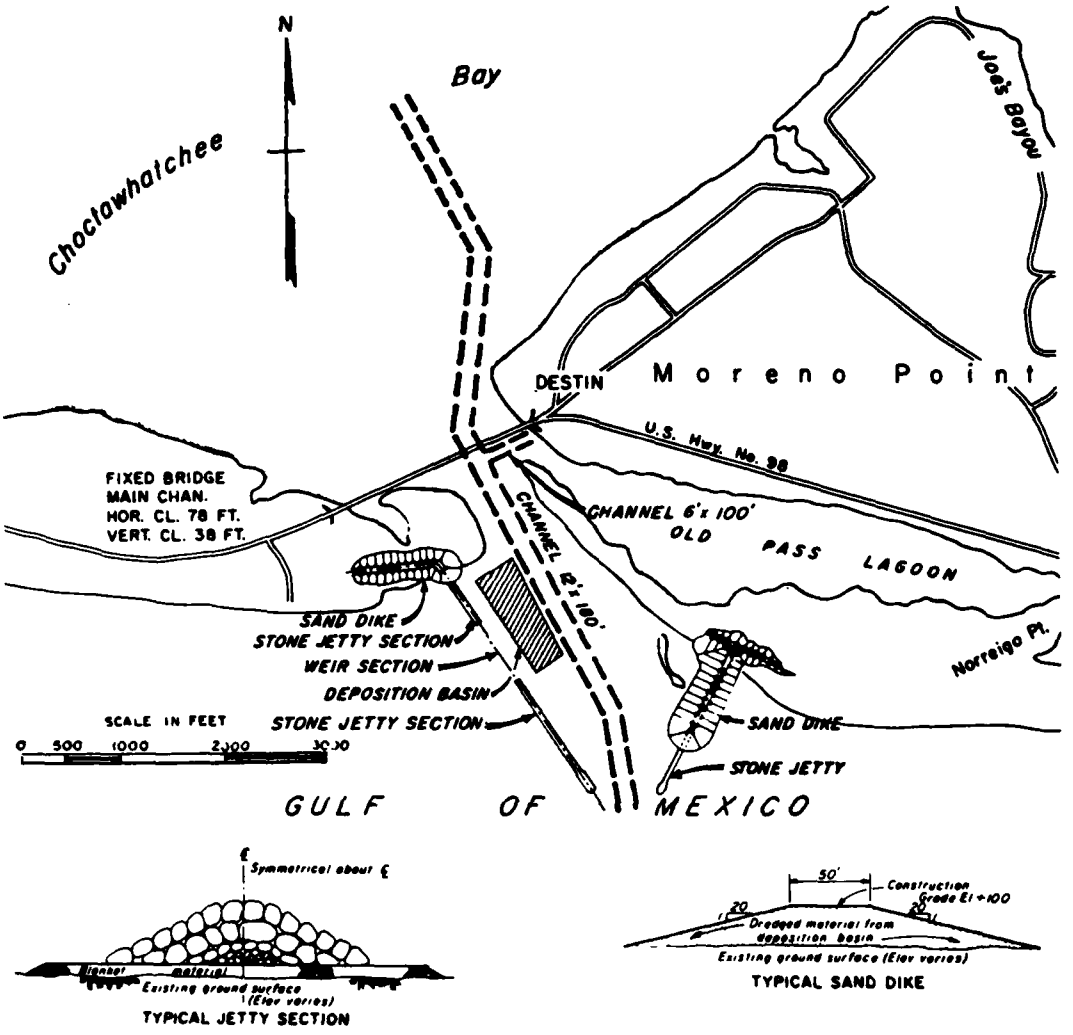

Figure 42. Destin East Pass, Florida, jetty alignment and deposition basin

to provide a rigid member. Waves breaking onto the sheet piling caused separation of some of the piles sufficient to allow currents and littoral material to pass, and scour holes up to 14 ft deep developed at the weir. Ebb currents on the order of 6 to 10 fps were not uncommon. Excessive torque developed in the wales, bolts sheared, and 100 ft of the weir section collapsed into the scour hole. The damaged section of the weir jetty was repaired by construction of a rubble-mound section instead of the originally designed concrete sheet piling.

Murrells Inlet, South Carolina

205. Until 1978, Murrells Inlet, South Carolina, was an unimproved inlet about 19 miles northeast of the city of Georgetown. Physical model tests were performed by WES (Perry, Seabergh, and Lane 1978) to aid in determining the optimum solution to navigation problems at Murrells Inlet. The final plan included a north weir jetty, a south jetty, and a sand dike at +10 ft mlw elevation parallel to the south shore to provide the landward end of the rubble-mound south jetty which would be constructed across the existing ebb current outflow channel and onto the shoal area. Murrells Inlet north jetty was completed in early 1979 and included a foundation blanket of filter material for bearing strength and erosion control. Scour was minimal to nonexistent during construction of the north jetty.

206. Construction of the south jetty was initiated upon completion of the north jetty in February 1979. Since the south jetty was planned to be constructed across the offshore shoal region, it was necessary to excavate some areas in order to reach the design grade for the structure foundation. It was anticipated (desired) that as construction of the south jetty proceeded from the south shoreline across the ebb channel, beneficial scour would result from combined strong ebb tidal current and potentially significant wave climate. It was expected that as closure of the channel proceeded, the reduced cross-sectional area for flow would experience an increased current velocity sufficient to initiate sediment movement and assist in necessary excavation of the shoal, estimated about 2 ft of material, to reach the design grade of the south jetty.

207. Scouring action that resulted from partial closure of the ebb channel was more severe and intense than anticipated, and the channel bottom scoured to approximately 5 ft below the design grade for the structure. More importantly, the ebb current was so intense that the foundation bedding material, which was being placed in the channel, would not remain long enough for the stabilizing core stone to be placed. Emergency operation procedures were initiated when it became apparent that ordinary construction techniques would not be sufficient to permit

further placement of structure material. It was necessary to divert the dredging operation from the navigation channel to provide fill material by pumping sand along and in front of the new jetty section. This was successful to the extent that the contractor was able to stay ahead of the stone placement and the jetty construction could continue.

Tillamook Bay, Oregon

208. A severe case of scour during construction occurred while building the south jetty at Tillamook Bay entrance channel, Oregon. This configuration is quite similar to that at Murrells Inlet, South Carolina, in that the south jetty would extend from the shore across a flood channel and onto a large shoal region. It had been anticipated that 3 to 5 ft of scour would result from strong ebb tidal currents and severe wave climate known to exist in the area. As jetty construction progressed across the channel, scour and erosion began to undermine the end of the structure; the channel proceeded to migrate at the same rate as the new jetty construction. The result was that a 40-ft-deep scour hole (unaccounted for in cost estimates) had to be filled. During the first year of construction, substantial overruns of stone quantities were experienced, reflected by the fact that approximately 5,000 ft of structure had been expected to be built and less than 3,000 ft was actually constructed.

209. During the second construction year of the Tillamook Bay south jetty, the technique of "accelerated core placement" was developed. To minimize scour of the ocean bottom ahead of the jetty, rapid placement of core stone was essential. The contractor was required to work all daylight hours, seven days per week, except as prevented by weather or sea conditions. Core stone placement was accomplished only when predicted tides for the 10-day period following were not expected to exceed a 9-ft differential between lower low water and higher high water. It was intended to place stone during a period when scouring tidal current velocities ahead of core construction were lowest and most favorable for the work. This accelerated placement technique reduced the depth of the scour hole by about 50 percent, from a 40-ft-deep hole during the first construction year to about 20 ft for subsequent construction periods.

PART VIII: SCOUR CONTROL TECHNIQUES

210. Rubble-mound coastal structures (breakwaters, groins, jetties, and seawalls) and the riprap used around ocean outfall pipelines and oil production structures constitute the most common types of marine construction presently in use. Rubble-mound structures have good wave energy dissipation characteristics which reduce wave runup and, thus, bottom scour and erosion. These structures are also relatively easy to construct and/or maintain and are relatively economical (compared with use of caissons or concrete armor units) since quarries are abundant. Unfortunately, many rubble-mound structures have failed because of scour and erosion both during and after construction. Many times scour during and after construction was not a design consideration. The interaction between waves, storm surges, currents, and the structures is extremely complex and not well understood. Most emphasis in structure design is placed on the size and weight of armor unit necessary for stability against wave attack or on foundation conditions for withstanding the bearing capacity of the huge structure. Inadequate foundation protection has been a contributing factor to partial or complete failure of many existing structures and has sometimes resulted in substantial cost overruns where scour during construction required the purchase and placement of additional material not included in the initial cost estimate.

211. Scour and erosion problems that occur around the toe of major structures are basically of two different types: (a) local scour due to sediment movement caused by intense current patterns generated by the existence of the structure itself and (b) general bed movement caused by wave effects or by longshore, tidal, or other currents of a regional nature. Several different erosion control techniques have been tested over the past few years and can be grouped into six fundamentally different categories:

a. Graded stone filters
b. Hot mastic asphalt
c. Synthetic fabrics
d. Filled plastic containers

e. Soil-cement

f. Prefabricated units

Not all of these categories of erosion control techniques are suitable for all situations, and some are much more adaptable to the local environment than others. Hence, the design engineer has only a limited degree of freedom in selecting and evaluating the optimum scour control technique for a particular location.

Graded Stone Filters

212. Graded stone foundation blankets are considered essential in the design and construction of rubble-mound structures, not only for an erosion control technique but also to provide a bearing surface on which to place the stone and/or artificial armor units that comprise the structure. Partial or a complete failure of some of these structures (rubble-mound seawalls and revetments) can be expected if a filter system is not provided or if the stone gradation specifications are improper. Some failures have been attributed to internal erosion where materials are removed by percolating water. As the tide rises or wave runup occurs, water fills the voids of the pervious section, and this water must be permitted to escape or hydrostatic pressure will cause slumping (instability) of the face of the structure (armor) or embankment.

213. Carver (1980) conducted hydraulic model tests at WES to determine the stability response of stone-armored breakwaters for a selected range of first underlayer weights. More specifically, it was desired to quantify, as a function of first underlayer weight, variations in the stability coefficient, wave runup, and wave rundown. Runup data are useful in selecting a crown elevation that will prevent excessive wave overtopping, and rundown data are useful in selecting the minimum depth below the still-water level to which the armor units should extend to prevent failure of the cover layer. Based on these test results in which stone armor was used on breakwater trunks and subjected to nonbreaking waves with a direction of approach of 90 deg, it was concluded that: (a) variations in first-underlayer stone weights

from 1/5 to 1/20 of the armor weight do not have a significant effect on armor stability, (b) armor stability will not be significantly influenced by relative depth (d/L) or wave steepness (H/L) over the range of conditions tested ($0.10 \leq d/L \leq 0.25$ and $0.026 \leq H/L \leq 0.079$), and (c) wave runup and rundown are not significantly affected by variations in first-underlayer stone weights in these ranges.

214. A properly designed graded filter must possess the following two properties: (a) it must be many times more pervious than the base on which it sits in order to effectively drain the structure which it supports (a reverse filter), and (b) it must be of such gradation that the base material will not migrate through the voids. Laboratory tests have been conducted by WES (Mansur and Olsen 1948) to develop the proper design for a filter system for Enid and Grenada Reservoirs. Results of these tests indicated that the gradation curve of the filter should be more or less parallel to the gradation curve of the base or material being drained for adequate stability. In general, the ratio d_{15} of the filter to d_{15} of the base should be less than 20, and the ratio d_{50} of the filter to d_{50} of the base should be less than 25 (d_{15}, d_{50}, etc., represent the grain size on a mechanical analysis curve corresponding to the percentage of particles by weight having diameters smaller than the percentage indicated by the subscript). The filter should be well graded from its maximum to its minimum size, with no large excess or lack of intermediate sizes, since this would increase the tendency toward segregation.

215. The gradation of the filter material depends on the characteristics of the backfill or bed materials and on the voids of rubble stones. The filter should be uniformly graded from fine sands, coarse sands, gravel, small stone, and large stone and can be placed in more than one protective layer. Seelye (1956) and more recent WES (1953) and Sherman (1978) studies recommend that

$$\frac{d_{15}\ \text{filter}}{d_{85}\ \text{base}} < 5$$

$$4 < \frac{d_{15}\ \text{filter}}{d_{15}\ \text{base}} < 20$$

$$\frac{d_{50}\ \text{filter}}{d_{50}\ \text{base}} < 25$$

$$\frac{d_{85}\ \text{filter}}{d_{\text{stone voids}}} > 2$$

The thickness of the filter blanket should be adequate for a complete coverage of all subgrade and backfill material. The foundation bedding material specified for many jetties and breakwaters consists of quarry-run spoils varying in gradation up to 12 in. This permits a keying action to develop as the smaller stones fill voids between larger stones, and the use of up to 80 percent of the quarry spoils frequently allows for a lower unit cost.

216. An important element of the erosion process, especially where it concerns wave action over a cohesionless bed, is the underflow induced in the bed by the variation of water pressure on it. Posey and Sybert (1961) have studied the scour that developed around Gulf of Mexico oil production platforms, and later Posey (1969) performed model tests of movable-bed materials to duplicate these prototype patterns. The production platforms were located in the Chevron Field of the Standard Oil Company of Texas at distances of up to 4 km from Padre Island. In this area the bottom material is a mixture of fine sand and silt, with small shell sometimes present. The depths of water at the platform sites varied up to 14 m; and although the area is subject to tropical hurricanes, none had visited the region between the time the platforms were completed and the scour protection measures were initiated. However, during winter storms the waves had reached up to 8 m in height, and this was sufficient to cause large motion of bottom material. Records of scour at these structures were kept and are summarized as follows:

Structure	No. of Months Structure in Place	No. of Months Scour Protection in Place	Max Scour Depth, m
No. A, Mar 1954,	30		2.7
2 km offshore	41		2.9
	48		3.6
	57		3.3
	63		3.3
	70		3.0
	74		3.6
	82		3.2
No. B, Sep 1954,	24		2.3
2.5 km offshore	42		4.0
	51		3.6
	57	5	0.0
	63	11	0.0
	74	22	0.0
No. D, Oct 1956,	17		3.0
2.6 km offshore	26		3.3
	32		3.0
	38		3.3
	43		3.2
	50	0	2.9
	51	1	0.0

The scour patterns observed did not consist of steep-sided conical holes around each pile, but were deep smooth-bottom saucers much larger than the entire structure and representing a large volume of removed foundation material. The appearance was as if the local scouring around each pile had overlapped until the cluster of piles had become one large obstruction.

217. Physical model tests were conducted at the Rocky Mountain Hydraulic Laboratory at a scale of 1:50 using fine sand as bed material and a uniform velocity of 0.3 m/sec in an effort to duplicate the scour patterns that had developed around these production platforms. The first erosion pattern did not resemble that observed in the prototype, as no general bed lowering in the vicinity of the model occurred. In an effort to duplicate the scour patterns, a number of distortions were attempted. Posey (1969) reports that it was necessary to abandon the sand bed and resort to movable beds composed of gilsonite (sp gr 1.06), in conjunction with mild currents and wave with heights of 0.2 m

and lengths up to 4 m. The saucer-like depressions were very similar in proportion to the prototype scour, and the mechanism observed seemed to be a possible one for action in the prototype. However, difficulties of working with gilsonite prevented testing details of the protective mat design.

218. To combat this erosion problem around the production platforms, it was decided to install a graded filter based on the criteria established by WES (Mansur and Olsen 1948). Layers of heavy pervious material were placed over the bed material, each layer having a grain size distribution so related to the layer below it that flow of water would not be able to move any of the fine material up into the coarser material above it. Steel mill slag was found to be the most economical, satisfactory material available, and it was used as the foundation mat around Structure No. B. Notwithstanding some inadequacies in the gradation of the material that was actually placed (Figure 43), the mat appears to be successful in preventing additional scour (Posey 1971).

Hot Mastic Asphalt

219. The need for quick and economical methods for making dike revetments in the Netherlands led to the widespread use of bituminous materials on and above the waterline. The idea then evolved that these same bituminous materials might be used for replacing or reinforcing the existing fascine and crushed stone foundation mattresses that were used to protect the shifting sandy bottom from current scour. In this region, large areas of the sandy bottom in the channels and closure gaps must be protected against scour by tidal currents and small wave action. The objective was to develop a quick and economical procedure by means of which a seamless slab of bituminous material of uniform thickness could be laid directly on the sand, or to evenly grout the rubble stone lying on the bottom so that less stone would be required and which could, moreover, be of a smaller size. The most attractive method should be a process by which the liquid material is conveyed to the bottom through pipes, because the material could flow to the required

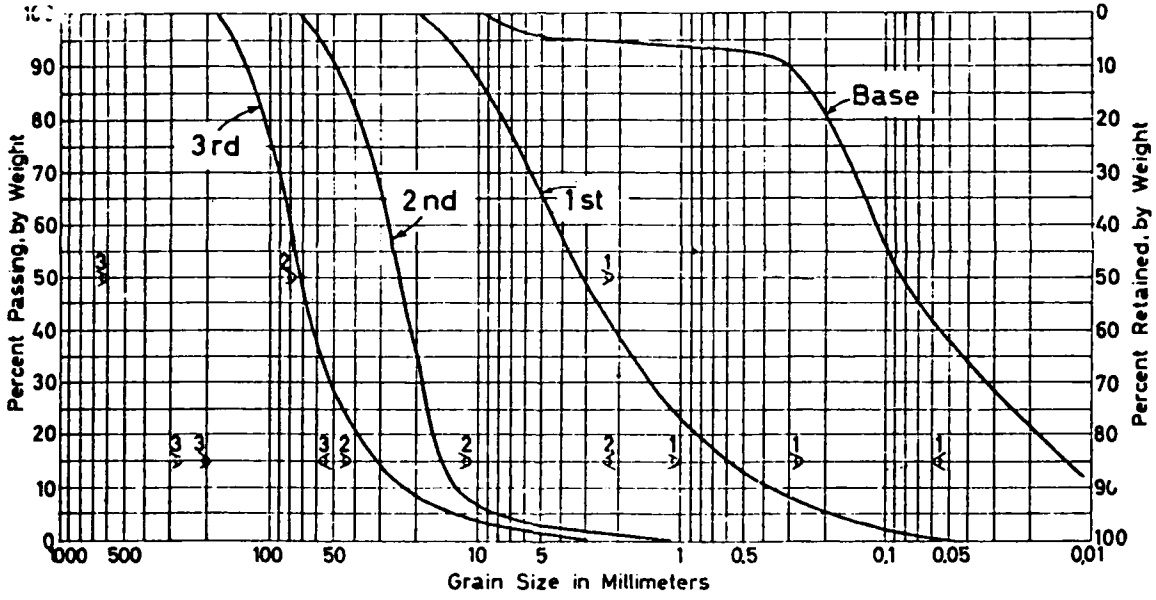

Figure 43. Prototype bed material and three gradation layers used to combat scour around oil production platforms in the Gulf of Mexico in water depth of 14 m, Structure No. B (after Posey 1961)

location under its own gravity from an asphalt mixer that might be installed on a ship. It has been shown that bituminous material can be made to flow out underwater at depths up to 400 m through unheated, uninsulated vertical pipes of only 15 cm in diameter without a high pumping pressure being necessary (Kerkhoven 1963). By fitting a specially designed piece of equipment to the outlet end of the pipe, the asphalt can be distributed evenly, with the speed of the work depending on the capacity of the asphalt mixer. It was found that 200 tons/hr could be placed which is equivalent to an asphalt mat 10 cm thick covering an area of approximately 1,000 m^2/hr, where the specific gravity of the mastic asphalt is about 2.

220. The bottom on which the protective layers were spread consisted of sand or rubble and was quite uneven with slopes occasionally existing of more than 1:10. Since it was not possible to drag the exit section over the rubble and stones, provisions were made to keep the mouthpiece at a fixed distance above the bottom. The depth of water in which mastic asphalt had been spread varied from 2 to 30 m; and because of tidal effects and slopes of the bottom, the depth continually changed during an operation. Current velocities of about 2 m/sec were encountered, on the average, although the finished surface experienced much higher currents as gap closure became smaller. The operations were carried out in water temperatures of around 10°C, wind forces of about 6 or 7, and a wave height of around 0.5 m. Schematics of the placement are shown in Figure 44.

221. The hot mastic asphalt is required to have certain material properties if the placement is to be effective. The material will need to be viscous in order to flow through the apparatus. The proper viscosity can be prepared by adding the proper quantities of asphaltic bitumen to a mixture of sand and filler. To avoid steam formation underwater, the temperature of the mixture should not be higher than about 100 to 130°C. Thus, the viscosity of the mixture should not exceed 10^4 poises in order to flow well, and should not be lower than about 10^3 poises to prevent intrusion of seawater.

222. In 1960, the Netherlands Delta Service commissioned the

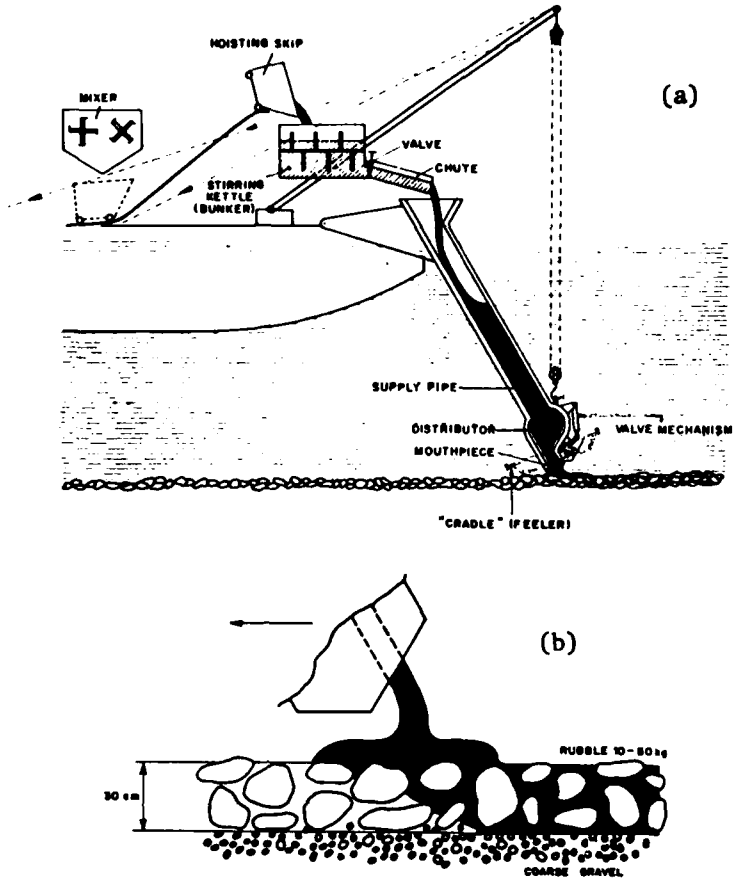

Figure 44. Placement of hot mastic asphalt on sand bottom or rubble for scour control (after Kerkhoven 1963)

grouting with mastic asphalt in a closure gap of the Zandkreek Dam. The closure was to consist of caissons placed on a layer of rubble of about 30 cm diameter, which was in turn imbedded in a layer of coarse gravel. The grout was intended to be placed at the rate of 300 kg/m^2 so as to ensure that scour and erosion by the strong tidal currents would not occur. After each day's operation, the work was inspected by divers who reported they could clearly see that the mastic asphalt penetrated between the stones, producing a compact and smooth layer of asphalt from which the stones protruded in many places. This was precisely the condition the Delta Service considered most suitable, with

the caissons coming to rest on the stone while the stones were yet firmly embedded and the bottom of the caissons were thus well sealed. The operation was regarded as a complete success. The divers also reported they could see the mix flow well and evenly from all openings of the placement apparatus, with about 2 min being required for the mix to penetrate between all the stones.

Synthetic Fabrics

223. Synthetic or man-made filter fabrics have in recent years come into wide use in solving a variety of civil engineering problems, especially those concerned with coastal structures and drainage problems. The fabrics are generally made from nylon, polyester, polypropylene, polyamide, polyethylene, or combinations of these. They are formed by weaving via traditional textile manufacturing methods or by bonding into a nonwoven form. There are at the present time approximately 25 different fabric types with some having as many as 11 different styles to choose from, according to Welsh and Koerner (1979). Various types of these filter fabrics have been found quite effective in increasing the stability of shore protection structures such as rubble revetments, seawalls, jetties, groins, and breakwaters.

224. Laboratory experiments were conducted by Lee (1972) to test the stability and sensitivity of rubble-mound breakwaters designed with graded and/or plastic filter systems. Particular attention was given to the characteristics of scour at the toe and under the foundation of the structure. Many hydraulic model studies on breakwater stability have neglected the effect of a movable bed on stability, including the problem of scour under the foundation. It was found that to prevent scouring under the structure it was necessary to extend a layer of core materials beyond the armor stone toe and then place two layers of secondary stones over this core layer with proper gradation. Alternatively, a plastic filter fabric may be placed under the breakwater and extend beyond the toe with secondary stones over it.

225. Compared with synthetic fabrics, the merits of the graded

stone filter system are that it is most likely available and has been widely accepted in practice. Its effectiveness is not susceptible to biodeterioration. On the other hand, the graded filter blanket is difficult to construct to specifications underwater, as the void ratio of the armor stone is necessary for the proper design of the filter and is not always easy to obtain. In general, the plastic filter fabrics have independent tensile strength and the screening process associated with graded stone filters is eliminated in construction. Consistency in design is obtainable and can usually be applied at any geographic location. However, the initial cost of the plastic filter fabrics may be higher than the graded stone; and the effectiveness over long-term operations may be reduced due to biodegradable characteristics.

226. Experience indicates it is necessary to offer plastic filter fabric of various permeabilities and tensile strengths to meet individual project requirements. Just as no one graded stone filter can suffice for every soil condition, neither is one type of filter fabric the answer to all filter problems. Depending upon local foundation conditions and void ratio of cover layers, the particle retention and permeability requirements of the fabric may vary from one location to another in the same structure. Where thickness is required, this element must be realized by the addition of a layer of gravel or crushed stone. Important considerations include type of structure, weight and type of armoring, method of construction, and forces the structure is designed to withstand. These variables determine the necessary abrasion resistance, tensile strength, and puncture strengths of the selected fabric. Barrett (1966) cited various types of membrane filters which had proven to be unsatisfactory. As a follow-up, Calhoun (1972) developed design criteria and acceptance specifications for plastic filter cloths to be used on U. S. Army Corps of Engineers projects. However, as pointed out by Dunham and Barrett (1974), since that time many new synthetics have been introduced on the market, and the acceptance specifications cover only a small portion of the fabrics available.

227. More recently, Keown and Dardeau (in preparation) have investigated the use of filter fabric for streambank protection, and

reevaluated filter fabric design considerations. They determined that two factors must be carefully weighed during selection and placement of a specific filter fabric for a given project application. These factors are: (a) filtration--the fabric must act as a filter, since the flow path through the fabric must be fine enough to prevent continuous infiltration of bed particles, yet large enough to allow water to pass freely, and (b) chemical and physical properties--the fabric's composition must be such that it will resist deterioration from chemicals found in the environment, and it must be strong enough to prevent tearing or puncturing during placement.

228. The equivalent opening size (EOS) of a fabric and the gradient ratio (GR) of the fabric-soil filtration system determine the filtration characteristics of a given fabric. For a given field application, the EOS must be known for the various fabrics available. The correct fabric can then be selected to ensure that fabric and bed material are properly matched to provide an effective foundation blanket. OCE (1975) guidelines to be used in selecting the correct filter fabric are:

> For fabric to be placed adjacent to granular materials containing 50% or less fines (those soils that will pass a U. S. Standard Sieve No. 200) by weight, the following ratio must be satisfied:
>
> $$\frac{d_{85} \text{ bed material (mm)}}{\text{EOS of filter cloth (mm)}} \geq 1$$
>
> For fabric to be placed adjacent to all other type soils: EOS no larger than the openings in the U. S. Standard Sieve No. 70. Filter fabric should not be placed on soils where 85% or more of the soil materials are fines.

To reduce the chance of clogging, no fabric should be specified with an EOS smaller than the openings of a No. 100 sieve. When possible, it is preferable to specify a fabric with openings as large as allowed by the criteria.

229. The GR of a given fabric-soil filtration system is the ratio of the hydraulic gradient over the 1 in. of soil immediately next to the fabric (i_f), to the hydraulic gradient over the 2 in. of material between 1 and 3 in. from the fabric (i_g).

$$GR = i_f/i_g \tag{117}$$

If the fine particles in the soil adjacent to the fabric get trapped in or on the fabric (clogging), the GR will increase. Likewise, if the fine soil particles move through the filter fabric (piping), the GR will decrease. As a general rule, the GR should not exceed 3.

230. Current Corps of Engineers specifications required that the plastic yarn used to manufacture filter fabric should consist of a long-chain synthetic polymer composed of at least 85 percent by weight of propylene, ethylene, ester, amide, or vinylidene-chloride, and shall contain stabilizers and/or inhibitors added to the base plastic (if necessary) to make the filaments resistant to deterioration due to ultraviolet and heat exposure. No guidelines are provided for non-plastic materials.

231. Synthetic filter fabric used on Corps of Engineers projects must conform to the physical strength requirements provided in Table 1. In addition, the fabric should be fixed so that yarn filaments will retain their relative position with respect to each other, and the edges of the fabric should be finished to prevent the outer yarn filament from pulling away from the fabric. In general, woven fabrics are considerably stronger in uniaxial tension than nonwoven fabrics, with the general ranking, in order of decreasing strength being: (a) heavy to intermediate weight woven fabrics, (b) intermediate to lightweight woven and heavy to intermediate weight nonwoven fabrics, and (c) lightweight nonwoven fabrics. Woven fabrics generally fail from localized strand breaking in tension or diagonal tearing suggestive of shear failure. Nonwoven fabrics fail primarily from diagonal tearing, excessive elongation, or strength drop without outward signs of fabric rupture or tearing.

232. Placement of any filter system underwater as required beneath jetties and breakwaters has always been a difficult problem. Some designers try to compensate for wave and tidal action by overdesign of the filter system, but even this offers no assurance that the filter bedding is actually placed properly. If properly placed, the use of synthetic filter fabrics eliminates much of the uncertainty regarding the condition of the filter when the heavier stones are placed upon it. Different placement methods have been applied at various locations, including the unrolling of large rolls and fixing the fabric to the bottom by stone anchors. Other methods include fastening the fabric to prefabricated steel frames and then placing the assembled frames permanently on the seabed beneath the proposed jetty or breakwater. Several manufacturers have developed techniques for deploying filter fabric, such as that of Figure 45 by Carthage Mills. Plastic filter fabric has been used at depths of up to 150 ft in the North Sea; hence, this is a versatile material which is adaptable to many adverse situations.

Filled Fabric Containers

233. Sand-filled or grout-filled fabric bags of various sizes have been used effectively for low-cost shoreline protection and scour control around coastal structures in many areas of the country. The bags, woven with nylon and coated with polyvinyl-chloride or acrylic to prevent fiber degradation by ultraviolet rays, are fabricated by several manufacturers. The bags are usually filled in place with available beach sand or pumped full of a grout mixture of cement and sand. The bags have been used to protect the toe of bulkheads, jetties, and groins. Depending upon wave climate, tidal range, and littoral drift characteristics, sand- or grout-filled bags have been used to fabricate entire groin sections. Shoreline revetments have been constructed by stacking layers of filled bags over an initial layer of filter fabric to prevent loss of supporting soil under wave attack at the toe of the structure. The first cost of any coastal defense system is usually high, and the cost-effectiveness of the filled bags depends largely on the

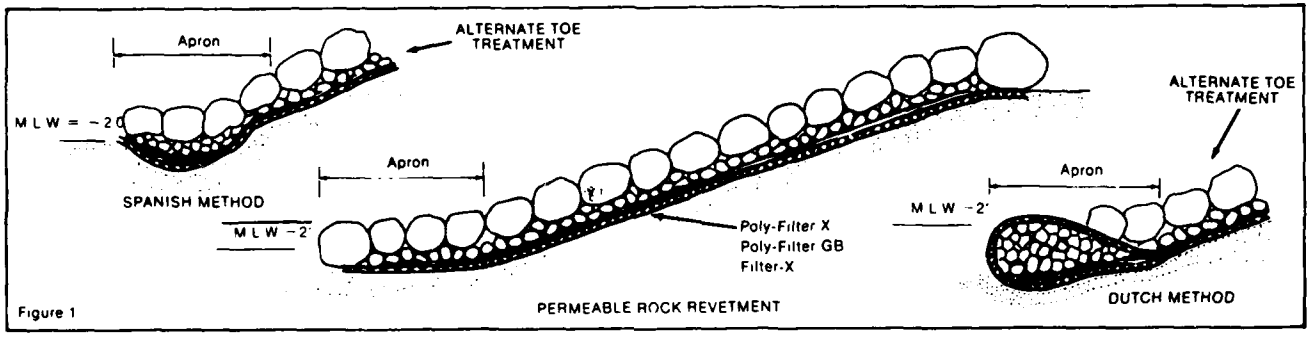

a.

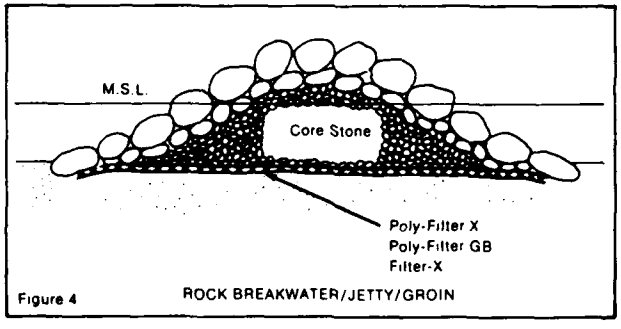

b.

Figure 45. Suggested procedures for placement of synthetic filter fabric under various type coastal structures, by Carthage Mills, Erosion Control Division

price of more traditional revetments. Experience has shown that unless the bags are filled with grout which hardens chemically, holes will be created by floating debris, pedestrian traffic, or vandalism. When placed in front of existing structures such as bulkheads or seawalls, it has been found expedient to make the placement after the winter waves have lowered the beach profile. Subsequent seasonal accretion will partially or completely cover the bags (Gutman 1979).

234. Different manufacturing companies have developed various types of units for a wide range of environmental conditions and market these products under several brand names. The Fabricast System of Intrusion-Prepakt Corporation was developed in response to a need for a reliable and less-costly coastal protection measure and utilizes large bags of high-strength synthetic fabric as forms for casting concrete blocks in place underwater. These blocks interlock inherently and may be rigidly connected by reinforcing steel bars or flexibly connected by means of steel inserts and cable connectors. The bags are filled with transit-mixed concrete delivered to the site and pumped into the bags through flexible hose lines which may be several hundred feet in length. An example of a Fabricast groin is shown in Figure 46 which was estimated to have been built at less than half the cost of rubble mound.

235. The Longard tube (manufacturered in Denmark and distributed

Figure 46. Concrete-filled plastic fiber bags comprising units of groin system

by the Edward Gillen Company of Milwaukee, Wisconsin) is a polyvinyl-coated outer shell of woven material. The tube is lined with polyvinyl sheeting for maintaining sand filler. The Longard tube is essentially an envelope of material which is given structural stability by filling the tube with pumped sand which provides weight and strength to the structure. The sand is pumped as a slurry into the tube, with a trap of filter cloth at the opposite end retaining the sand and allowing the water to drain out.

236. Longard tubes are used essentially to prevent beach erosion, and have been applied with success around the world. In the United States, these tubes have been installed at Grand Isle, Louisiana, which was the site of an emergency sand dune and beach replenishment project following Hurricane Carmen in 1974. This project, discussed by DeMent (1977), utilized two design concepts. The first consisted of a low-sill mound of sand covered by plastic filter cloth 18 ft wide and anchored by two 10-in. Longard tubes sewn to the outer edges of the plastic filter cloth. The top of the sand mound was built to approximately 1.0 ft msl.

237. The second design concept specified the building of a groin field by using six 40-in. Longard tubes 300 ft long and spaced 400 ft apart. In conjunction with this groin field a 40-in. tube 2,000 ft long running parallel to the beach was installed 50 ft from the landward edge of the groins. The 2,000-ft-long segment was the main element of the protection designed to retain the hydraulically placed sand fill. The top elevation of the Longard tube was built to 3.0 ft msl, with the design calling for placing the tubes initially on the existing beach profiles and then filling behind the tubes with sand to achieve the desired cross section. The completed project appears to be working well. Other field applications of a similar nature have been documented by Armstrong and Kureth (1979).

Soil-Cement

238. During the past 30 years a useful technique has been

developed by designers of embankments for slope stability and scour protection purposes, although the technique is not applicable to placement underwater. Soil-cement can be broadly defined as a mixture of natural soils, portland cement, and water. In its moist-compacted state, it forms a strong, durable, and economical material with properties similar to concrete and natural rock. American Society for Testing Materials standard tests in conjunction with other criteria are used to determine for a specific location the cement content and moisture content necessary to produce the strength, durability, and other characteristics that may be desired. A typical mixture contains about 10 percent cement and 10 percent water by weight of dry soil, but actual cement contents have ranged from less than 7 percent to more than 14 percent by weight.

239. While soil-cement is essentially impervious, some cracking is inevitable; therefore, the facing cannot be considered to be totally watertight and the toe should be stabilized with rock riprap or other elements to prevent underscour from eroding behind the stabilized beach slope. Also, leakage may sometimes take place through the bonding surfaces between layers, and the possibility exists that water may get behind the facing. The weight and strength of the facing are considered to be sufficient to resist any uplift pressures that may develop, particularly since outward drainage through cracks will exist. The revetment slope should be designed so that its least permeable zone is immediately adjacent to the soil-cement facing. Field applications of soil-cement have been discussed by Wilder and Dinchak (1979), and deficiencies in the present practice are evaluated. Proper control of the layer width and thickness is essential for adequate mixing of the cement. Material should be spread uniformly over the slope to be stabilized, with the mixture thickness varying from 6 to 9 in. A lack of uniformity often exists in distributing the cement spatially in the field. The soil fraction of the soil-cement is frequently beach sand and gravel which contains too many gravel particles larger than 1 in. and too much nonmineral debris, all of which adversely affect the density and overall quality of the soil-cement.

Prefabricated Units

240. In recent years, the concept of utilizing prefabricated units instead of graded stone filter blankets under jetties and breakwaters has been improved and applied in several locations. Also, preformed concrete units have been applied for slope stability and other scour and erosion control problems, particularly at the base of coastal structures to prevent scour of the toe and foundation.

Gabion units

241. Gabions are relative newcomers to American construction but have been installed in their present form in Europe since the late 1800's when the metal gabion was developed. This form (Figure 47) provides the necessary structural strength, and galvanizing adds durability with economy, thus broadening the field applicability. Gabions are compartmented rectangular containers made of galvanized steel hexagonal wire mesh and filled with stones. Compartments are formed of equal capacity by wire netting diaphragms or partitions. These partition walls add strength to the container and help retain its shape during the filling

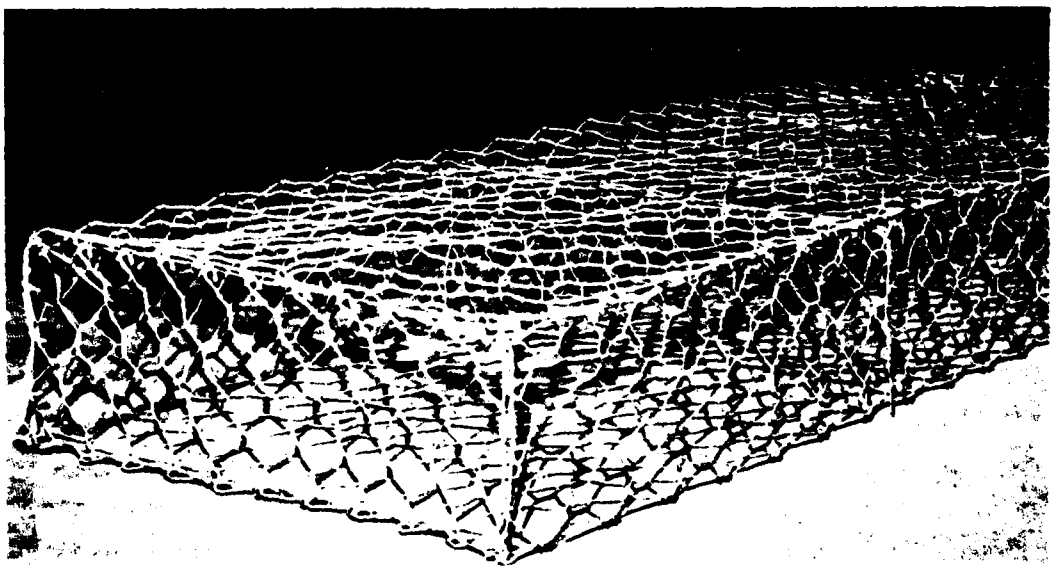

Figure 47. Gabion unit prior to filling with stone (after Terra Aqua Conservation, Bekaert Corporation 1977)

operation. They also provide assurance that the fill will remain evenly distributed, even after extensive settlement.

242. Gabion units are normally filled with hand-size stones, usually dumped into it mechanically. The filled gabion then becomes a large, flexible, and permeable building block from which a broad range of structures can be built. This is done by setting and wiring individual units together in courses and filling them in place, or by filling and then placing individual units. The wire mesh used in gabions is heavily galvanized. It may be safely used in fresh water and in areas where the pH (acidity indicator) of liquid in contact with it is not greater than 11. For highly corrosive conditions, a polyvinyl-chloride coating must be used over the galvanizing. Such treatment is an economical solution to deterioration of the wire in the ocean, in some industrial areas, and in polluted streams.

243. A favorable feature of the gabion unit is its flexibility. The triple-twist hexagonal mesh construction of the basket permits it to tolerate differential settlement without fracture. This property is especially important when the structure is placed on unstable ground in areas where scour from waves or currents can undermine it. The pervious nature of the gabion allows it to dissipate portions of the energy to which it is exposed. Gabion units have been known to remain effective long after the structure which they were protecting has passed its useful life. The flexible gabion apron designed for shore protection and other coastal structures is planned to settle without fracture and adhere to the ground as scour may occur. The foundation need not be completely level; however, if large holes are in existence before the initial construction begins, these should be filled with quarry-run material (frequently used to fabricate the foundation bedding material blanket under major coastal structures).

244. Gabion units have been used extensively to build up and widen beaches, due to their flexibility and ability to absorb wave action. They usually extend perpendicularly, or nearly so, from beyond low water to the shoreline. Their purpose is to trap or retard littoral drift and modify offshore currents. To be effective, the gabion groin

system should be used in a group rather than an isolated unit or groin. The system should be gradually built up, as complex factors are involved and conditions may vary widely along a section of beach. Gabions are well suited to the construction of the groin system as the individual building blocks forming the structure can be added or removed easily. Also, the permeability of the gabion groin permits a more uniform buildup of the beach than do impermeable groins.

245. The sea-type gabions recommended for seawall installations have the same triple-twist galvanized steel wire hexagonal mesh used under jetties and breakwaters, but they are given the additional protection of a coating of polyvinyl chloride to increase corrosion resistance. Successive levels of gabions in seawalls are usually set back 12 in. or more from the course below to give the wall an appreciable batter and to break up wave action and reduce spray. A flexible gabion apron should be used to protect the toe of the seawall, with the top of the apron flush with the existing shoreline. The rough exterior and the interstices in the stone-filled unit tend to retain the sand, and the pervious nature allows water which may splash over to drain through, thus eliminating some of the causes of seawall collapse. The installed gabion units become an immediate platform from which additional reaches of the wall may be fabricated, eliminating the necessarily long wait for curing necessary in concrete construction.

Gobimat units

246. The Gobimat system of slope protection for coastal applications consists of pretested, custom-designed concrete control blocks bonded to a hydraulic plastic filter cloth which can be very simply hoisted by a small crane and laid like a blanket on any slope where scour and erosion is a problem. This often eliminates the costly bulkhead and riprap method with the net result being a concrete revetment that will be completely covered with natural or planted grass above the waterline and affording scour control measures at the toe of the slope. Typical dimensions are shown in Figure 48.

247. Gobimat was developed in the Netherlands and Louisiana to combat the many severe erosion problems native to delta country. The

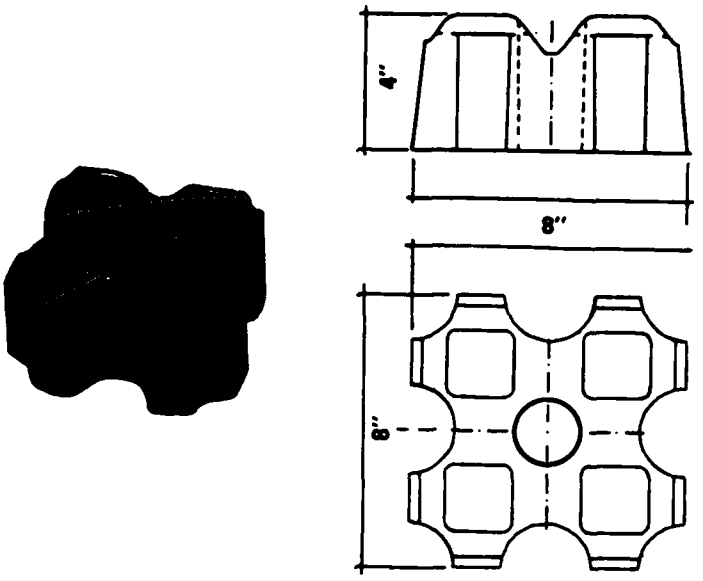

Figure 48. Typical configuration of Gobi units

system has been extensively tested at Delft Hydraulics Laboratory (1973a, 1973b), and is now being widely used throughout that nation. More recent tests have been conducted at CERC by McCartney and Ahrens (1975). Gobimat units are typically fabricated in sections 4 ft wide and up to 18 ft in length, with a 1-ft fabric overlap all around; hence, the sections may be joined lengthwise or widthwise. The filter fabric is made from a combination of polyethylene and polyester monofilament yarn which under normal conditions are chemically inert. The filter fabric is protected from the sun by the blocks so degradation by ultraviolet rays is rare. The concrete blocks are glued to the filter fabric with a two-component chemically inert polyurethane.

248. As a typical example of the application, erosion protection had long been needed at Holly Beach, Louisiana, and in 1970 the Louisiana State Highway Department constructed a 3-mile revetment project at this location to stabilize a section of Louisiana Highway 82 which lies directly adjacent to the beach. The importance of this coastal highway which connects Louisiana and Texas is related to the fact that it serves as a hurricane evacuation route. This highway had been seriously damaged

in the 1950's and 1960's by winter storms passing directly over the area, with wind setup from the Gulf of Mexico overtopping the highway which is approximately 7 ft above mean sea level. Major storms in this region are capable of generating significant waves at the coastline of 3 to 4 ft in height with maximum waves approaching 6 ft. Wave periods are estimated to be from 5 to 8 sec, according to DeMent (1977). This section of the State Highway is only 50 ft from the gulf.

249. A 200-ft portion of the revetment project was constructed of Gobi Blocks for test purposes. This prototype test section was divided into two 100-ft-long reaches. Both sections consisted of hand-placed blocks and differed only in the type of filter cloth used in the underlayment. The Gobi Blocks are approximately 4 in. by 8 in. by 8 in., weigh 13-1/2 lb each, and have an open area of 35 percent. For a design wave of 3.6 ft and placed on a 1:3 slope, the 13-lb Gobi Block provides a stability coefficient exceeding 50, which is greater than other known methods of erosion protection. This corresponds to a W_{50} size of riprap stone which varies from 150 to 360 lb.

250. The prototype test section was put through a very severe test only two weeks after completion when a winter storm inundated the highway and caused extensive damage along parts of the road. Prior to placement of the blocks, the filter cloth had been anchored by excavating a trench to the -3 ft mean low gulf elevation, which is approximately 2 ft below mean sea level. The bottom row of Gobi Blocks had been set against a 3- by 12-in. timber header. Currents running parallel to the shore eroded sand at the toe but did not displace any of the blocks. The experience at Holly Beach clearly proved that a filter cloth used in conjunction with Gobi Blocks in a structure subject to wave attack can have a high retention of the local soil while having a high ratio of open area in relation to the bank material area; i.e., the percent open area should exceed the porosity of the bank material to relieve hydrostatic pressure. A secondary filter of coarse beach sand and shell fragments was placed under the filter cloth which prevented the very fine sand from leaching out, but there was no clogging of the filter cloth at this installation. Success in this initial effort led to

successive installations, along with pertinent fundamental research on the subject by McCartney and Ahrens (1975).

PART IX: NUMERICAL TECHNIQUES FOR PREDICTING MOVABLE-BED EVOLUTION

251. When major structures are erected in the coastal zone, the normal current patterns may be altered to such an extent that changes are induced in sediment transport patterns. The existing equilibrium can be disturbed, resulting in large changes in bathymetry (i.e. scour) in the vicinity of the structures. In order to predict the extent of bathymetric changes induced by structures, the fluid-sediment-structure interaction must be understood. This involves the computation of current patterns and magnitudes around structures in the presence of a diffracting and refracting wave field. The theories and analytical studies that have been developed to this time are in many cases unable to provide comprehensive solutions to large-scale problems; they do, however, form the basic foundation upon which more sophisticated numerical procedures will be constructed. These numerical techniques are capable of cycling the physical phenomena to obtain the temporal as well as spatial solution.

252. A major objective of this investigation is to develop techniques for predicting the probable magnitude of scour that may result as a function of wave climate, tidal currents, or an interaction of these two. Numerical techniques to be developed will incorporate both refraction and diffraction effects near the structure, will compute wave-induced and other velocities in the vicinity of the structure, and will apply these results to estimate sediment transport characteristics at the particular location. The flux of material around the structure will be accounted for; consequently, an estimate can be made of the extent of erosion or accretion as a function of wave climate, tidal currents, or a combination of these phenomena.

253. Fully analytical models are quite restricted in application because the set of equations that describe the behavior of water masses has been solved analytically for very few cases and then only for very simple geometry. The mathematical model will consist of the equations of motion, together with the appropriate boundary conditions and

empirical parameters, and will be solved by numerical techniques as this is usually the most productive approach.

Numerical Modeling of Tides

254. The numerical modeling of water wave behavior, especially long waves and tides, has progressed rapidly in the past few years and is now recognized as a valuable tool for the solution of many coastal engineering problems. The principal features of the water movement that must be reproduced are the tidal current velocity patterns, the water-surface elevations, and the dispersion of concentrates such as contaminants, heat, or sediment throughout the region of interest.

255. Many different estuarine tidal circulation models have been developed in recent years in response to the user needs. The range of models indicates the wide variation of requirements and techniques. The basic equations for all the models are the Reynolds equations of motion, the conservation equation of mass, and the conservation equation for each concentrate under consideration. The principal simplifications usually made to the Navier-Stokes equations are: (a) to average out the turbulence, (b) to use empirical resistance coefficients to represent shear stresses, and (c) to average the equations over one or more spatial dimensions.

256. As discussed by Hinwood and Wallis (1975a, 1975b), three different temporal averaging periods have historically been used in developing water quality or tidal flow models. When the hydrodynamic, conservation of mass, and transport equations are derived by averaging over a relatively short time period (long compared with the turbulence time scale but short compared with the tidal period), the time period is taken to be an interval of a few minutes. If the temporal averaging period is made equal to a tidal period, then tidally averaged equations are obtained. With a very long averaging period (many tidal cycles), the temporal variability of concentrates may not be significant, and the equations obtained represent steady-state conditions.

257. To simplify the fully three-dimensional aspects of the

fundamental equations of motion of a viscous fluid, averaging over one or more spatial dimensions has been employed: (a) averaging over the depth (the most frequently used method) leads to a two-dimensional model in plan view; (b) averaging over the width leads to a two-dimensional model in side elevation; (c) averaging over the cross-sectional area leads to a true one-dimensional model; and (d) finally, averaging over the volume of the bay or estuary leads to essentially a zero-dimensional model. Hydrodynamic models are considered to be those in which the velocity field is computed by solving the equations of motion; kinematic models are those in which the velocity field is computed from the equation of mass conservation. On the other hand, transport models require that the velocity field be supplied and the bulk movement and dispersion of contaminants or sediments are then simulated.

258. In order to mathematically model and predict the dispersion of sediments, it is essential to be able to predict accurately the time-dependent currents of the region. Three-dimensional, time-dependent models are required, and they can generally be classified as free-surface or rigid-lid models (Sheng et al. 1978). The three-dimensional time-dependent flow in the Western Basin of Lake Erie has been calculated numerically by Sheng et al. (1978) by means of both a rigid-lid model and a two-mode free-surface model. For rigid-lid models it is assumed that the vertical velocity at the undisturbed location of the free surface is zero. This eliminates the motion and time scales associated with the surface gravity waves and allows much larger numerical time-steps than is possible for free-surface models. In the two-mode free-surface model, the surface elevation is treated separately from the internal three-dimensional flow variables (vertically integrated quantities are calculated). Short time-steps are thus needed only for the two-dimensional free-surface calculations and much longer time-steps can be used for calculations of the three-dimensional structure.

259. Detailed comparisons of the results of the free-surface and rigid-lid models were presented for two wind conditions by Sheng et al. (1978): (a) a constant wind suddenly imposed, and (b) an actual wind which is variable in both space and time. For relatively short time

intervals, it was found that significant differences between the results of the two models occur since the seiche motion of the lake is eliminated in the rigid-lid model. Long-term time-averaged circulation computed by the two models agrees well in periods of strong wind, but differs appreciably in periods of light wind and active seiching.

260. Sheng and Lick (1979) investigated the time-dependent flow and dispersion of suspended sediments in the Western Basin of Lake Erie by means of numerical models utilizing data from remote-sensing studies and flume experiments. The time-dependent currents were computed by means of a free-surface hydrodynamic model, and a wave-hindcasting model was used to compute the wave parameters needed for estimation of shear stress generated at the sediment-water interface under given wind conditions. The rate of sediment resuspension as a function of bottom shear stress and sediment properties was based on data from flume experiments using lake sediments. Computations were also performed for a two-dimensional lake with a variable bottom representing a section of the lake. It was found that wind direction and fetch length can significantly affect the sediment dispersion patterns.

261. Many numerical models have been developed for treating specific situations, for example, Abbott and Marshall (1969), Banks (1969), Dronkers (1969), Wada (1969), Leendertse (1970), Dean and Taylor (1972), Abbott, Rodenhuis, and Verwey (1973), and Boericke and Hall (1974). The Corps of Engineers has been required for some time to provide reliable estimates of estuarine circulation, velocity patterns, and coastal flooding from tides and hurricane surges; hence, the necessity for a generalized numerical model for treating these hydrodynamic problems has been apparent for some time. A numerical model, WES Implicit Flooding Model (WIFM), was first devised for application in simulating tidal hydrodynamics of Great Egg Harbor and Corson Inlets, New Jersey (Butler 1978a). Program WIFM originally employed an implicit solution scheme similar to that developed by Leendertse (1970), and a variable-grid system was developed for simulation of tidal hydrodynamics of the Coos Bay-South Slough, Oregon, complex by Butler (1978b).

262. Basic features of Program WIFM, developed by Butler (1979),

include inundation simulation of low-lying terrain, treatment of subgrid barrier effects, and a variable grid option. Included in the model are actual bathymetry and topography, time and spatially variable bottom roughness, inertial forces due to advective and Coriolis accelerations, rainfall, and spatial and time-dependent wind fields. Horizontal diffusion terms in the momentum equations are optionally present and can be used, if desired, for aiding stability of the numerical solution. Solution schemes include choices of both implicit and explicit formulations written in terms of velocity- or transport-dependent variables. The model also employs a one-dimensional channel routine that can be coupled dynamically to any cell in the grid system.

263. The hydrodynamic equations used in Program WIFM are the classical shallow-water wave equations. Expressed in a Cartesian coordinate system (Figure 49), the equations of motion are given as:

MOMENTUM

$$\frac{\partial U}{\partial t} + \frac{\partial}{\partial x}\left(\frac{U^2}{d}\right) + \frac{\partial}{\partial y}\left(\frac{UV}{d}\right) - fV + gd\,\frac{\partial \eta}{\partial x} = -\frac{gU}{C^2 d^2}\left(U^2 + V^2\right)^{1/2} + F_x \quad (118)$$

$$\frac{\partial V}{\partial t} + \frac{\partial}{\partial x}\left(\frac{UV}{d}\right) + \frac{\partial}{\partial y}\left(\frac{V^2}{d}\right) + fU + gd\,\frac{\partial \eta}{\partial y} = -\frac{gV}{C^2 d^2}\left(U^2 + V^2\right)^{1/2} + F_y \quad (119)$$

CONTINUITY

$$\frac{\partial \eta}{\partial t} + \frac{\partial U}{\partial x} + \frac{\partial V}{\partial y} = R \quad (120)$$

The fluid has been assumed incompressible and homogeneous and all density variations are neglected. In these equations, U and V are the vertically integrated transports per unit of width at time t in the x and y directions, respectively; η is the water-surface elevation with respect to the given datum; $d = \eta - h$ is the total water depth at (x,y,t); f is the Coriolis parameter; C is the Chezy coefficient; F_x and F_y are terms representing external forcing functions such as wind effects; g is the acceleration due to gravity; and R is a term

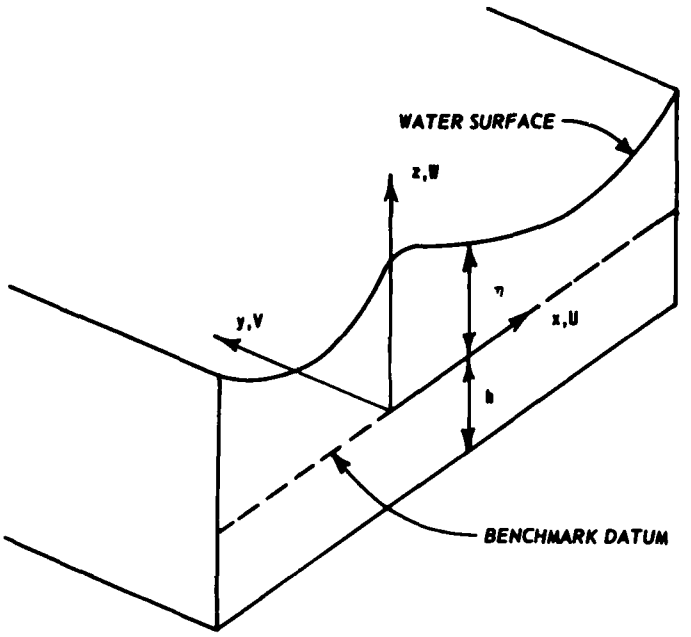

Figure 49. Coordinate system for Program WIFM problem formulation (after Butler 1978b)

representing the rate at which additional water is introduced into or taken from the system.

264. The initial version of Program WIFM only permitted the use of a regular-spaced rectilinear grid system. Due to the nature of the Coos Bay-South Slough complex and the relatively small dimensions of plan modifications to be tested, it was necessary to develop a variable grid procedure to permit economical simulation of the study region. A coordinate transformation given by

$$x = a + b\alpha^c \tag{121}$$

where a, b, and c are arbitrary constants, was applied piecewise for each axis. One may consider this transformation as mapping prototype space, discretized with a smoothly varying grid, into computational space (α-space) employing a regular-spaced grid. The transformation is such that in α-space all derivatives are centered. By applying a

smoothly varying grid whose functional as well as first derivatives are continuous, stability problems usually associated with variable grid schemes are eliminated. This type of transformation permits simulation of a complex landscape by locally increasing grid resolution and/or aligning coordinates along physical boundaries. The equations of motion in α-space can be written as

MOMENTUM

$$\frac{\partial U}{\partial t} + \frac{1}{\mu_1}\frac{\partial}{\partial \alpha_1}\left(\frac{U^2}{d}\right) + \frac{1}{\mu_2}\frac{\partial}{\partial \alpha_2}\left(\frac{UV}{d}\right) - fV + \frac{gd}{\mu_1}\frac{\partial \eta}{\partial \alpha_1} = -\frac{gU}{C^2 d^2}\left(U^2 + V^2\right)^{1/2} + F_{\alpha_1} \tag{122}$$

$$\frac{\partial V}{\partial t} + \frac{1}{\mu_1}\frac{\partial}{\partial \alpha_1}\left(\frac{UV}{d}\right) + \frac{1}{\mu_2}\frac{\partial}{\partial \alpha_2}\left(\frac{V^2}{d}\right) + fU + \frac{gd}{\mu_2}\frac{\partial \eta}{\partial \alpha_2} = -\frac{gV}{C^2 d^2}\left(U^2 + V^2\right)^{1/2} + F_{\alpha_2} \tag{123}$$

CONTINUITY

$$\frac{\partial \eta}{\partial t} + \frac{1}{\mu_1}\frac{\partial U}{\partial \alpha_1} + \frac{1}{\mu_2}\frac{\partial V}{\partial \alpha_2} = R \tag{124}$$

where

$$\mu_1 = \frac{\partial x}{\partial \alpha_1} = b_1 c_1 \alpha_1^{(c_1 - 1)} \tag{125}$$

$$\mu_2 = \frac{\partial y}{\partial \alpha_2} = b_2 c_2 \alpha_2^{(c_2 - 1)} \tag{126}$$

The quantities μ_1 and μ_2 define the stretching of the regular-spaced computational grid in α-space (spatial steps of $\Delta\alpha_1$ and $\Delta\alpha_2$) to approximate a study region in real or prototype space (x,y space).

265. Program WIFM was applied to the Coos Bay-South Slough complex and found to reproduce satisfactorily the hydrodynamic response of

the system to a specified astronomical tide. The verification procedure substantiates the model's ability to reliably predict the impact of proposed modifications on tidal elevations, current velocities, and circulation patterns within the study area. Most velocity and circulation changes associated with proposed modifications were confined to the local vicinity of the proposed plans.

Combined Wave Refraction and Diffraction

266. When surface gravity waves propagate shoreward, they are influenced by six dominant phenomena: diffraction, refraction, reflection, shoaling, dissipation, and resonance. The primary effect of all of these phenomena is to alter wave height which, in turn, directly influences the scouring potential of the wave climate. Diffraction and refraction are the primary influences on wave height except when they reach a boundary where dissipation and reflection manifest themselves.

267. Wave refraction. Wave celerity or phase velocity is dependent on wave period and water depth. Celerity decreases with decreasing depth, thus celerity varies along the wave crest which moves at an angle to the underwater contours. That part of the wave crest in deeper water is moving faster than that part in shallower water. This variation in phase speed or celerity causes the wave crest to bend toward alignment with the contours, and this bending effect is called wave refraction.

268. Refraction has a significant influence on the wave height and distribution of wave energy along the coast, since the change of wave direction results in convergence and divergence of wave energy. Its effect on erosion and deposition of beach sediments contributes to bathymetric alterations. Practically all engineering applications of wave refraction theory use the linear theory which is based on the assumptions that there is energy conservation between orthogonals and that the direction of wave advance is normal to the wave crest. A discussion of the limit of applicability of linear wave refraction theory is given by Whalin (1971, 1972).

269. Wave diffraction. Diffraction refers to the propagation of

energy laterally along a wave crest (i.e. energy will propagate from a region of larger height to a region of smaller height). The classically used example of wave diffraction is the case of a wave propagating past a breakwater, which results in a lateral transfer energy along the wave crest and across wave orthogonals to produce a wave behind or in the shadow zone of the breakwater. When the depth of water behind the obstruction is constant, no refraction occurs and diffraction effects can be easily isolated. Penny and Price (1952) proposed the original solution for the breakwater diffraction problem based on the fact that surface gravity waves of small amplitude passing a semi-infinite breakwater create the same boundary-value problem as that in light diffraction. Wiegel (1962) developed diffraction diagrams for a uniform depth adjacent to an impervious structure. These diagrams can be scaled so that a particular wavelength corresponds to the scale of the hydrographic survey data being applied.

270. In actual practice, it is rare indeed that water of constant depth exists behind and adjacent to structures on the coastline. Of more direct concern in solving real-world engineering problems is that a combined solution of the refraction/diffraction problem is necessary to calculate wave transformations in intermediate and shallow water since any refraction (causing a variation in height along a crest) automatically results in simultaneous energy diffraction which tends to make the height uniform along the wave crest. The procedure developed by Blue and Johnson (1949), and considered to be the state of the art until the early 1970's, evaluated both refraction and diffraction separately by approximation techniques. The procedure consisted of performing refraction analyses shoreward from deep water to the breakwater or other structure. At this point, diffraction diagrams were prepared that carried the successive crests shoreward three or four wavelengths. With the wave crest and wave direction indicated by the last shoreward wave crest determined from the diffraction diagram, construction of a new refraction diagram to the breaker line was prepared. The validity of this technique has come into question regarding its ability to determine effects on bottom currents around structures from the scour and sediment

transport standpoint. In order to refine the precision of computations of near-bottom velocities, techniques have been developed which solve the fundamental differential equations that govern both refraction and diffraction.

271. One of the first investigations of the combined effects of refraction and diffraction was performed experimentally by Mobarek (1962). The main purpose of that investigation was to study the effect of bed slope on wave diffraction through a gap in a breakwater normal to the incident wave travel direction. The study was conducted, however, in a very small facility, and scale effects may have been important. More experiments on a larger scale and with more equipment were strongly recommended by the author in order to obtain quantitative results. One such experiment was conducted by Whalin (1971).

272. Worthington and Herbich (1970) developed a computer program to estimate the combined effect of refraction and diffraction around a semi-infinite breakwater. The technique used is to initiate orthogonals as in usual refraction computations. Then as each point along an orthogonal is located, the refraction and shoaling coefficients are calculated. Following this, the coordinates of the point are transformed into coordinates used in the diffraction coefficient calculations, and a wavelength at that point is calculated. With this information, a diffraction coefficient is calculated and the wave height at that point becomes the product of the shoaling, refraction, and diffraction coefficients applied to the deepwater wave height. Once all the primary orthogonals have been plotted, the program initiates a second series of orthogonals in the lee of the breakwater . The orthogonals of this series all start at the breakwater tip but differ from each other in the direction each takes initially. This direction is established by the program itself which assigns the first radial orthogonal a direction 15 deg clockwise from the breakwater line. Each successive radial orthogonal is assigned an initial direction 15 deg clockwise from the preceding one; and the initiation of radial orthogonals is continued until finally an orthogonal is propagated out of the lee of the breakwater.

273. The program developed by Worthington and Herbich (1970) is limited to predicting the wave height and direction under the combined influence of refraction and diffraction by a semi-infinite breakwater. The wave heights obtained from the program have been demonstrated to be accurate to within 13 percent of actual values obtained in laboratory investigations. The program is flexible within its intended framework, but should not be used without a thorough understanding of its limitations. It is intended to apply to breakwater gaps of five wavelengths or more, and there is assumed to be no wave generation within the zone of study. Bottom friction effects are not included in the computations.

274. A method was developed by Ito and Tanimoto (1972) for obtaining numerically the wave patterns in any region of arbitrary shape from deep water to shallow water. The principle is to solve the linearized wave equations under the given boundary conditions from a certain initial state. The wave equation is derived from the Eulerian equations of motion and of continuity and includes only unknown functions at the water surface. By using this approach, it is possible to investigate various problems of wave propagation in the region of arbitrary shape and variable water depth.

275. The nondimensional basic differential equations are converted into finite-difference equations as:

$$\eta(i,j)^{t+\Delta t/2} = \eta(i,j)^{t-\Delta t/2} - \frac{\Delta t}{\Delta x}\left[u(i+1,j)^{t} - u(i,j)^{t}\right] - \frac{\Delta t}{\Delta y}\left[v(i,j+1)^{t} - v(i,j)^{t}\right] \tag{127}$$

$$u(i,j)^{t+\Delta t} = u(i,j)^{t} - \frac{\Delta t}{\Delta x}\left[\eta(i,j)^{t+\Delta t/2} - \eta(i-1,j)^{t+\Delta t/2}\right] \tag{128}$$

$$v(i,j)^{t+\Delta t} = v(i,j)^{t} - \frac{\Delta t}{\Delta y}\left[\eta(i,j)^{t+\Delta t/2} - \eta(i,j-1)^{t+\Delta t/2}\right] \tag{129}$$

The computations are performed by propagating a sinusoidal wave train in the negative x-direction as the incident wave. Time is initialized when

the front of the incident wave train reaches the front of the structure, and the initial wave conditions are given by conventional small amplitude wave theory (Airy Theory).

276. The applicability of the method of Ito and Tanimoto (1972) was confirmed by determining the distribution of wave height over a submerged shoal by both numerical calculation and hydraulic model tests. This comparison for a caustic problem in the region of ray convergence is shown in Figure 50. The calculated wave heights agree quite well with those obtained from the model tests with the maximum wave height being 2.1 H_i at the rear of the shoal where linear refraction theory indicates infinite wave height. This method of analysis can be applied to regions of more realistic bottom topography as well. Simultaneous hydraulic model tests by Whalin (1972) at WES with a circular shoal region which penetrated the surface also indicated that linear refraction theory was inadequate for predicting the refraction coefficients in a convergence zone, even when the refraction coefficients were as low as 1.1 to 1.2. In those situations where a convergence zone exists it is imperative to include diffraction effects on wave transformation.

277. A two-dimensional differential equation that describes the combined effect of refraction and diffraction of water waves has been sought by researchers for many years. The disadvantage of the expressions prior to 1972, according to Berkhoff (1972), is that they do not reduce precisely to the appropriate refraction equations. Also, they do not transform to the well-known linear shallow-water equations in the case of small water depth. The Berkhoff (1972) development

$$\nabla \cdot (CC_g \nabla \phi_o) + \omega^2 \frac{C_g}{C} \phi_o = 0 \tag{130}$$

where

$$n = \frac{1}{2}\left[1 + \frac{2k_o d}{\sinh (2k_o d)}\right] \tag{131}$$

$$C_g = nC \tag{132}$$

and

$$C = \omega / k_o \tag{133}$$

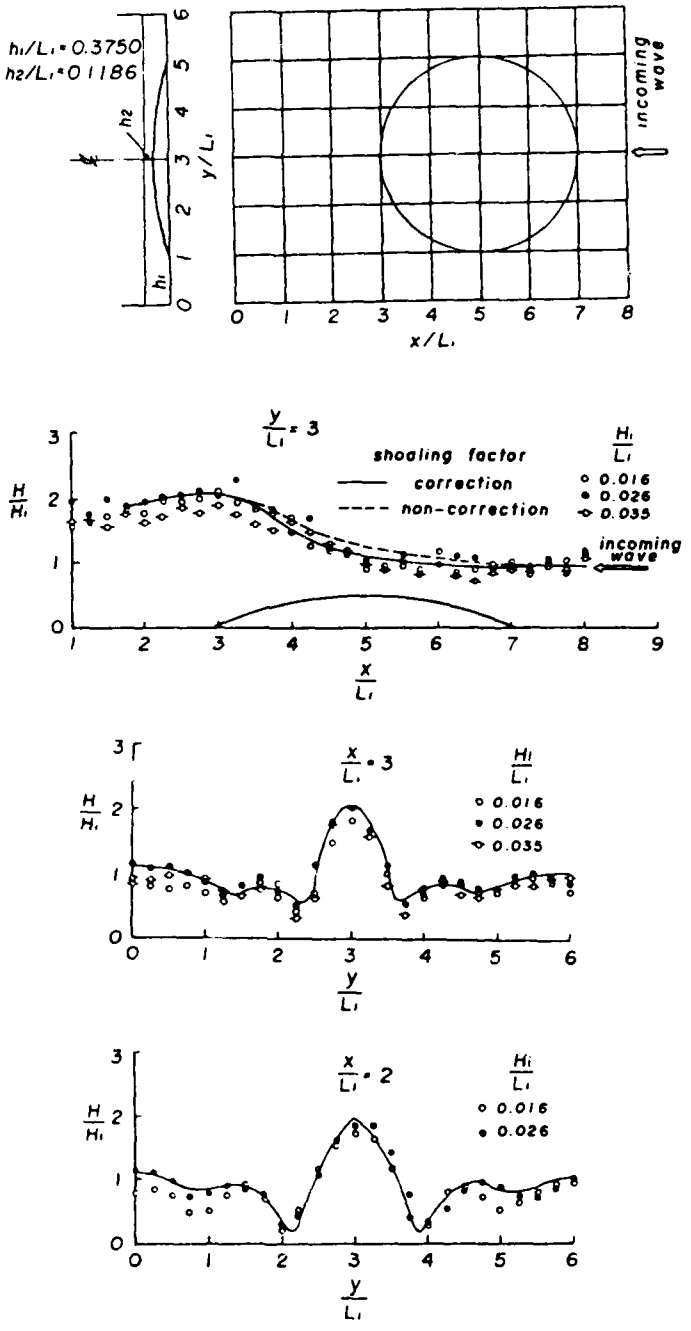

Figure 50. Comparison of calculated wave heights with experimental results for waves propagating over a submerged shoal (after Ito and Tanimoto 1972. By permission of American Society of Civil Engineers)

becomes the diffraction Helmholtz equation in the case of deep water or constant water depth, and corresponds to the linear shallow-water equation which can also be derived from the shallow-water approximation. Thus, Equation 130 describes both the refraction and the diffraction phenomena.

278. Berkhoff (1976) also developed two-dimensional wave propagation expressions for diffraction alone and for refraction alone. In the diffraction model, water depth is either constant or deep and the velocity potential ϕ is a solution of the Helmholtz equation with a constant wave number k_o :

$$\frac{\partial^2 \phi}{\partial x^2} + \frac{\partial^2 \phi}{\partial y^2} + k_o^2 \phi = 0 \tag{134}$$

Introducing a wave amplitude function, a , and a phase function, S , by

$$\phi = a\, e^{iS} \tag{135}$$

$$\frac{1}{a}\left(\frac{\partial^2 a}{\partial x^2} + \frac{\partial^2 a}{\partial y^2}\right) + \left(\frac{\partial S}{\partial x}\right)^2 + \left(\frac{\partial S}{\partial y}\right)^2 - k_o^2 = 0 \tag{136}$$

and

$$\frac{\partial}{\partial x}\left(a^2 \frac{\partial S}{\partial x}\right) + \frac{\partial}{\partial y}\left(a^2 \frac{\partial S}{\partial y}\right) = 0 \tag{137}$$

In the refraction model a slow variation of water depth was considered, but variation of the wave amplitude in the horizontal plane was ignored:

$$\left(\frac{\partial S}{\partial x}\right)^2 + \left(\frac{\partial S}{\partial y}\right)^2 - k_o^2 = 0 \tag{138}$$

and

$$\frac{\partial}{\partial x}\left(\frac{k_s}{k_o^2} a^2 \frac{\partial S}{\partial x}\right) + \frac{\partial}{\partial y}\left(\frac{k_s}{k_o^2} a^2 \frac{\partial S}{\partial y}\right) = 0 \tag{139}$$

where

k_o = a variable wave number corresponding to the local water depth d

k_s = a variable shoaling coefficient, also a function of depth

In the combined refraction and diffraction model of Berkhoff (1976), again a slow variation of water depth was assumed; and the variation of the wave amplitude was included in the formulation

$$\frac{1}{a}\left(\frac{\partial^2 a}{\partial x^2}+\frac{\partial^2 a}{\partial y^2}\right)+\frac{k_o^2}{k_s a}\left[\frac{\partial a}{\partial x}\frac{\partial}{\partial x}\left(\frac{k_s}{k_o^2}\right)+\frac{\partial a}{\partial y}\frac{\partial}{\partial y}\left(\frac{k_s}{k_o^2}\right)\right] + \left(\frac{\partial S}{\partial x}\right)^2+\left(\frac{\partial S}{\partial y}\right)^2-k_o^2=0 \tag{140}$$

and

$$\frac{\partial}{\partial x}\left(\frac{k_s}{k_o^2}a^2\frac{\partial S}{\partial x}\right)+\frac{\partial}{\partial y}\left(\frac{k_s}{k_o^2}a^2\frac{\partial S}{\partial y}\right)=0 \tag{141}$$

Equations 140 and 141 can be combined into:

$$\frac{\partial}{\partial x}\left(\frac{k_s}{k_o^2}\frac{\partial \phi}{\partial x}\right)+\frac{\partial}{\partial y}\left(\frac{k_s}{k_o^2}\frac{\partial \phi}{\partial y}\right)+k_s\phi=0 \tag{142}$$

and this equation can be reduced to Equation 130. This combined refraction and diffraction model has a great disadvantage for solving practical engineering problems due to the amount of computing time needed to obtain a solution over a large area in the horizontal plane. Berkhoff (1976) recommended use of the more simple refraction or diffraction models where possible, and to connect the solutions in whatever way that can be judged to be appropriate.

279. Equation 130 is derived with the aid of a small parameter development, and the method of solution is based on the finite element technique with a source distribution. The theory is restricted to linear waves, and loss of energy due to friction or breaking is not taken into account. The equation is applicable to waves in the range from shallow water to deep water. The solution of the differential equation in an arbitrary area can be found by minimizing the corresponding functional expression over the area, taking into account the conditions at the boundaries of full reflection at rigid walls and the

Sommerfeld radiation condition at sea. The solution at the sea boundary is a superposition of the incident and an outgoing wave which is caused by the presence of the structure. The solution at the boundary is continuous with respect to wave height and phase. As noted by Chen and Mei (1974), Berkhoff (1972, 1976) did not use a proper functional in his finite element model formulation with the consequence that his global stiffness matrix was nonsymmetric and thus inconvenient numerically for all but the simplest problems.

280. Houston (in preparation) solved Equation 130 in a region of variable depth using a hybrid finite element method originally developed by Chen and Mei (1974) to solve the diffraction Helmholtz equation in a constant depth region. Variational principles are used in this approach that incorporate the matching conditions between a region covered with regular finite element cells and an infinite region covered by a super element as natural conditions. Thus a symmetric global stiffness matrix is obtained that is very advantageous for highly complex problems. Houston demonstrates use of this model for very large problems involving combined refraction diffraction.

281. For plane regular waves of small amplitude, incident on a parabolic island, Jonsson, Skovgaard, and Brink-Kjaer (1976) calculated the wave field according to two different approaches: a diffraction theory and a depth refraction theory. The solutions were compared for periods where the Coriolis force can be neglected. It was found that for L_a/r_a between 1.5 and 2.5 (L_a is wavelength at the shoreline and r_a is the radius of the island), the complete refraction solution can predict the critical wave periods quite well. For L_a/r_a smaller than about 0.4, the amplitudes at the middle of the front face of the island are rather well predicted by the primary orthogonal. For L_a/r_a greater than this, the amplitudes from refraction theory deviate more and more from the diffraction solution. Beyond $L_a = 2.5\ r_a$, the refraction calculations become quite meaningless. The complete refraction solution was only calculated for shallow-water waves. This was the first time the diffraction solution had been given for an island of this form, using intermediate depth theory and a mild-slope wave

equation that is a variation of Equation 130:

$$\nabla \cdot (CC_g \nabla \eta) + \frac{C_g}{C} \omega^2 \eta = 0 \tag{143}$$

Generally, this equation may be replaced by the well-known linear long-wave equation when periods exceed 7 min. All nonlinear effects were neglected.

282. A uniformly valid asymptotic solution for water waves was presented by Liu and Lozano (1979) which accounts for the combined effects of refraction due to slowly varying water depth and diffraction by a long breakwater. The asymptotic solutions are developed by assuming there is no reflection from the variable bottom bathymetry. Recent developments in formal geometrical optics approximations were extended to include the effects of diffraction. The breakwater is assumed to have zero thickness and is located on a uniformly sloping beach. The bottom topography is assumed to be varying slowly in the onshore-offshore direction. The theory provides a uniform asymptotic representation of the wave field everywhere, including the neighborhood of the edges of the breakwater, except in the surf zone where the waves break. Physical hydraulic model tests were conducted at the WES in 1979 (Hales in preparation) to confirm the analytic solution of Liu and Lozano (1979). Typical results of these experiments are displayed in Figure 51. This analytical development was an extension of original work by Liu and Mei (1976a).

283. Engineering practice has long been concerned with the behavior of short waves in shallow water. These waves are instrumental in bringing sediments into suspension as they refract and diffract around structures, and they often induce the currents that transport these sediments to quieter regions for deposition. For the control of coastal erosion a knowledge of short-wave motions and the currents that these waves induce is of fundamental importance. The effort expended in numerical modeling of short waves, although considerably less than that used in physical modeling, has still produced several useful results. Most of the techniques are based upon periodic wave propagation and

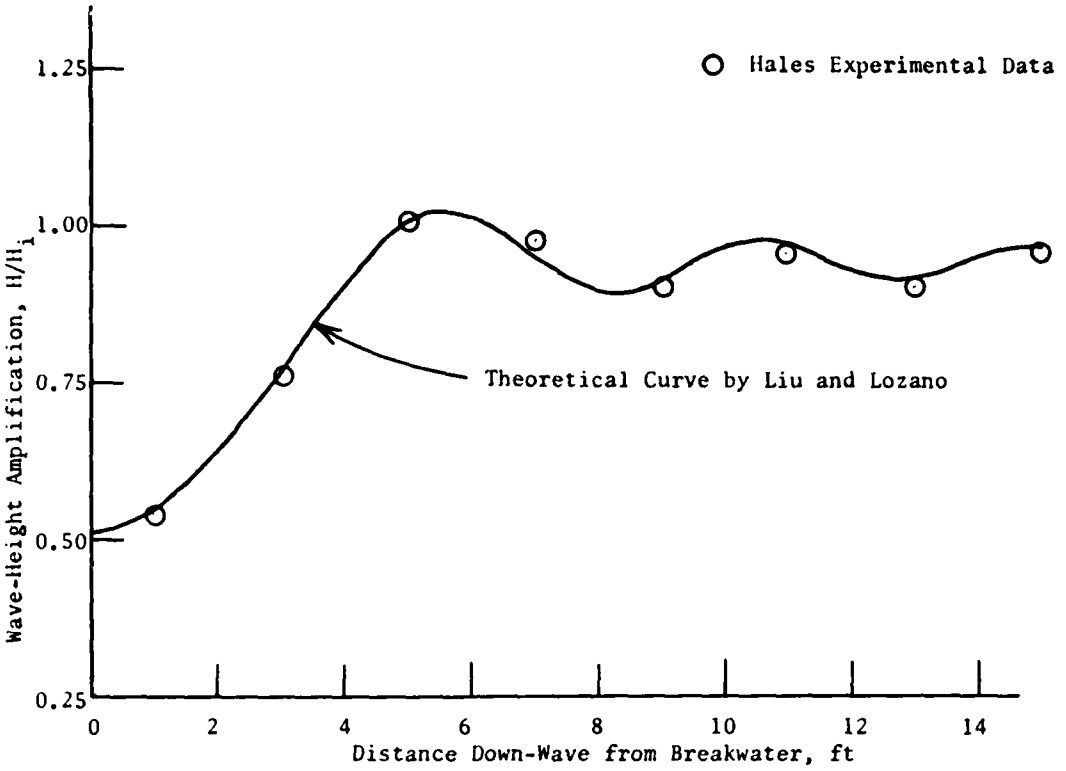

Figure 51. Comparison of experimental data from Hales (in preparation) with theoretical development of Liu and Lozano (1979). Model distance from end of breakwater = 5 ft, still-water depth at section = 0.50 ft, wave period = 0.75 sec, angle of incidence = 20 deg from the left

geometric optics. The range of water waves that can be so treated is restricted, being essentially limited to small-amplitude periodic waves described by linearized wave theories. Experience of physical modeling suggests that the restriction of small amplitude waves may give unacceptable errors in some situations.

284. A numerical modeling system is described by Abbott, Petersen, and Skovgaard (1978) that generates and runs models of short waves of any form (periodic or irregular), with any desired physically realistic current field over any given bathymetry. The system-generated models are based upon Boussinesq equations in which the vertical velocity is supposed to increase linearly from zero at the bed to a maximum magnitude at the surface, in two independent (horizontal) space

variables and time. The Boussinesq equations are formulated as mass and momentum conservation laws while, by virtue of the high order of accuracy of the difference approximations, there is very little numerical energy falsification. This system has been tested against analytical results in one- and two-dimensions and also against physical model tests, for all of its main capabilities. In all cases, the agreement of the system numerical model results with the analytical and physical results were satisfactory, according to Abbott, Petersen, and Skovgaard (1978).

Nearshore Circulation and Resulting Current Patterns

285. Observations of nearshore circulation patterns indicate a longshore periodicity for both normal and oblique wave incidence. Noda (1974) developed a theory to explain the nearshore circulation patterns analytically by the use of a longshore periodic beach bathymetry. The following assumptions were imposed on flow conditions within the surf zone: (a) the circulation system was steady and mean wave characteristics were used, (b) the horizontal velocities were independent of depth, so that the equations of motion and continuity could be integrated with depth (i.e. long wave theory), (c) convective acceleration terms were neglected, (d) energy dissipation for the induced circulation was provided by a bottom friction term, and (e) the circulation velocities were assumed small so that the incoming wave-current interaction can be neglected.

286. The analytic model that resulted from Noda's (1974) assumptions incorporates the incoming wave-bathymetry interaction to produce spatial variations of wave characteristics as the driving mechanism. Analytic functions representing actual field bathymetry were developed, and the resulting model circulation patterns yielded quite good results when compared with field measurements. The assumption that the circulation pattern is steady in time has been subject to some criticism. Field observations by Arthur (1962) and Sonu (1972) indicate that nearshore circulation patterns undergo regular pulsations; and these

pulsations can be associated with the formation of a rip current and its ejection from the nearshore circulation field.

287. The numerical results of Noda (1974) indicate that bathymetry greatly influences the circulation pattern. The development of analytic representations of the prototype bottom configuration in conjunction with the derived fluid motion shows that if the imposed bathymetry is not in equilibrium with the current motion, large current velocities and associated bottom shear stress will develop. Hence, extensive bottom scour and sediment movement will occur until an equilibrium bottom configuration is formed. Unfortunately, the model of Noda (1974) has no provision for sediment movement.

288. The primary objective of an investigation by Liu and Mei (1975) was to study nearshore currents due to breaking waves inside and near the surf zone. The incident waves were assumed to be interrupted by two kinds of coastal structures: (a) a shore-connected breakwater and (b) a breakwater offshore and parallel with the shoreline. Extending the Fresnel diffraction approximation, the first order wave field accounting for diffraction and refraction was derived. Results were then used to calculate the radiation stresses and mean sea level in the shoaling zone. The governing equations of the nearshore currents were solved numerically assuming lateral turbulent diffusion and convective inertia are negligible. Bottom friction was assumed to be proportional to the current velocity. An iterative procedure of finite differences was developed to solve the resulting problem.

289. The most significant result of the study by Liu and Mei (1975) was the formation of cells. Whether in the diffraction zone or in the reflection zone, these cells are associated with variations in the breaking wave height which is closely related to variations in the breaker line position, surf zone width, and mean sea level. For the shore-connected breakwater, diffraction features in the down-wave zone are very much like the neighborhood of the downstream cell of the offshore breakwater. In the up-wave reflection zone near the breakwater, the wave field is essentially that of two incident waves approaching from different directions. Liu and Mei (1975) found that the larger

the friction coefficient C_f the weaker the current and the farther apart the streamlines. The mean sea level does not change very much for different friction coefficients, suggesting that the incident waves play a direct role in generating the mean setup and setdown and that the currents only modify it slightly. In general, the current velocity is strongly affected by the value of C_f, which is difficult to determine in the field. Representative examples of this work are shown in Figures 52 and 53 for the up-wave side of the shore-connected breakwater with two coefficients of friction, and Figures 54 and 55 for the down-wave side with the same two friction coefficients. The angle of incidence of the wave train is 45 deg in each case. This work has been summarized by Liu and Mei (1976b).

290. A finite element model for computing wave-induced currents in the nearshore environment has been presented by Liu and Lennon (1978). Due to the flexible nature of the finite element layout and the fact that no iteration procedure is needed in this model, Liu and Lennon (1978) claim that their finite element model is more efficient than the finite difference model developed by Noda (1974). The model presented is constructed on the basis of linear theory; i.e., the bathymetric variation in the alongshore direction is small compared with local water depth. Wave current interactions and the nonlinear convective acceleration terms have been neglected, although they are by no means negligible for many problems.

291. An explicit finite difference model for predicting nearshore circulation which includes convective accelerations and lateral mixing was developed by Ebersole (1980). This model also includes a quadratic bottom friction term that considers the velocity vectors due to both mean and wave-induced currents. The equations that govern both wave refraction and shoaling as a result of wave-current interactions used in this model are those of Noda et al. (1974). The advantage of this method is that it predicts the wave angles and wave heights at certain points rather than along a wave ray. This procedure lends itself well to use in the finite difference model because calculations are performed at points that lie in the center of rectangular grid elements which are

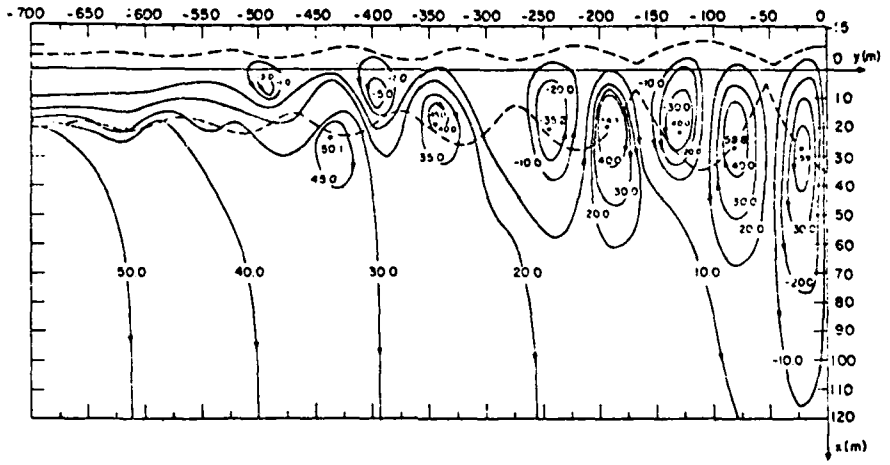

Figure 52. Streamline pattern on up-wave side of shore-connected breakwater. Coefficient of friction = 0.01. Angle of incidence = 45 deg from the left (after Liu and Mei 1978)

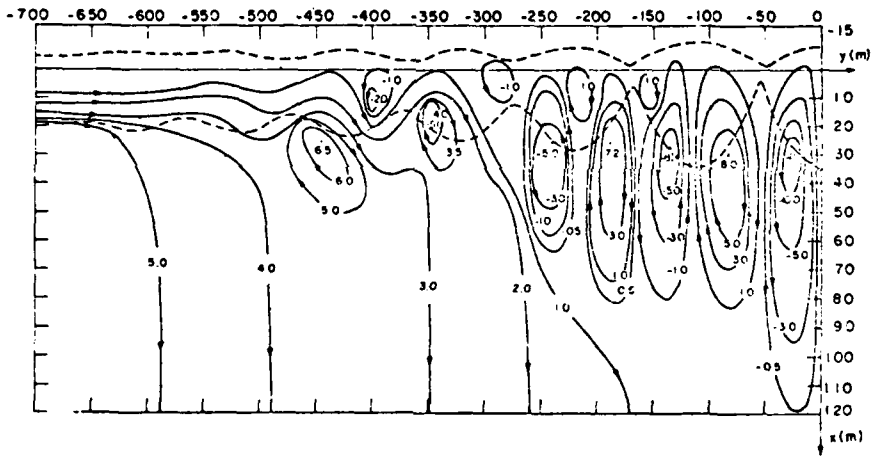

Figure 53. Streamline pattern on up-wave side of shore-connected breakwater. Coefficient of friction = 0.09. Angle of incidence = 45 deg from the left (after Liu and Mei 1978)

part of a larger grid. Steady-state conditions are achieved by time-stepping the model until current variations with time are negligible. Example current patterns for intersecting wave trains are shown in Figure 56 for a plane beach of slope = 0.025 after 1,500 time-steps.

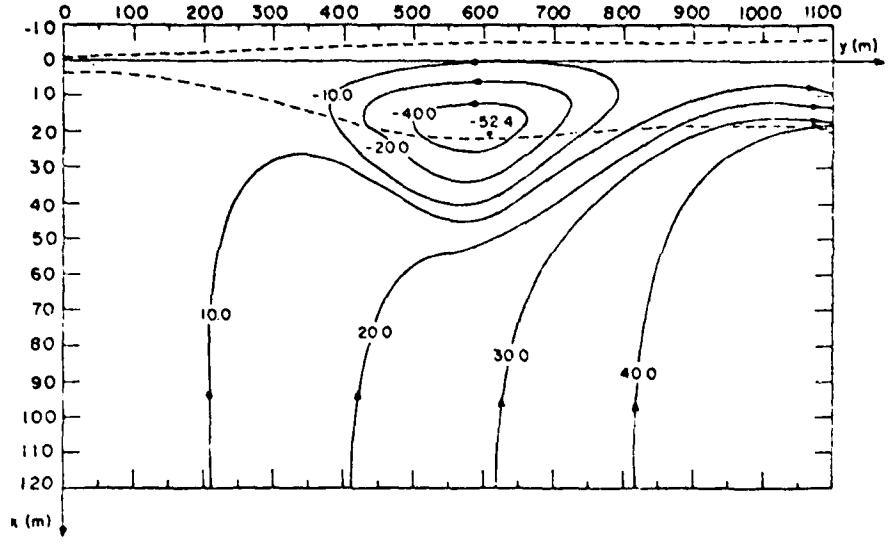

Figure 54. Streamline pattern on down-wave side of shore-connected breakwater. Coefficient of friction = 0.01. Angle of incidence = 45 deg from the left (after Liu and Mei 1978)

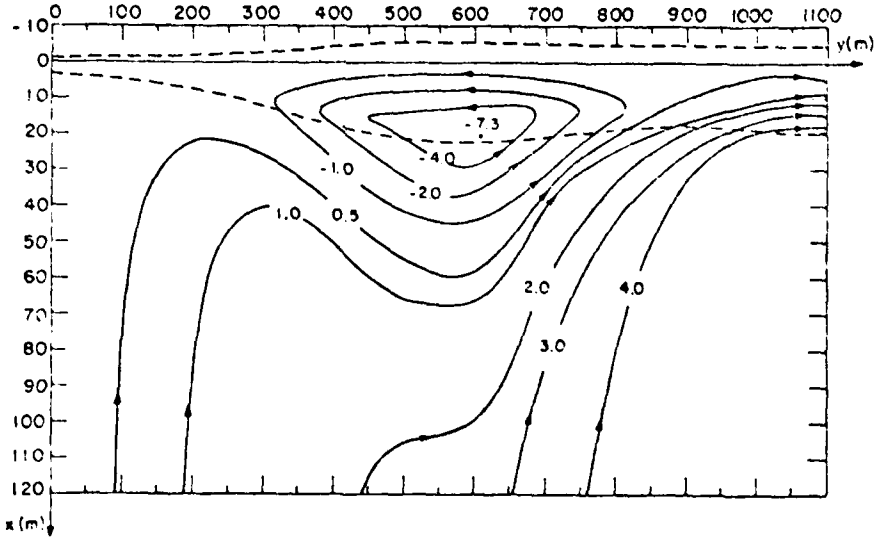

Figure 55. Streamline pattern on down-wave side of shore-connected breakwater. Coefficient of friction = 0.09. Angle of incidence = 45 deg from the left (after Liu and Mei 1978)

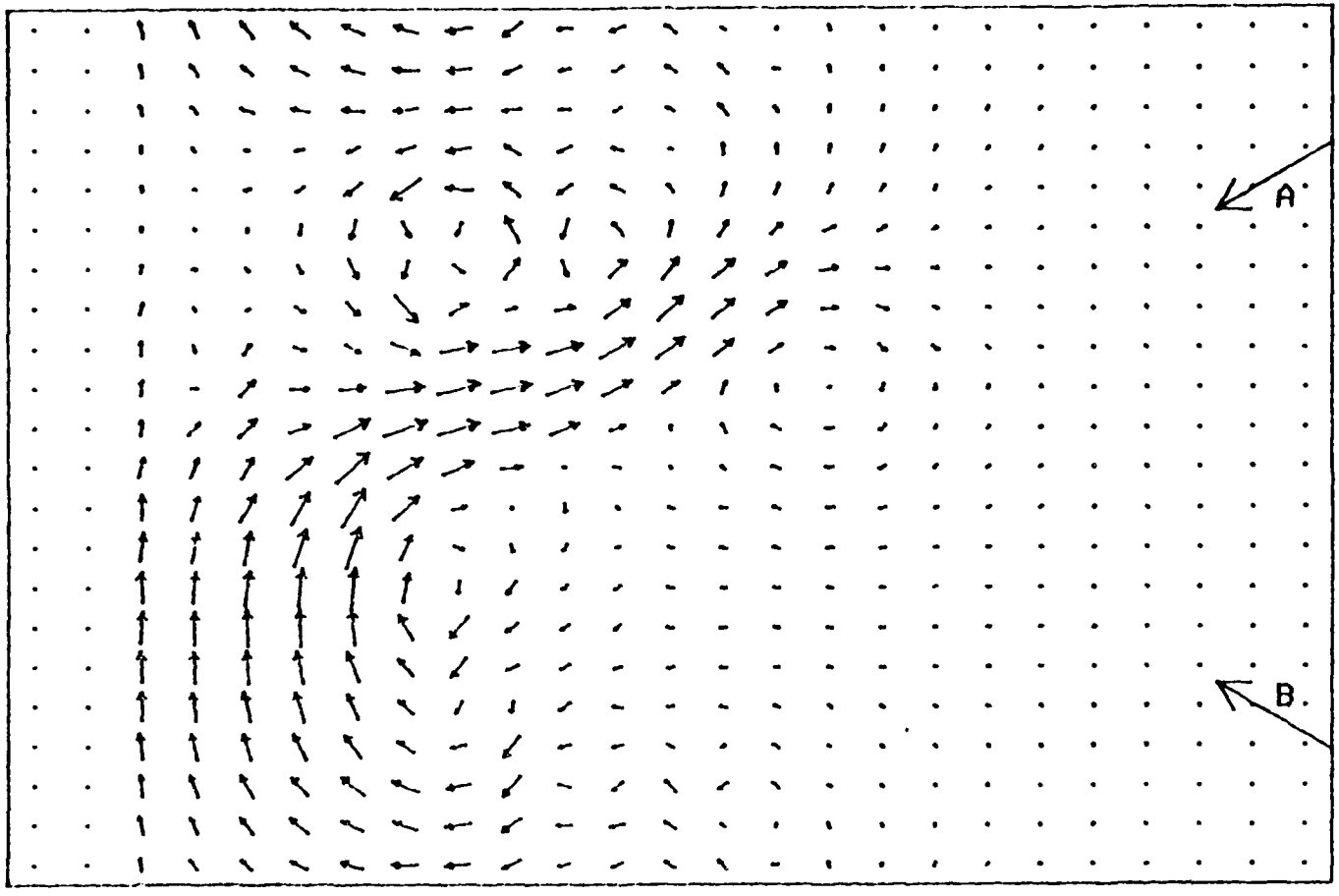

Figure 56. Current vectors for a meandering circulation pattern. Intersecting wave trains, plane beach (slope = 0.025), wave height A = 0.1 m, wave height B = 0.4 m, wave angle A = 30 deg, wave angle B = 30 deg, wave periods = 7.2 sec, Δx = 5.0 m, Δy = 4.0 m, Δt = 0.2 sec, iterations = 1,500 (after Ebersole 1980)

Sediment Transport by Numerical Techniques

292. A mathematical model for sediment transport under waves was developed by Fleming and Hunt (1976) from concepts that have been used successfully for unidirectional flow. This model was combined interactively with numerical models for wave refraction, wave diffraction, longshore currents, and circulation currents in order to predict local bathymetric changes in the vicinity of a structure. The sediment model was calibrated using field data of sediment concentration profiles. Verification and adjustments were made by analyzing deepwater wave statistics and periodic beach and hydrographic surveys. This model can be used to investigate the effects of wave climate on sediment transport and different layouts of coastal structures can be examined.

293. The sediment transport model used assumes that sediment is transported in a bed-load region adjacent to the stationary part of the bed where the grains are supported by interparticle collisions, and a suspended load region where gravitational forces are overcome by fluid turbulence. The exact definition of the transition level was not considered significant since the flux of sediment immediately above and below this level will be similar. This unidirectional model was tested against the best existing empirical theories and found to give comparable estimates of sediment transport rates.

294. The case of flow in the combined wave and current field is treated as a quasi-steady condition with respect to the shear stresses acting on the bed and the dispersion of shear stress due to wave motion. Wave motion is assumed to be the primary forcing function responsible for putting the sediment in suspension, while the current acts as the principal transporting agent. Application of the wave model requires evaluation of wave heights, wave directions, and nearshore currents over a region. This is achieved by using a wave-refraction model combined with a longshore current model.

295. It has been shown by Madsen and Grant (1976) that the Shields criterion for incipient sediment motion in unidirectional flow also can be applied to oscillatory flow when the bottom shear stress is

evaluated using Equations 43 and 46. It is assumed that the bed-load layer is supported entirely by grain interaction, and that the local change in dispersed shear is proportional to the local concentration, where the concentration distribution is implied as:

$$C = C_m(C_e/C_m)^{y/e} \tag{144}$$

where

C_m = maximum concentration at the bed

C_e = concentration at the upper boundary of the bed-load layer

e = bed-load thickness

$$e = \left[\tau_d \ln (C_e/C_m)\right] \Big/ \left[g(\rho_s - \rho)(C_e - C_m)(\tan\alpha + \tan\theta)\cos\theta\right] \tag{145}$$

τ_d is the dispersion shear stress, defined as

$$\tau_d = \tau_w - \tau_c \tag{146}$$

where

α = friction angle of the bed material

θ = bottom slope

τ_w = mean wave shear stress

τ_c = critical shear stress

The bed-load transport rate is

$$Q_{bed} = \int_0^e C\, u\, dy \tag{147}$$

The current velocity distribution is assumed to be of the form:

$$u_c = u_{cmax}(y/d)^{1/7} + \text{const} \tag{148}$$

maximum current velocity at the free surface

The suspended load transport can therefore be expressed as:

$$Q_{sus} = \int_{e}^{d} C\, u_c\, dy \qquad (149)$$

296. Sediment sampling in the surf zone is extremely difficult due to the presence of waves; however, some concentration profiles both inside and outside the surf zone have been obtained for a range of wave heights. Using these profiles, it is possible to evaluate the eddy viscosity above the bed. A wave-refraction model is then used to evaluate the wave directions and heights above the bed, and the longshore current model of Longuet-Higgins (1970) is used to calculate wave induced currents inside and outside the surf zone. Given any combination of offshore wave period, direction and height, the refraction and longshore current models can be used to provide the required parameters at each point in the grid. Predictions of local bathymetric changes can be made by applying the sediment transport model at these points.

297. The sediment transport model of Fleming and Hunt (1976) is not universal insofar as there are certain parameters that must be calculated from field data. There is a general scarcity of detailed field or experimental data for either concentration profiles or sediment transport rates under waves, and it is therefore not possible to generalize this particular model. Any further development of this model to include such nonlinear effects as mass transport will probably be difficult to confirm.

298. Lepetit and Hauguel (1978) introduced a numerical two-dimensional model for sediment transport that allows the computations of the impact of a coastal structure on the bottom evolution. The introduction of current disturbances and some assumptions about difference of time scale between currents and bottom evolutions allows the development of a propagation equation that drives the bottom evolution. The model has been calibrated for the case of local scour around a jetty or breakwater and has been applied to prototype situations. This mathematical sediment transport model takes into account the influence of bottom evolution on the current patterns. While the study of sediment

drifting and movable-bed evolution is difficult from the standpoint of the physics involved, the problem ultimately reduces to a conservation of flux.

299. When the initial bottom configuration d_o has been determined, the depth averaged flow pattern is (u_o, v_o). This current modifies the bottom shape, which, in turn, modifies the current to $[u_1(t), v_1(t)]$. At time t, the current pattern is given by $[u_o + u_1(t), v_o + v_1(t)]$, and the bottom level is $d(t)$. The bottom evolution is defined as:

$$d_s = d - d_o \tag{150}$$

The resulting disturbance (u_1, v_1) is assumed to be without effect upon the surface elevation. This assumption is equivalent to neglect of the characteristic response time of the surface wave propagation compared with the characteristic response time of the bottom evolution. The fluid continuity equation can be written in two parts: the first part comes directly from the bottom elevation and expresses the flow conservation along the streamlines of the undisturbed flow fields; the second part is a deviation of the flow due to the bottom slope (u_{11} and v_{11}). These two components can be introduced into the bed continuity equation, and results in the bottom evolution equation:

$$\begin{aligned}\frac{\partial d_s}{\partial t} + C\left(\frac{u}{w}\frac{\partial d_s}{\partial x} + \frac{v}{w}\frac{\partial d_s}{\partial y}\right) = {} & T_{xu}\left[\frac{\partial}{\partial x}(u_o + u_{11}) + d_s\frac{\partial}{\partial x}\left(\frac{u_o}{d_o}\right)\right] \\ & - T_{xv}\left[\frac{\partial}{\partial x}(v_o + v_{11}) + d_s\frac{\partial}{\partial x}\left(\frac{v_o}{d_o}\right)\right] \\ & - T_{yu}\left[\frac{\partial}{\partial y}(u_o + u_{11}) + d_s\frac{\partial}{\partial y}\left(\frac{u_o}{d_o}\right)\right] \\ & - T_{yv}\left[\frac{\partial}{\partial y}(v_o + v_{11}) + d_s\frac{\partial}{\partial y}\left(\frac{v_o}{d_o}\right)\right]\end{aligned} \tag{151}$$

where

$$C = \frac{1}{d}\left(u\frac{\partial T}{\partial u} + v\frac{\partial T}{\partial v}\right) \tag{152}$$

$$T_{xu} = \frac{u}{w}\frac{\partial T}{\partial u} + T\frac{v^2}{w^3} \tag{153}$$

$$T_{xv} = \frac{u}{w}\frac{\partial T}{\partial v} - T\frac{uv}{w^3} \tag{154}$$

$$T_{yu} = \frac{v}{w}\frac{\partial T}{\partial u} - T\frac{uv}{w^3} \tag{155}$$

$$T_{yv} = \frac{v}{w}\frac{\partial T}{\partial v} + T\frac{u^2}{w^3} \tag{156}$$

$$T = 8(g/\gamma)^{1/2}\frac{1}{\gamma_s - \gamma}(\tau - \tau_c)^{3/2} \quad \text{if} \quad \tau > \tau_c \tag{157}$$

$$T = 0 \quad \text{if} \quad \tau < \tau_c \tag{158}$$

and

$$w = (u^2 + v^2)^{1/2} \tag{159}$$

where

τ = bottom shear stress

τ_c = critical bottom shear stress from Shields parameter

Equation 151 governs ripple propagation in the direction of the initial current pattern with celerity C. This is the direct result of the inclusion of the current disturbance, the neglect of which would have indicated no ripple propagation.

300. To develop the fluid equation, an irrotational current disturbance is assumed so that the three-dimensional stream function ψ may be obtained which yields a Poisson-type equation. The current pattern is defined as:

$$u = u_o + u_o\frac{d_s}{d} + \frac{1}{d}\frac{\partial \psi}{\partial y} \tag{160}$$

$$v = v_o + v_o\frac{d_s}{d} - \frac{1}{d}\frac{\partial \psi}{\partial x} \tag{161}$$

d is the actual depth, and ψ can be obtained from:

$$\Delta\psi = d \frac{\partial}{\partial x}\left(v_o \frac{d_s}{d}\right) - \frac{\partial}{\partial d}\left(u_o \frac{d_s}{d}\right) + \frac{1}{d}\frac{\partial\psi}{\partial y}\frac{\partial d}{\partial y} - \frac{1}{d}\frac{\partial\psi}{\partial x}\frac{\partial d}{\partial x} \qquad (162)$$

301. A finite difference scheme is used to solve Equations 151 and 162, where each time step involves two stages: (a) computation of the bottom elevation d by the characteristic method where all functions are explicit, and (b) computation of the new velocities by an iterative process. This numerical technique has been compared with results of a physical hydraulic model study of scour and erosion around the tip of a breakwater or jetty. The comparison between the computed and measured erosion was quite good, except for a region very near the structure. Lepetit and Hauguel (1978) attribute this deviation to the initial current pattern in the physical model which was not conservative. This problem was mathematically eliminated in the numerical model.

PART X: CONCLUSIONS

302. When major structures are erected in the coastal zone for the protection of beaches, harbors, etc., they alter the existing current field. Wave effects on the structure can cause suspension of bottom material allowing it to be transported from the region by longshore or other currents. The scour that develops often requires large quantities of material for rehabilitation and may even endanger the integrity of the structure itself.

303. A substantial amount of work has been performed to investigate and understand local scour of noncohesive material in unidirectional flow. Relatively little effort has been spent on the study of the problem of local scour around structures subjected to wave action, probably because of the unsteady nature of the flow field. Even less work has been performed on the problem of scour under the dual processes of wave motion and unidirectional flow. An understanding of local scour processes around coastal structures will come only through investigations that include both unidirectional and oscillatory flow fields. Scouring by tidal currents, to a first approximation, can be considered the result of a unidirectional current having a long period. The transport process is generally considered to be the result of sediment suspension by wave action and transport by currents. The currents could conceivably be weak in magnitude and still account for a large transport since the sediment is already in suspension due to wave action.

304. Many theoretical investigations concerning scour and erosion due to wave action are based on earlier work regarding scour and sediment transport mechanics developed from river hydraulics and potamology. These unidirectional theories have been modified in an attempt to account for the increased shear stress and pressure variations induced by the oscillatory wave field. This report is a survey of existing literature that has been directed toward understanding sediment transport by waves and currents, and the scour and erosion problems that result during or shortly after construction of coastal structures. The primary forcing function is usually due to wind waves, and refraction by local bathymetry

can cause concentrations of wave energy that increases the scouring potential. As bathymetry is altered by scour, a change in refraction patterns results. Theoretical and numerical work to couple wave characteristics, refraction and diffraction, and sediment transport mechanics to deduce bottom evolution is truly in its infancy. However, the basic groundwork has been laid on which more sophisticated and analytically sound developments can be built.

REFERENCES

Abbott, M. B., and Marshall, G. 1969. "A Numerical Model of a Wide Shallow Estuary," Proceedings, Thirteenth International Congress of the International Association of Hydraulic Research, Kyoto, Japan, pp 123-130.

Abbott, M. B., Petersen, H. M., and Skovgaard, O. 1978. "On the Numerical Modeling of Short Waves in Shallow Water," Journal of Hydraulic Research, Vol 16, No. 3, pp 173-203.

Abbott, M. B., Rodenhuis, G., and Verwey, A. 1973. "System 11, a Design System for Rivers and Estuaries," Proceedings, International Symposium on River Mechanics, Bangkok, Thailand, pp 207-213.

Abou-Seida, M. M. 1963. "Sediment Scour at Structures," Technical Report HEL-4-2, University of California, Berkeley, Calif.

_____. 1965. "Bed Load Function Due to Wave Action," Technical Report HEL-2-11, University of California, Berkeley, Calif.

Ackers, P., and White, W. R. 1973. "Sediment Transport: New Approach and Analysis," Journal, Hydraulics Division, American Society of Civil Engineers, Vol 99, No. HY11, pp 2041-2060.

Ahmad, M. 1962. Discussion of "Scour at Bridge Crossings," Transactions, American Society of Civil Engineers, Vol 127, Part II, pp 198-206.

Anderson, A. G. 1974. "Scour at Bridge Waterways--A Review," Report No. FHWA-RD-75-89, St. Anthony Falls Hydraulic Laboratory, Minneapolis, Minn.

Armstrong, J. M., and Kureth, C. L. 1979. "Some Observations on the Longard Tube as a Coastal Erosion Protection Structure," Proceedings, Coastal Structures 79, Vol I, pp 250-269.

Arthur, R. S. 1962. "A Note on the Dynamics of Rip Currents," Journal of Geophysical Research, Vol 67, No. 7, pp 2777-2779.

Bagnold, R. A. 1946. "Motion of Waves in Shallow Water, Interaction Between Waves and Sand Bottom," Proceedings, Royal Society of London, Series A, Vol 187, pp 1-15.

_____. 1966. "An Approach to the Sediment Transport Problem from General Physics," Professional Paper No. 422-J, U. S. Geological Survey, Washington, D. C.

Banks, J. E. 1969. "A Numerical Model to Study Tides and Surges in a River-Sea Combination," Report 19, Tidal Institute and Observatory, University of Liverpool, Liverpool, United Kingdom.

Barrett, R. J. 1966. "Use of Plastic Filters in Coastal Structures," Proceedings, Tenth Conference on Coastal Engineering, Tokyo, Japan, pp 1048-1067.

Bekaert Steel Wire Corp. 1977. "Bekaert Gabions," Technical Memorandum, Terra Aqua Conservation, Reno, Nev.

Berkhoff, J. C. W. 1972. "Computation of Combined Refraction-Diffraction," Proceedings, Thirteenth Coastal Engineering Conference, Vancouver, British Columbia, Canada, Vol I, pp 471-490.

_____. 1976. "Mathematical Models for Simpl Harmonic Linear Water Waves--Wave Diffraction and Refraction," Publication No. 163, Delft Hydraulics Laboratory, Delft, the Netherlands.

Bijker, E. W. 1971. "Longshore Transport Computations," Journal, Waterways, Harbors, and Coastal Engineering Division, American Society of Civil Engineers, Vol 97, No. WW4, pp 687-701.

Blench, T. 1969. Mobile Bed Fluviology, University of Alberta Press, Edmonton, Alberta, Canada.

Blue, F. L., Jr., and Johnson, J. W. 1949. "Diffraction of Water Waves Passing Through a Breakwater Gap," Transactions, American Geophysical Union, Vol 30, No. 5, pp 705-718.

Boericke, R. R., and Hall, D. W. 1974. "Hydraulics and Thermal Dispersion in an Irregular Estuary," Journal, Hydraulics Division, American Society of Civil Engineers, Vol 100, No. HY1, pp 85-102.

Breusers, H. N. C. 1965. "Scour Around Drilling Platforms," Bulletin of Hydraulics Research, 1964 and 1965, International Association for Hydraulic Research, Vol 19, p 276.

_____. 1972. "Local Scour near Offshore Structures," Publication No. 105, Delft Hydraulics Laboratory, the Netherlands.

Butler, H. L. 1978a (Jun). "Numerical Simulation of Tidal Hydrodynamics, Great Egg Harbor and Corson Inlets, New Jersey," Technical Report H-78-11, U. S. Army Engineer Waterways Experiment Station, CE, Vicksburg, Miss.

_____. 1978b (Dec). "Numerical Simulation of the Coos Bay-South Slough Complex," Technical Report H-78-22, U. S. Army Engineer Waterways Experiment Station, CE, Vicksburg, Miss.

_____. 1979. "Evolution of a Numerical Model for Simulating Long-Period Wave Behavior in Ocean-Estuarine Systems," Proceedings, Workshop on Wetlands and Estuarine Processes and Water Quality Modeling, New Orleans, La.

Calhoun, C. C., Jr. 1972 (Jun). "Development of Design Criteria and Acceptance Specifications for Plastic Filter Cloths," Technical Report S-72-7, U. S. Army Engineer Waterways Experiment Station, CE, Vicksburg, Miss.

Carver, R. D. 1980 (Jan). "Effects of First Underlayer Weight on the Stability of Stone-Armored Rubble-Mound Breakwater Trunks Subjected to Nonbreaking Waves with No Overtopping; Hydraulic Model Investigation," Technical Report HL-80-1, U. S. Army Engineer Waterways Experiment Station, CE, Vicksburg, Miss.

Chen, H. S., and Mei, C. C. 1974. "Oscillations and Wave Forces on an Offshore Harbor," Report No. 190, Massachusetts Institute of Technology, Cambridge, Mass.

Chesnutt, C. B., and Schiller, R. E., Jr. 1971. "Scour of Simulated Gulf Coast Sand Beaches Due to Wave Action in Front of Sea Walls and Dune Barriers," Sea Grant Publication No. 71-207, Texas A&M University, College Station, Tex.

Chitale, S. V. 1962. Discussion of "Scour at Bridge Crossings," Transactions, American Society of Civil Engineers, Vol 127, Part I, pp 191-196.

Cook, D. O., and Gorsline, D. S. 1972. "Field Observations of Sand Transport by Shoaling Waves," Marine Geology, Vol 13, No. 1, pp 31-55.

Cunha, L. V. 1976. "Time Evolution of Local Scour," Technical Memorandum No. 477, Laboratorio Nacional De Engenharia Civil, Lisbon, Portugal.

Dalrymple, R. A. 1974. "Water Waves on a Bilinear Shear Current," Proceedings, Fourteenth Conference on Coastal Engineering, Copenhagen, Denmark, Vol 1, pp 626-641.

Das, M. M. 1971. "Mechanics of Sediment Suspension Due to Oscillatory Water Waves," Technical Report HEL-2-32, University of California, Berkeley, Calif.

Daugherty, R. L., and Franzini, J. B. 1965. Fluid Mechanics with Engineering Applications, 6th ed., McGraw-Hill, New York.

Davies, A. G., and Wilkinson, R. H. 1977. "The Movement of Non-Cohesive Sediment by Surface Water Waves," Report No. 45, Part I, Institute of Oceanographic Sciences, Wormley, England.

Dean, R. G., and Taylor, R. B. 1972. "Numerical Modeling of Constituent Transport in Bay Systems," Proceedings, Thirteenth Conference on Coastal Engineering, Vancouver, British Columbia, Canada, Vol 3, pp 227-249.

Delft Hydraulics Laboratory. 1973a. "Gobi-Blocks as Slope Revetments: Stability Under Wave Attack," Report No. M-11884, Delft, Netherlands.

_____. 1973b. "Stability of Gobi-Mat and Its Permeability to Sand in Turbulent Flow," Report No. R-788, Delft, Netherlands.

DeMent, L. W. 1977. "Two New Methods of Erosion Protection for Louisiana," Shore & Beach, Vol 45, No. 1, pp 31-38.

Dietz, J. W. 1976. "The Reproduction of Scour Processes in Model Tests," Bundesanstalt Fuer Wasserbau, Communication No. 40, pp 71-85.

Dingler, J. R., and Inman, D. L. 1976. "Wave-Formed Ripples in Nearshore Sands," Proceedings, Fifteenth Coastal Engineering Conference, Honolulu, Hawaii, Vol II, pp 2109-2126.

Donnelly, P., and Boivin, R. 1968. "Pattern of Wave-Induced Erosion Under Caisson-Type Breakwater," Proceedings, Eleventh Conference on Coastal Engineering, London, England, Vol I, pp 599-605.

Downing, J. J., Jr. 1977. "Sediment Transport Measurement in the Nearshore Environment: A Review of the State of the Art," Proceedings, Workshop on Instrumentation for Nearshore Processes, Sea Grant Publication No. 62, Nearshore Sediment Transport Study, LaJolla, Calif.

Dronkers, J. J. 1969. "Tidal Computations for Rivers, Coastal Areas, and Seas," Journal, Hydraulics Division, American Society of Civil Engineers, Vol 95, No. HY1, pp 29-78.

Dunham, J. W., and Barrett, R. J. 1974. "Woven Plastic Cloth Filters for Stone Seawalls," Journal, Waterways, Harbors, and Coastal Engineering Division, American Society of Civil Engineers, Vol 100, No. WW1, pp 13-22.

Eagleson, P. S., and Dean, R. G. 1966. "Chapter 1: Small Amplitude Wave Theory," Estuary and Coastline Hydrodynamics, McGraw-Hill, New York.

Eagleson, P. S., Dean, R. G., and Peralta, L. A. 1958. "The Mechanics of the Motion of Discrete Spherical Bottom Sediment Particles Due to Shoaling Waves," Technical Memorandum No. 104, U. S. Army Engineer Beach Erosion Board, Washington, D. C.

Ebersole, B. A. 1980. A Numerical Model for Nearshore Circulation Including Convective Accelerations and Lateral Mixing, M.S. Thesis, University of Delaware, Newark, Del.

Einstein, H. A. 1950. "The Bed Load Function for Sediment Transportation in Open Channel Flows," Bulletin No. 1026, Soil Conservation Service, U. S. Department of Agriculture, Washington, D. C.

_____. 1972. "Sediment Transport by Wave Action," Proceedings, Thirteenth Coastal Engineering Conference, Vancouver, British Columbia, Canada, Vol II, pp 933-952.

Engelund, F., and Hansen, E. 1967. "A Monograph on Sediment Transport in Alluvial Streams," Technical University of Denmark, Copenhagen, Denmark.

Fleming, C. A., and Hunt, J. N. 1976. "Application of a Sediment Transport Model," Proceedings, Fifteenth Coastal Engineering Conference, Honolulu, Hawaii, Vol II, pp 1184-1202.

Foley, M. G. 1975. "Scour and Fill in Ephemeral Streams," Report No. KH-R-33, California Institute of Technology, Pasadena, Calif.

Garde, R. J., and Albertson, M. L. 1958. Discussion of "The Total Sediment Load of Streams," Journal, Hydraulics Division, American Society of Civil Engineers, Vol 84, pp 1856-59 - 1856-64.

Graf, W. H. 1971. Hydraulics of Sediment Transport, McGraw-Hill, New York.

Gutman, A. L. 1979. "Low-Cost Shoreline Protection in Massachusetts," Proceedings, Coastal Structures 79, Vol I, pp 373-387.

Hales, L. Z. "Experimental Studies of Combined Wave Refraction and Diffraction near Shore-Connected Breakwaters" (in preparation), U. S. Army Engineer Waterways Experiment Station, CE, Vicksburg, Miss.

Herbich, J. B. 1976. "Scour Around Model Pipelines Due to Wave Action," Proceedings, Fifteenth Conference on Coastal Engineering, Honolulu, Hawaii, Vol II, pp 1624-1645.

Herbich, J. B., and Ko, S. C. 1968. "Scour of Sand Beaches in Front of Seawalls," Proceedings, Eleventh Conference on Coastal Engineering, London, England, pp 622-643.

Highway Research Board. 1970. "Scour at Bridge Waterways," Synthesis of Highway Practice Report No. 5, National Cooperative Highway Research Program, National Research Council, Washington, D. C.

Hinwood, J. B., and Wallis, I. G. 1975a. "Classification of Models of Tidal Waters," Journal, Hydraulics Division, American Society of Civil Engineers, Vol 101, No. HY10, pp 1315-1331.

_____. 1975b. "Review of Models of Tidal Waters," Journal, Hydraulics Division, American Society of Civil Engineers, Vol 101, No. HY11, pp 1405-1421.

Hjorth, P. 1975. "Studies on the Nature of Local Scour," Bulletin Series A, No. 46, Department of Water Resources Engineering, University of Lund, Lund, Sweden.

Hjulstrom, J. 1935. "The Morphological Activity of Rivers as Illustrated by Rivers Fyris," Bulletin, Geological Institute of Uppsala, University of Uppsala, Sweden, Vol 25.

Hopkins, G. R., Vance, R. W., and Kasraie, B. 1975. "Scour Around Bridge Piers," Report No. FHWA-RD-75-56, West Virginia University, Morgantown, W. Va.

Horikawa, K., and Watanabe, A. 1968. "Laboratory Study on Oscillatory Boundary Layer Flow," Proceedings, Eleventh Conference on Coastal Engineering, London, England, Vol I, pp 467-486.

Hotta, S., and Marui, N. 1976. "Local Scour and Current Around a Porous Breakwater," Proceedings, Fifteenth Conference on Coastal Engineering, Honolulu, Hawaii, Vol II, pp 1590-1604.

Houston, J. R. "Modeling of Short Waves Using the Finite Element Method" (in preparation), Proceedings, Third International Conference on Finite Element in Water Resources, University of Mississippi, Oxford, Miss.

Huang, N. E., et al. 1972. "Interactions Between Steady Non-Uniform Currents and Gravity Waves with Applications for Current Measurements," Journal of Physical Oceanography, Vol 2, No. 4, pp 420-431.

Inglis, C. C. 1949. "The Behaviour and Control of Rivers and Canals," Central Power, Irrigation and Navigation Research Station, Poona, India, p 327.

Inman, D. L., and Bowen, A. J. 1963. "Flume Experiments on Sand Transport by Waves and Currents," Proceedings, Eighth Conference on Coastal Engineering, Mexico City, Mexico, pp 137-150.

Ito, Y., and Tanimoto, K. 1972. "A Method of Numerical Analysis of Wave Propagation--Application to Wave Diffraction and Refraction," Proceedings,

Thirteenth Coastal Engineering Conference, Vancouver, British Columbia, Canada, Vol 1, pp 503-522.

Johnson, J. W. 1949. "Scale Effects in Hydraulic Models Involving Wave Motion," Transactions, American Geophysical Union, Vol 30, No. 4, pp 517-527.

Johnson, J. W., and Eagleson, P. S. 1966. "Chapter 9: Coastal Processes," Estuary and Coastline Hydrodynamics, McGraw-Hill, New York.

Jonsson, I. G. 1965. "Friction Factor Diagrams for Oscillatory Boundary Layers," Basic Research Progress Report No. 10, Part 2, Coastal Engineering Laboratory, Technical University of Denmark, Copenhagen, Denmark.

_____. 1970. "Interaction Between Waves and Currents," Proceedings, Twelfth Conference on Coastal Engineering, Washington, D. C., Vol 1, pp 489-507.

_____. 1978. "A New Approach to Oscillatory Rough Turbulent Boundary Layers," Series Paper No. 17, Technical University of Denmark, Copenhagen, Denmark.

Jonsson, I. G., Skovgaard, O., and Brink-Kjaer, O. 1976. "Diffraction and Refraction Calculations for Waves Incident on an Island," Journal of Marine Research, Vol 34, No. 3, pp 469-497.

Kalinske, A. A. 1947. "Movement of Sediment as Bed Load in Rivers," Transactions, American Geophysical Union, Vol 28, pp 615-620.

Kalkanis, G. 1963. "Transportation of Bed Material Due to Wave Action," Technical Report HEL-2-4, University of California, Berkeley, Calif.

Kana, T. W. 1978. "Surf Zone Measurements of Suspended Sediment," Proceedings, Sixteenth Coastal Engineering Conference, Hamburg, Germany, Vol II, pp 1725-1743.

_____. 1979. "Suspended Sediment in Breaking Waves," Technical Report No. 18-CRD, University of South Carolina, Columbia, S. C.

Karaki, S. S. 1959. "Hydraulic Model Study of Spur Dikes for Highway Bridge Openings," No. CER59SSK36, Colorado State University, Fort Collins, Colo.

Kato, H., and Tsuruya, H. 1978. "Experimental Study of Wind Waves Generated on Currents," Proceedings, Sixteenth Conference on Coastal Engineering, Hamburg, Germany, Vol 1, pp 742-755.

Keown, M. P., and Dardeau, A. E., Jr. "Utilization of Filter Fabric for Streambank Protection Applications" (in preparation), U. S. Army Engineer Waterways Experiment Station, CE, Vicksburg, Miss.

Kerkhoven, R. E. 1963. Application of Hot Mastic Asphalt Under Water for Bottom Protection, 2d ed., Koninklijke/Shell Laboratorium, Amsterdam, the Netherlands.

Kieslich, J. M., and Mason, C. 1975. "Channel Entrance Response to Jetty Construction," Proceedings, Civil Engineering in the Oceans III, Vol 1, pp 689-705.

Komar, P. D. 1971. "The Mechanics of Sand Transport on Beaches," Journal of Geophysical Research, Vol 76, pp 713-721.

_____. 1975. "Longshore Currents and Sand Transport on Beaches," Proceedings, Ocean Engineering III Conference, Newark, Del.

_____. 1976. "Chapter 7: Boundary Layer Flow Under Steady Unidirectional Currents," Marine Sediment Transport and Environmental Management, Wiley, New York.

_____. 1976. "Chapter 8: The Transport of Cohesionless Sediments on Continental Shelves," Marine Sediment Transport and Environmental Management, Wiley, New York.

Komar, P. D., and Miller, M. C. 1973. "The Threshold of Sediment Movement Under Oscillatory Water Waves," Journal of Sedimentary Petrology, Vol 43, No. 4, pp 1101-1110.

_____. 1974. "Sediment Threshold Under Oscillatory Waves," Proceedings, Fourteenth Coastal Engineering Conference, Copenhagen, Denmark, pp 756-775.

Lane, E. W., and Kalinske, A. A. 1941. "Engineering Calculations of Suspended Sediment," Transactions, American Geophysical Union, Vol 22, pp 603-607.

Larras, J. 1963. "Maximum Depths of Erosion in Shifting Beds Around River Piles," Annales des Ports et Chaussees, Vol 133, No. 4, pp 411-424.

Laursen, E. M. 1951. "Scour Around Bridge," Research Report No. 13-B, Highway Research Board, National Research Council, Washington, D. C.

_____. 1962. "Scour at Bridge Crossings," Transactions, American Society of Civil Engineers, Vol 127, Part I, pp 166-180.

Lee, T. T. 1972. "Design of Filter System for Rubble-Mound Structures," Proceedings, Thirteenth Conference on Coastal Engineering, Vancouver, British Columbia, Canada, Vol III, pp 1917-1933.

Leendertse, J. J. 1970. "A Water-Quality Simulation Model for Well-Mixed Estuaries and Coastal Seas," Principles of Computation, Vol 1, Rand Corp., Santa Monica, Calif.

Lepetit, J. P., and Hauguel, A. 1978. "A Numerical Model for Sediment Transport," Proceedings, Sixteenth Coastal Engineering Conference, Hamburg, Germany, Vol II, pp 1715-1724.

Letter, J. V., Jr., and McAnally, W. H., Jr. 1977 (Nov). "Physical Hydraulic Models: Assessment of Predictive Capabilities; Movable-Bed Model of Galveston Harbor Entrance," Research Report H-75-3, Report 2, U. S. Army Engineer Waterways Experiment Station, CE, Vicksburg, Miss.

Liu, P., and Lennon, G. P. 1978. "Finite Element Modeling of Nearshore Currents," Journal, Waterway, Port, Coastal, and Ocean Division, American Society of Civil Engineers, Vol 104, No. WW2, pp 175-189.

Liu, P., and Lozano, C. J. 1979. "Combined Wave Refraction and Diffraction," Proceedings, Coastal Structures 79, Vol II, pp 978-997.

AD-A088 893 ARMY ENGINEER WATERWAYS EXPERIMENT STATION VICKSBURG--ETC F/G 8 3
EROSION CONTROL OF SCOUR DURING CONSTRUCTION; REPORT 2. LITERAT-- TC(U)
AUG 80 L Z HALES
UNCLASSIFIED WES/TR/HL-80-3-2 NL

END
DATE FILMED
10 80
DTIC

Liu, P., and Mei, C. C. 1975. "Effects of a Breakwater on Nearshore Currents Due to Breaking Waves," Technical Memorandum No. 57, U. S. Army Engineer Coastal Engineering Research Center, CE, Fort Belvoir, Va.

_____. 1976a. "Water Motion on a Beach in the Presence of a Breakwater--Part I, Waves," Journal of Geophysical Research, Vol 81, No. 18, pp 3079-3084.

_____. 1976b. "Water Motion on a Beach in the Presence of a Breakwater--Part II, Mean Currents," Journal of Geophysical Research, Vol 81, No. 18, pp 3085-3094.

Longuet-Higgins, M. S. 1962. "The Directional Spectrum of Ocean Waves, and Processes of Wave Generation," Proceedings, Royal Society of London, Series A, Vol 265, No. 30, pp 285-315.

_____. 1970. "Longshore Currents Generated by Obliquely Incident Sea Waves, 1," Journal of Geophysical Research, Vol 75, No. 33, pp 6788-6801.

Longuet-Higgins, M. S., and Stewart, R. W. 1960. "Changes in the form of Short Gravity Waves on Long Waves and Currents," Journal of Fluid Mechanics, Vol 8, pp 565-583.

_____. 1964. "Radiation Stresses in Water Waves; A Physical Discussion with Applications," Deep-Sea Research, Vol II, pp 529-562.

Lundgren, H. 1962. "The Concept of the Wave Thrust," Progress Report No. 3, pp 1-5, Coastal Engineering Laboratory, Technical University of Denmark.

MacDonald, T. C. 1973. "Sediment Transport Due to Oscillatory Waves," Technical Report HEL-2-39, University of California, Berkeley, Calif.

Machemehl, J. L. 1979. "Damage and Repairs to Coastal Structures," Proceedings, Coastal Structures 79, Vol I, pp 314-332.

Machemehl, J. L., and Abad, G. 1975. "Scour Around Marine Foundations," Proceedings, Offshore Technology Conference, Houston, Tex., Paper No. OTC 2313.

Madsen, O. S., and Grant, W. D. 1975. "The Threshold of Sediment Movement Under Oscillatory Waves: A Discussion," Journal of Sedimentary Petrology, Vol 45, pp 360-361.

_____. 1976. "Quantitative Description of Sediment Transport by Waves," Proceedings, Fifteenth Coastal Engineering Conference, Honolulu, Hawaii, Part II, pp 1093-1112.

Manohar, M. 1955. "Mechanics of Bottom Sediment Movement Due to Wave Action," Technical Memorandum No. 75, U. S. Army Engineer Beach Erosion Board, CE, Washington, D. C.

Mansur, C. I., and Olson, G. E. 1948 (Jan). "Laboratory Investigation of Filters for Enid and Grenada Dams," Technical Memorandum No. 3-245, U. S. Army Engineer Waterways Experiment Station, CE, Vicksburg, Miss.

McCartney, B. L., and Ahrens, J. P. 1975. "Stability of Gobi Block Revetment to Wave Attack," Technical Memorandum No. 55, U. S. Army Engineer Coastal Engineering Research Center, CE, Washington, D. C.

Meulen, T. V., and Vinje, J. J. 1977. "Three-Dimensional Local Scour in Non-Cohesive Sediments," Publication No. 180, Delft Hydraulics Laboratory, Delft, the Netherlands.

Mobarek, I. 1962. "Effect of Bottom Slope on Wave Diffraction," Technical Report HEL-1-1, University of California, Berkeley, Calif.

Murphy, T. E. 1971 (Mar). "Control of Scour at Hydraulic Structures," Miscellaneous Paper H-71-5, U. S. Army Engineer Waterways Experiment Station, CE, Vicksburg, Miss.

Naheer, E. 1979. "Incipient Motion of Arbitrary Shape Particles Under Solitary Waves," Coastal Engineering, Vol 2, pp 277-296.

Nakagawa, H., and Suzuki, K. 1976. "Local Scour Around Bridge Pier in Tidal Current," Coastal Engineering in Japan, Vol 19.

Neill, C. R. 1964. "River Bed Scour," Technical Publication No. 23, Canadian Good Roads Association, Ottawa, Canada.

_____. 1965. "Measurements of Bridge Scour and Bed Changes in a Flooding Sand-Bed River," Proceedings, Institute of Civil Engineers, London, England.

_____. 1967. "Mean Velocity Criterion for Scour of Coarse Uniform Bed Material," Proceedings, Twelfth Congress, International Association for Hydraulic Research, Fort Collins, Colo., Vol 3, pp 46-54.

Nielsen, P. 1979. "Some Basic Concepts of Wave Sediment Transport," Series Paper No. 20, Technical University of Denmark, Lyngby, Denmark.

Noda, E. K. 1974. "Wave-Induced Nearshore Circulation," Journal of Geophysical Research, Vol 79, No. 27, pp 4097-4106.

Noda, E. K., et al. 1974. "Nearshore Circulations Under Sea Breeze Conditions and Wave-Current Interactions in the Surf Zone," Report TC-149-4, Tetra Tech Corporation, Pasadena, Calif.

Nordstrom, C. E., and Inman, D. L. 1975. "Sand Level Changes on Torrey Pines Beach, California," Miscellaneous Paper No. 11-75, U. S. Army Engineer Coastal Engineering Research Center, CE, Washington, D. C.

Office, Chief of Engineers, Department of the Army. 1975. "Civil Works Construction Guide Specifications, Plastic Filter Cloth," CW 02215, Washington, D. C.

Ostendorf, D. W., and Madsen, O. S. 1979. "An Analysis of Longshore Currents and Associated Sediment Transport in the Surf Zone," Sea Grant Communications MIT-SG-79-13, Massachusetts Institute of Technology, Cambridge, Mass.

Palmer, H. D. 1969. "Wave-Induced Scour on the Sea Floor," Proceedings, Civil Engineering in the Oceans--II, Miami Beach, Fla., pp 703-715.

Penny, W. G., and Price, A. T. 1952. "The Diffraction Theory of Sea Waves and the Shelter Afforded by Breakwaters," Philosophical Transactions, Royal Society of London, Series A, Vol 244, pp 236-253.

Perry, F. C., Jr., Seabergh, W. C., and Lane, E. F. 1978 (Apr). "Improvements for Murrells Inlet, South Carolina; Hydraulic Model Investigation," Technical Report H-78-4, U. S. Army Engineer Waterways Experiment Station, CE, Vicksburg, Miss.

Posey, C. J. 1969. "Erosion Prevention Experiments," Proceedings, Thirteenth International Association for Hydraulic Research, Kyoto, Japan, Vol 2, pp 211-219.

_____. 1971. "Protection of Offshore Structures Against Underscour," Journal, Hydraulics Division, American Society of Civil Engineers, Vol 97, No. HY7, pp 1011-1016.

Posey, C. J., and Sybert, J. H. 1961. "Erosion Protection of Production Structures," Proceedings, Ninth International Association for Hydraulic Research, Dubrovnik, Yugoslavia, pp 1157-1161.

Rance, P. J., and Warren, N. F. 1968. "The Threshold of Movement of Coarse Material in Oscillatory Flow," Proceedings, Eleventh Conference on Coastal Engineering, London, England, Vol I, pp 487-491.

Resio, D. T. 1978. "Estimation of Longshore Drift Rates from Numerical Models," Proceedings, Coastal Zone 78, Vol III, pp 2289-2307.

Riedel, H. P., Kamphuis, J. W., and Brebner, A. 1972. "Measurement of Bed Shear Stress Under Waves," Proceedings, Thirteenth Coastal Engineering Conference, Vancouver, British Columbia, Canada, Vol I, pp 587-603.

Rouse, H. 1938. "Transportation of Sediment," Fluid Mechanics for Hydraulic Engineers, McGraw-Hill, New York.

Russell, R. C. H., and Inglis, C. 1953. "The Influence of a Vertical Wall on a Beach in Front of It," Proceedings, Minnesota International Hydraulics Convention, Minneapolis, Minn., pp 221-226.

Sager, R. A., and Seabergh, W. C. 1977 (Nov). "Physical Model Simulation of the Hydraulics of Masonboro Inlet, North Carolina," GITI Report No. 15, U. S. Army Engineer Coastal Engineering Research Center, Fort Belvoir, Va., and U. S. Army Engineer Waterways Experiment Station, CE, Vicksburg, Miss.

Sato, S., Tanaka, N., and Irie, I. 1968. "Study on Scouring at the Foot of Coastal Structures," Proceedings, Eleventh Conference on Coastal Engineering, London, England, Vol I, pp 579-598.

Sawaragi, T. 1966. "Scouring Due to Wave Action at the Toe of Permeable Coastal Structure," Proceedings, Tenth Conference on Coastal Engineering, Tokyo, Japan, pp 1036-1047.

Sawaragi, T., and Deguchi, I. 1978. "Distribution of Sand Transport Rate Across a Surf Zone," Proceedings, Sixteenth Coastal Engineering Conference, Hamburg, Germany, Vol II, pp 1596-1613.

Schlichting, H. 1968. Boundary Layer Theory, 6th ed., McGraw-Hill, New York.

Seabergh, W. C. 1979. "Model Testing of Structures at a Tidal Inlet," Proceedings, Coastal Structures 79, Vol II, pp 690-709.

Seelye, E. E. 1956. Foundation Design and Practice, Wiley, New York.

Shen, H. W., Schneider, V. R., and Karaki, S. 1969. "Local Scour Around Bridge Piers," Journal, Hydraulics Division, American Society of Civil Engineers, Vol 95, No. HY6, pp 1919-1940.

Sheng, Y. P., and Lick, W. 1979. "The Transport and Resuspension of Sediments in a Shallow Lake," Journal of Geophysical Research, Vol 84, No. C4, pp 1809-1826.

Sheng, Y. P., et al. 1978. "Numerical Computation of Three-Dimensional Circulation in Lake Erie: A Comparison of a Free-Surface Model and a Rigid-Lid Model," Journal of Physical Oceanography, Vol 8, No. 4, pp 713-727.

Sherman, W. C., Jr. 1978. "Filter Concepts" (unnumbered memorandum), U. S. Army Engineer Waterways Experiment Station, CE, Vicksburg, Miss.

Simmons, H. B., and Boland, R. A., Jr. 1969 (Feb). "Model Study of Galveston Harbor Entrance, Texas; Hydraulic Model Investigation," Technical Report H-69-2, U. S. Army Engineer Waterways Experiment Station, CE, Vicksburg, Miss.

Song, W. O., and Schiller, R. E. 1973. "Experimental Studies of Beach Scour Due to Wave Action," Sea Grant Publication No. 73-211, Texas A&M University, College Station, Tex.

Sonu, C. J. 1972. "Field Observations of Nearshore Circulation and Meandering Currents," Journal of Geophysical Research, Vol 77, No. 18, pp 3232-3247.

Sorensen, R. M. 1978. Basic Coastal Engineering, Wiley, New York.

Steiman, D. B., and Watson, S. R. 1957. Bridges and Their Builders, Dover, New York.

Straub, L. G. 1942. "Mechanics of Rivers," Hydrology, Dover, New York.

Swart, D. H. 1974. "Offshore Sediment Transport and Equilibrium Beach Profiles," Publication No. 131, Delft Hydaulics Laboratory, Delft, the Netherlands.

_____. 1976. "Predictive Equations Regarding Coastal Transports," Proceedings, Fifteenth Coastal Engineering Conference, Honolulu, Hawaii, Vol II, pp 1113-1132.

Teleki, P. G. 1972. "Chapter 2: Wave Boundary Layers and Their Relation to Sediment Transport," Shelf Sediment Transport, Dowden, Hutchinson and Ross, Inc., Stroudsburg, Pa.

Terzaghi, K., and Peck, R. B. 1948. Soil Mechanics in Engineering Practice, Wiley, New York.

Thornton, E. B. 1970. "Variations of Longshore Current Across the Surf Zone," Proceedings, Twelfth Coastal Engineering Conference, Washington, D. C., Vol I, pp 291-308.

_____. 1972. "Distribution of Sediment Transport Across the Surf Zone," Proceedings, Thirteenth Coastal Engineering Conference, Vancouver, British Columbia, Canada, Vol II, pp 1049-1068.

Unna, P. J. H. 1942. "Waves and Tidal Streams," Nature, Vol 149, p 219.

U. S Army Engineer Coastal Engineering Research Center, CE. 1975. "Shore Protection Manual," Vol I, Washington, D. C.

U. S. Army Engineer Waterways Experiment Station, CE. 1953. "Filter Experiments and Design Criteria," Technical Memorandum No. 3-360, Vicksburg, Miss.

Van de Graaff, J., and Van Overeem, J. 1979. "Evaluation of Sediment Transport Formulae in Coastal Engineering Practice," Coastal Engineering, Amsterdam, the Netherlands, Vol 3, No. 1-32.

Van Hoften, J. D. A., and Karaki, S. 1976. "Interaction of Waves and a Turbulent Current," Proceedings, Fifteenth Conference on Coastal Engineering, Honolulu, Hawaii, Vol I, pp 404-422.

Vanoni, V. A. 1964. "Measurements of Critical Shear Stress for Entraining Fine Sediments in a Boundary Layer," Report No. KH-R-7, California Institute of Technology, Pasadena, Calif.

Wada, A. 1969. "Numerical Analysis of the Distribution of Flow and Thermal Diffusion Caused by Outfall of Cooling Water," Proceedings, Thirteenth International Congress of the International Association for Hydraulic Research, pp 335-342.

Walton, T. L., Jr., and Chiu, T. Y. 1979. "Littoral Sand Transport on Beaches," Report No. UFL-COEL-TR-041, University of Florida, Gainesville, Fla.

Wells, D. R., and Sorensen, R. M. 1970. "Scour Around a Circular Pile Due to Oscillatory Wave Motion," Sea Grant Publication No. 208, Texas A&M University, College Station, Tex.

Welsh, J. P., and Koerner, R. M. 1979. "Innovative Uses of Synthetic Fabrics in Coastal Construction," Proceedings, Coastal Structures 79, Vol I, pp 364-372.

Whalin, R. W. 1971 (Dec). "The Limit of Applicability of Linear Wave Refraction Theory in a Convergence Zone," Research Report H-71-3, U. S. Army Engineer Waterways Experiment Station, CE, Vicksburg, Miss.

_____. 1972. "Wave Refraction Theory in a Convergence Zone," Proceedings, Thirteenth Coastal Engineering Conference, Vancouver, British Columbia, Canada, Vol 1, pp 451-470.

_____. 1976 (Aug). "A Variational Approach to Nonlinear Wave Theory," Miscellaneous Paper H-76-16, U. S. Army Engineer Waterways Experiment Station, CE, Vicksburg, Miss.

Wiegel, R. L. 1962. "Diffraction of Waves by Semi-Infinite Breakwaters," Journal, Hydraulics Division, American Society of Civil Engineers, Vol 88, No. HY1, pp 27-44.

Wilder, C. R., and Dinchak, W. G. 1979. "Soil-Cement for Shore Protection," Proceedings, Coastal Structures 79, Vol I, pp 301-313.

Worthington, H. W., and Herbich, J. B. 1970. "A Computer Program to Estimate the Combined Effect of Refraction and Diffraction of Water Waves," Report No. 127-COE, Texas A&M University, College Station, Tex.

Yalin, M. S. 1959. "On the Full-Scale Similarity of Sediment Transport in Model Tests," Die Bautechnik, Vol 36, No. 3, pp 96-99.

_____. 1971. Theory of Hydraulic Models, Macmillan, New York.

Table 1

Physical Strength Requirements for Woven and Nonwoven Plastic Filter Fabric

Physical Property	Test Procedure	Acceptable Test Results*
Tensile strength (unaged fabric**)	ASTM D 1682 Grab Test Method using 1-in. square jaws and a travel rate of 12 in./min	200-lb minimum in any principal direction
Puncture strength (unaged fabric**)	ASTM D 751 Tension Testing Machine with Ring Clamp; steel ball replaced with a 5/16-in.-diam solid steel cylinder with a hemispherical tip centered within the ring clamp	80-lb minimum
Abrasion resistance	ASTM D 1682 as above, after abraded as in ASTM D 1175† Rotary Platform, Double Head Method; rubber-base abrasive wheels equal to CS-17 "Calibrase" by Taber Instrument Co.; 1 kg load per wheel; 1,000 revolutions	55-lb minimum in any principal direction

* Acceptable test results strengths may be reduced 50 percent for fabric to be used in drainage trenches, beneath concrete slabs, or to be cushioned from rock placement by a layer of sand or by zero drop height placement.

** Unaged fabric is defined as fabric in the condition received from the manufacturer or distributor.

APPENDIX A: NOTATION

a	Wave amplitude
A	Area, orbital diameter
A_y	Eddy viscosity coefficient
b	Obstruction width normal to flow lines
B	Coefficient of proportionality
B_s	Proportionality constant
C	Wave celerity, Chezy coefficient, concentration of suspended sediment
C_a	Sediment concentration, specific location
C_b	Wave celerity at breaking
C_D	Drag coefficient
C_e	Concentration at upper boundary of bed-load layer
C_f	Friction coefficient
C_g	Group velocity
C_L	Lift coefficient
C_m	Maximum concentration at the bed
C_o	Base concentration
C_r	Refraction coefficient
C_s	Sediment concentration, arbitrary location
C_l	Wave celerity in the presence of a current
d	Sediment particle diameter, depth of water
d_e	Equivalent effective roughness of the bottom
d_m	Mean diameter of bed material
d_o	Initial bottom configuration
d_s	Maximum scour depth

du/dy	Velocity gradient
d_{50}, d_{35}, etc.	Particle diameter (50, 30, etc., percent by weight exceeded in size)
D	Depth of uniform flow, width of pier
e	Bed-load thickness
E	Wave energy density
f	Coriolis parameter
f_w	Wave friction factor
F_D	Drag force
F_L	Lift force
F_r	Froude number
F, F_x, F_y	Applied forces
$F_{\alpha_1}, F_{\alpha_2}$	Applied forces in α-space coordinates
g	Acceleration due to gravity
G	Unique Einstein parameter
h	Local water depth
h	Water depth
h_c	Water depth at offshore bar
h_t	Water depth at nearshore trough
H	Wave height
H_b	Breaker height
H_i	Instant wave height
H_o	Deepwater wave height
H_r	Measured reflected wave height from structure
H_s	Deepwater standing wave height
i_f	Hydraulic gradient of 1 in. of soil immediately next to filter fabric

i_g	Hydraulic gradient of 2 in. of soil from 1 in. to 3 in. away from filter fabric
i,j	Finite difference increments
I_1, I_2	Einstein integrals
k	Von Karman's constant
k_o	Wave number
k_s	Measure of roughness elements
k_s	Variable shoaling coefficient
K	Pier shaped coefficient
ℓ	Ripple length, ripple factor
ℓ_e	Mixing length for sediment exchange
L	Wavelength
L_a	Wavelength at shoreline
L_o	Deepwater wavelength
L_s	Deepwater standing wavelength
m	Beach slope
M	Suspended load transport parameter
n	Manning's roughness coefficient, wave depth effect coefficient, ripple height
$n_{s/d}$	Sand scale ratio
p	Porosity of sediment material
P_{ls}	Alongshore component of wave energy flux per unit length of beach
pH	Acidity indicator
q	Instantaneous discharge
q_s	Sediment transport per unit width of channel
q_{cr}	Critical discharge

q_{bed}	Bed-load transport
q_{lso}	Unit longshore transport outside breaker zone
q_{sus}	Suspended load
Q_{AW}	Longshore transport based on Ackers-White formula
Q_{Bi}	Longshore transport based on Bijker formula
Q_{EH}	Longshore transport based on Engelund-Hansen formula
Q_{ls}	Longshore transport
Q_{SW}	Longshore transport based on SWANBY concept
r	Constant, bed roughness above the bed
r_a	Radius of the island
R	Water input to Program WIFM
R_{e*}	Shear Reynolds number
R_x	Rate of energy transfer in x-direction
RE	Wave Reynolds number
s_o	Suspended load velocity parameter
S	Slope of hydraulic gradient producing the uniform flow, depth of scour, phase function
S_x	Radiation stress in x-direction
SS_{10}	Suspended sediment concentration at 10 cm above bed
t	Time
t_r	Reference time
T	Wave period
T_{max}	Maximum depth of scour at nearshore trough
u	Average channel velocity
u'	Combined velocity due to current and waves
u_b	Bottom velocity

u_c	Current velocity at arbitrary location
u_o	Maximum orbital velocity at the bed
u_*	Friction velocity
u_{cr}	Critical average velocity required to move a substantial number of surface bed particles
u_{max}	Maximum particle velocity at the bottom
u_{cmax}	Maximum current velocity at free surface
u,v,w	Instantaneous velocity components in x, y, z directions
u',v',w'	Turbulent velocity components in x, y, z directions
U	Velocity, average horizontal component of velocity in x-direction
U_o	Average velocity of flow in laboratory flume
v	Exchange discharge through unit area, mean current velocity
V	Average horizontal component of velocity in y-direction
v_f	Fall velocity
v_{*c}	Shear stress velocity due to current
v_{*wc}	Shear stress velocity due to wave
V_{ls}	Velocity of longshore current
V_{lso}	Longshore velocity outside surf zone
W_{50},W_{30},etc.	Stone weight (50, 30, etc., percent by weight exceeded in size)
X	Wave friction factor and velocity parameter
X_b	Distance from shoreline to the point where wave breaks
y	Still-water depth
Y	Separation distance, elevation, or wave bed-load transport parameter
z	Verticle direction in Cartesian coordinate system

z_*	Fall velocity parameter
α	Coefficient, friction angle of bed material
α_b	Breaker angle
γ	Weight of liquid per unit volume
γ_s	Unit weight of the solids
δ	Boundary layer thickness
Δ	Relative apparent density of bed material
ε	Diffusion coefficient, Bijker's parameter
η	Instantaneous water-surface elevation
θ	Bottom slope
θ_t	Wave sediment movement threshold parameter
λ	Distortion factor of a sand scale to a flow depth scale
μ	Fluid kinematic viscosity
μ_1, μ_2	Coordinate stretching parameters
ν	Fluid dynamic viscosity
π	3.14159
ρ	Density of the liquid
ρ_s	Particle density
ρ_w	Water density
τ	Shearing stress
τ_c	Bottom shear stress due to current, critical shear stress
τ_d	Dispersion shear stress
τ_i	Critical tractive force
τ_o	Bottom shear stress
τ_w	Mean wave shear stress
Φ	Bed material angle of response, wave potential function

ψ Shields wave sediment movement parameter

ω Frequency of wave oscillation

In accordance with letter from DAEN-RDC, DAEN-ASI dated 22 July 1977, Subject: Facsimile Catalog Cards for Laboratory Technical Publications, a facsimile catalog card in Library of Congress MARC format is reproduced below.

Hales, Lyndell Z
Erosion control of scour during construction; Report 1: Literature survey of theoretical, experimental, and prototype investigations / by Lyndell Z. Hales. Vicksburg, Miss. : U. S. Waterways Experiment Station ; Springfield, Va. : available from National Technical Information Service, 1980.
194, [1], 7 p. : ill. ; 27 cm. (Technical report - U. S. Army Engineer Waterways Experiment Station ; HL-80-3, Report 2)
Prepared for Office, Chief of Engineers, U. S. Army, Washington, D. C.
References: p.182-194.

1. Construction practices. 2. Erosion control. 3. Prototypes. 4. Scour. I. United States. Army. Corps of Engineers. II. Series: United States. Waterways Experiment Station, Vicksburg, Miss. Technical report ; HL-80-3, Report 2.
TA7.W34 no.HL-80-3 Report 2